March
2014

“DAMP-ening inflammation caused by Interferon Inducible Protein 16 (IFI16) in systemic autoimmunity”

PHD THESIS

MANDAR BAWADEKAR

FACULTY OF MEDICINE - UNIVERSITY OF PIEMONTE ORIENTALE | Via Solaroli 17, 28100 – Novara, Italy

PhD in Clinical & Experimental Medicine

UNIVERSITÀ DEGLI STUDI DEL PIEMONTE ORIENTALE "AMEDEO AVOGADRO"

Dipartimento di Medicina Traslazionale

Corso di Dottorato di Ricerca in Medicina Clinica e Sperimentale

ciclo **XXVI**

DAMP-ening inflammation caused by Interferon Inducible Protein 16 (IFI16) in systemic autoimmunity

SSD: MED/07

Coordinatore
Prof. Marisa Gariglio

Tutor
Prof. Marisa Gariglio

Dottorando
Mandar Bawadekar

CONTENTS

1 RESEARCH SUMMARY

IFI16, a nuclear pathogenic DNA sensor induced by several pro-inflammatory cytokines, is a multifaceted protein with various functions. It is also a target for autoantibodies as specific antibodies have been demonstrated in the sera of patients affected by systemic autoimmune diseases. Following transfection of virus-derived DNA, or treatment with UVB, IFI16 delocalizes from the nucleus to the cytoplasm and is then eventually released into the extracellular milieu. In this PhD research study, using an in-house capture enzyme-linked immunosorbent assay we demonstrate that significant levels of IFI16 protein can also exist as circulating form in the sera of autoimmune patients. We also show that the rIFI16 protein, when added in-vitro to endothelial cells, does not affect cell viability, but severely limits their tubulogenesis and transwell migration activities. These inhibitory effects are fully reversed in the presence of anti-IFI16 N-terminal antibodies, indicating that its extracellular activity resides within the N-terminus. It was further demonstrated that endogenous IFI16 released by apoptotic cells bind neighboring cells in a co-culture. Immunofluorescence assays revealed existence of high-affinity binding sites on the plasma membrane of endothelial cells. Free recombinant IFI16 binds these sites on HUVEC with dissociation constant of 2.7nM, radioiodinated and unlabeled IFI16 compete for binding sites, with inhibition constant (K_i) of 14.43nM and half maximal inhibitory concentration (IC_{50}) of 67.88nM; these data allow us to estimate the presence of 250,000 to 450,000 specific binding sites per cell. Corroborating the results from functional assays, this binding could be completely inhibited using anti-IFI16 N-terminal antibody, but not with an antibody raised against the IFI16 C-terminal. By qPCR analysis, we were able to identify the cytokine stimulating activity of IFI16. IFI16 treatment on

primary endothelial cells lead to time-dependent increased m-RNA expression of various chemokines like IL-8, CCL2, CCL5, CCL20, adhesion molecules like ICAM1, VCAM1 and TLRs such as TLR3, TLR4 and TLR9. Such pro-inflammatory cytokine expression was mediated by Nf-κB dependent pathways. Altogether, these data demonstrate that IFI16 may exist as circulating protein in the sera of autoimmune patients which binds endothelial cells causing damage and stimulates the production of pro-inflammatory cytokines, suggesting a new pathogenic, DAMP-like alarmin function through which this protein triggers the development of autoimmunity.

IFI16 is highly implicated for its role in inflammasome signaling and DNA sensing, while in turn it acts as restriction factor for viral replication. Intracellular viral DNA sensors and restriction factors are critical components of host defence, which alarm and sensitize immune system against intruding pathogens. Recently demonstrated by Gariano GR *et.al*. PLoS Paths 2012, that the DNA sensor IFI16 restricts HCMV replication by down-regulating viral early and late but not immediate-early mRNAs and their protein expression. However, viruses are known to evolve numerous strategies to cope and counteract such restriction factors and neutralize the first line of host defense mechanisms. Our findings as described in the attached second manuscript, that during early stages of infection, IFI16 successfully recognizes HCMV DNA. However, in late stages HCMV mislocalizes IFI16 into the cytoplasmic viral assembly complex (AC) and finally entraps the protein into mature virions. This work clarifies the mechanisms HCMV relies to overcome intracellular viral restriction, which provides new insights about the relevance of DNA sensors during HCMV infection.

The outcomes of above discussed aspects of IFI16 related research are discussed wholly in the attached manuscripts as listed below:

1. Gugliesi F*, **Bawadekar M***, De Andrea M, Dell'Oste V, Caneparo V, Gariglio M and Landolfo S. Nuclear DNA Sensor IFI16 as Circulating Protein in Autoimmune Diseases Is a Signal of Damage that Impairs Endothelial Cells through High-Affinity Membrane Binding. PLoS ONE, 2013, 8(5): e63045. doi:10.1371/journal.pone.0063045 (* Contributed Equally).

2. Dell'Oste V, Gatti D, Gugliesi F, De Andrea M, **Bawadekar M**, Lo Cigno I, Biolatti M, Vallino M, Marschall M, Gariglio M and Landolfo S. Early stage IFI16 cytoplasmic translocation and late stage entrapment into egressing virions during HCMV infection (submitted).

2 INTRODUCTION

2.1 AUTOIMMUNITY

Autoimmunity is a diverse group of disorder that is characterized by the production of antibodies that react with host tissues or immune effector cells that are autoreactive to endogenous peptides. Autoimmune attack against "self" may be involved in the initiation and/or perpetuation of disease. The autoimmune processes seem to result, in certain instances, from a normal (or aberrant) immune reaction against an exogenous pathogen with subsequent "spreading" of the immune response to recognize self-tissue; this reaction can continue in the apparent absence of the initiating pathogen. Most often, however, autoimmune phenomena are simply phenomenological events (for example, false-positive autoantibody tests) without pathogenetic relevance. Autoimmune diseases are individually rare, but together they affect approximately 5 percent of the population in western countries, with the exception of more commonly occurring rheumatoid arthritis and autoimmune thyroiditis [6, 7].

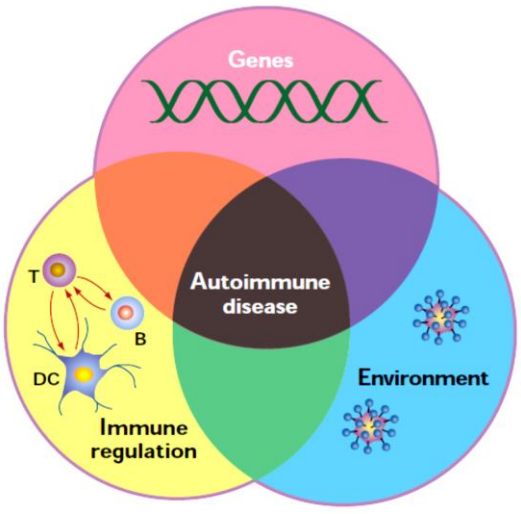

Figure 1. Factors contributing for the development of Autoimmunity [4].

Many patients with autoimmune disease have increased responsiveness to type I IFNs (a/b), and therapy with these cytokines has induced or unmasked autoimmune disease in many additional patients [8].

2.1.1 Interferons and Autoimmune Disorders

Interferon (IFN) was first identified in 1957. A protective role against RNA viruses was inferred from the ability of viral infections to induce IFN production [9]. Subsequently, IFN was found to decrease tumor growth, inflammation, and angiogenesis. The existence of many different IFNs was established. IFNs are now considered to play key roles in both innate immunity (IFN-α, IFN-β) and adaptive immunity (IFN-γ). The IFN pathways are increasingly well understood. These pathways are activated in many situations such as defense mechanisms against viral and bacterial infections, solid tumors, and hematological malignancies. They are also involved in several autoimmune diseases including systemic lupus erythematosus (SLE), Sjögren's syndrome, adult-onset rheumatoid arthritis (RA), polymyositis, and systemic sclerosis. Insights gained into the effects of IFNs, together with the ability to clone the main IFNs, have led to the development of new treatments designed either to support the IFN pathways (hepatitis C and B, adjuvant cancer treatment, treatment of some forms of multiple sclerosis) or to block the effects of IFNs (SLE). The significance of different IFNs in some common autoimmune diseases such as systemic sclerosis (SSc) and Rheumatoid Arthritis (RA) is discussed in the following sections.

Autoimmune rheumatic diseases (AIRD) affect 5-8% of the population with a female preponderance and come in two basic flavors: systemic [e.g. Systemic Lupus Erythematosus (SLE), Sjogren Syndrome (SjS)], and Systemic Sclerosis (SSc)], and organ-specific (e.g. type I diabetes, autoimmune thyroid disease, and multiple

sclerosis) diseases. SLE is a disease characterized by a broad spectrum of clinical manifestations and a multitude of laboratory abnormalities [10, 11]. In clinical practice, the diagnosis of SLE is usually made in a patient who has developed a combination of clinical and immunologic features specific to SLE. Similarly, SSc is a chronic multisystem autoimmune disease that is highly heterogeneous and has multiple overlapping and poorly defined clinical subsets. Primary SjS is considered to represent an ideal disease to study the mechanisms underlying autoimmunity because its manifestation are both organ specific and systemic in nature. Once again, there is no single test for the diagnosis of SjS, and criteria utilizing combinations of clinical and laboratory parameters are currently being used. All these diseases arise as a consequence of the breakdown in tolerance to self-antigens, and the diagnosis is also based on the detection of characteristic autoantibodies. Those autoantibodies may also be pathogenic reacting with the self-antigens in tissues and inducing an inflammatory response that results in damage and disease. Glomerulonephritis is one of the commonest and most serious manifestations of SLE [11]. Despite the overall improvement in the care of SLE in the past two decades, the prognosis of lupus nephritis (LN) remains unsatisfactory [12]. Up to 25% of patients still develop end stage renal failure 10 years after onset of renal disease. Current laboratory markers for LN such as proteinuria, urine protein-to-creatinine ratio, creatinine clearance, anti-dsDNA, and complement levels are unsatisfactory. They lack sensitivity and specificity for differentiating renal activity and damage in lupus nephritis. Besides exploring more effective but less toxic treatment modalities that will further improve the remission rate, early detection and treatment of renal activity may reduce renal damage. The investigation of novel accurate and predictive indexes of AIRD represents a primary

goal for the clinical research in this field. Early diagnosis and a better stratification of the autoimmune disease process is crucial for an early therapeutic intervention which may significantly increase the probability of disease remission and improve patient prognosis. Moreover, new diagnostic techniques need to be established that can help pathologists recognize histology patterns, correctly diagnose the disease, and identify people who are at high risk of developing lethal systemic complications. Systemic autoimmune diseases, like SLE, are characterized by the production of autoantibodies mainly directed against ubiquitous nuclear targets [13]. The skin has long been recognized as a prominent target tissue, with cutaneous disease sometimes manifesting de novo after extended exposure to sunlight, and established disease being exacerbated by such exposure. Skin lesions are present in at least 80% of patients and constitute the primary sign in about 25% of these individuals [14, 15]. The microvascular endothelium in SSc and LN is severely damaged, basal laminae are usually thickened and reduplicated, and a vast number of capillaries are missing or obliterated with the absence of new vessel formation. Microvascular endothelial cell (MVEC) injury and apoptosis is a central event in the pathogenesis of SSc and LN vasculopathy that leads to microcirculatory dysfunction and eventual organ failure. MVEC apoptosis may eventually activate the immune-inflammatory system by dendritic cells and macrophage presentation of self-antigen present in the apoptotic debris to CD4+ T cells and the subsequent triggering of autoantibodies by activated B cells.

2.1.2 Systemic Sclerosis

Type I and II IFNs inhibit collagen production both in vivo and in vitro when they are added to normal or scleroderma fibroblasts. This effect prompted a number of therapeutic trials in patients with diffuse systemic sclerosis, which met

with little success. Oddly enough, there have been several reports of systemic sclerosis induced by IFN-α therapy for hepatitis C or myeloproliferative diseases or by IFN-β therapy for multiple sclerosis. A study of the transcriptome of circulating leukocytes from patients with systemic sclerosis showed amplification of mRNAs for a few genes involved in the IFN pathway [16], although the IFN signature was less typical than in SLE. Serum from patients with systemic sclerosis and antitopoisomerase I (Scl70) antibodies induces a higher level of IFN-α production by normal peripheral blood mononuclear cells than does serum from patients with anticentromere antibody. IFN-α production is higher in patients with diffuse systemic sclerosis and in those with interstitial lung disease. Among the genes induced by IFN, IFI16 encodes a protein found in large amounts in the epidermis and inflammatory dermis of scleroderma lesions. IFI16 plays a role in endothelial cell proliferation. An immunohistochemistry study showed an infiltrate of CD123+ pDCs in scleroderma-affected skin specimens [17]. In a study of candidate genes, increased frequencies of some IRF5 allelic variants were found in patients with systemic sclerosis, and these variants were significantly associated with interstitial lung disease [18]. IRF5 encodes a transduction protein involved in the pro-inflammatory cytokine pathway.

2.1.3 Rheumatoid Arthritis

Growing evidence indicates that adult-onset RA is a syndrome. In patients who produce rheumatoid factor and anticitrullinated protein antibodies (ACPA or anti-CCP) and who carry a susceptibility allele of the PTPN22 gene and the shared epitope of the HLADRB1* alleles, the disease is often erosive and involves TNF-α as the key inflammatory cytokine. In another form of RA, there are no rheumatoid factors or erosions and the HLA phenotype is often DR3; this form is associated with

several polymorphisms of the IRF5, STAT4 genes encoding transduction proteins involved in IFN pathways [19, 20] and of TRAF1, which encodes a negative regulator of TNF-α signaling [21]. This form of RA shares similarities with SLE and Sjögren's syndrome, including involvement of IFNs in the inflammatory response. The two forms of RA correspond to the model that contrasts two categories of autoimmune diseases, one driven by TNF-α and the other by IFN-α [22].

2.1.4 Other Autoimmune Diseases

IFNα/β exert stimulating or inhibitory effects in various autoimmune diseases that fall outside the scope of rheumatology. For instance, in type I insulin-dependent diabetes mellitus, reliable animal models indicate a deleterious role for type I IFNs. IFNs are also harmful in multiple sclerosis and its animal model of acute encephalitis, and IFN-β is used to treat relapsing/remitting forms of multiple sclerosis. Other examples include thyroiditis, some forms of autoimmune hemolytic anemia, and some forms of uveitis such as Behçet's disease uveitis in which IFN-α is used to treat flares.

2.2 Etiopathogenic Role of Type I IFNs in Systemic Autoimmunity

Since their initial use in the 1980s, IFNs have become an essential component of the therapies for many diseases such as hepatitis, multiple sclerosis and some hematological malignancies. Although they have been extremely useful in conditions that pose therapeutic challenges, complications associated with their use have been widely reported, including emerging reports of several autoimmune diseases [23-25]. Many patients with autoimmune disease have increased responsiveness to type I IFNs (α/β); moreover, therapy with these cytokines has been found to induce or unmask autoimmune disease in many patients. Therefore, it is now well accepted that IFNs play a critical role in the pathogenesis of several

autoimmune diseases, including SLE, SjS, SSc, and type 1 diabetes. In particular, long-standing data indicating elevated circulating levels of IFN-α in SLE patients have recently been supplemented by gene expression analyses of patient cells studied ex vivo, and studies of the induction mechanisms of IFN-α production. Administration of recombinant IFN-α, as a therapy for malignancies or hepatitis infection, was reported to induce SLE in some cases. More importantly, immune complexes bearing anti-nuclear autoantibodies and either RNA or DNA antigens have been shown to induce IFN- production. Deregulation of IFN-α in SLE is also evident in the gene expression profile of SLE peripheral blood mononuclear cells [26-28].

Gene microarray studies have revealed the upregulation of IFN stimulated genes (ISGs) in about half of lupus patients, including genes encoding anti-viral proteins, apoptosis regulators, MHC molecules, and chemokines. This "IFN signature" is generally associated with active disease states, and renal and CNS involvement. Altogether, these findings strongly support a pathogenic role for IFN-α in SLE. Consistent with these observations, increased expression of IFN-regulated genes has been described in the salivary glands of patients affected by Sjogren's syndrome, and plasmacytoid dendritic cells (pDCs) were identified as being the main source of IFN-β in these patients [29, 30]. Emerging data have also indicated a role for IFNs in the pathogenesis of SSc [16, 31]. Increased mRNA expression of two classical ISGs in SSc-affected skin has also been described, namely double-stranded RNA dependent protein kinase (PKR) and 2'5'-oligoadenylate synthetase (2'-5' OAS) [17]. Our group found an enhanced expression of the IFN-inducible protein IFI16 in the epidermis and dermal inflammatory infiltrate obtained from SSc and SLE lesions [32]. Altogether, these observations identify type I IFN as the

initiator and ISGs as the executioners in the etiopathogenesis of systemic autoimmune diseases. As a whole, this finding indicates that similar etiopathogenic mechanisms may be involved in different systemic autoimmune diseases and it is likely that dysregulation of common molecular pathways will be found across the various autoimmune diseases. However, the mechanisms actually driving the autoimmune reactions remain elusive, and there are currently no validated biomarkers for disease activity or assessment of organ-specific risk.

2.3 The Interferon-Inducible p200 (IFI-200) Family of Proteins

Upon binding to specific receptors, type I IFN lead to the activation of signal transduction pathways that activate a broad range of ISGs that are responsible for the antiviral, antiproliferative, pro-apoptotic, and immunomodulatory activities of type I IFN. One family of IFN-inducible genes is the HIN-200/Ifi-200 gene family, which encodes evolutionary related human (IFI16, IFIX, MNDA, and AIM2) and murine (Ifi202a, Ifi202b, Ifi203, Ifi204, Ifi205/D3, and Ifi206) proteins [33]. The human and murine gene clusters are located on syntenic genomic regions of chromosome 1 and probably stem from repeated gene duplications of one ancestral gene. The HIN-200 proteins contain at least a 200-amino acid repeat that constitutes the HIN domain, which is always near the C-terminus. The common domain architecture PYD-HIN of these protein families consists of one or two copies of the HIN domain (domains A and B) and an N-terminal PYD domain, also named PAAD, DAPIN, or Pyrin, a member of the death domain superfamily [34, 35]. The PYD domain, commonly found in cell death-associated proteins such as Pyrin, ASC, and zebrafish caspase, is present in the N-terminus of most Ifi200/HIN200 proteins, suggesting a role of these proteins in inflammation and apoptosis [36-38].

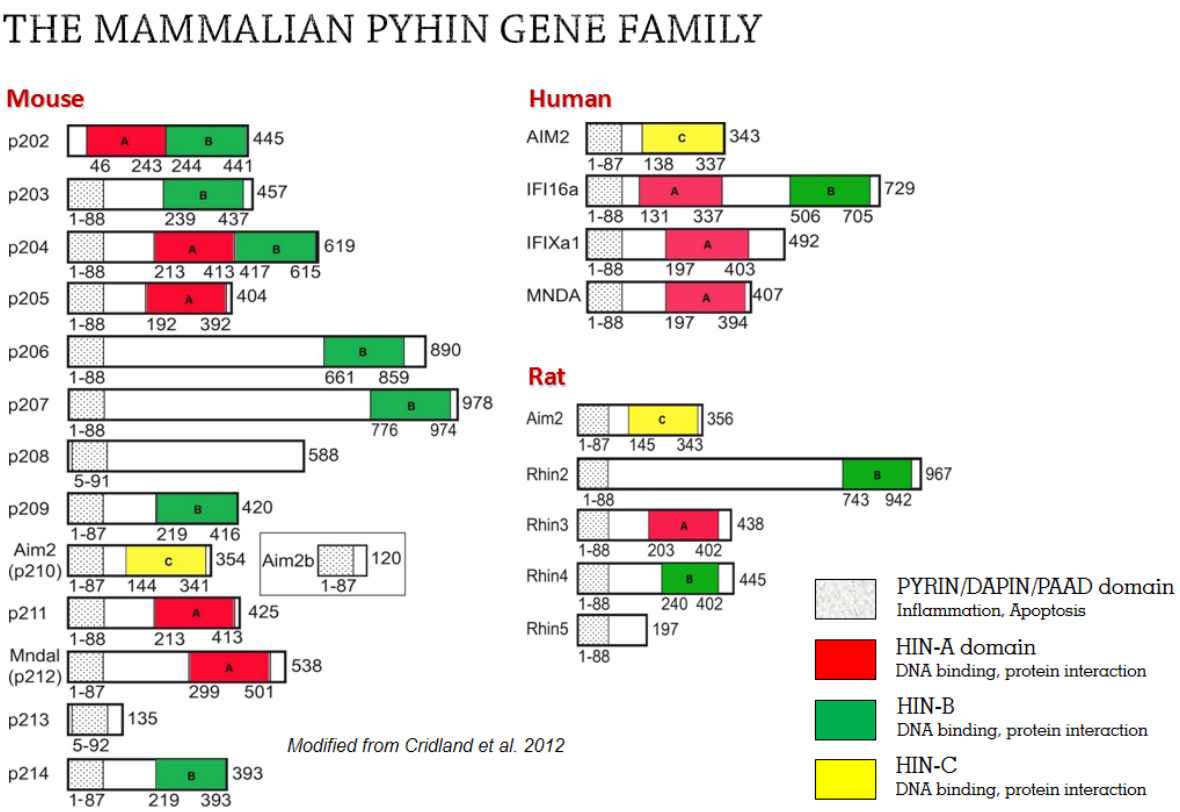

Figure 3: The Mammalian PHYIN Gene Family – Domain Architecture

2.4 The Interferon Inducible 16 (IFI16) Protein

In the human IFI16 protein, the PYD domain is followed by two copies of a HIN domain (A and B respectively). These are separated by a serine-threonine-proline (S/T/P)-rich spacer region. The size of the spacer region is regulated by mRNA splicing and can contain one, two, or three copies of the highly conserved 56-aa S/T/P domain, giving rise to the isotypic variants IFI16a, IFI16b, and IFI16c respectively. A comprehensive bioinformatics analysis revealed the presence of 2 oligonucleotide/oligosaccharide binding (OB) folds in each HIN domain [39] and biophysical approaches demonstrated that the A and B domains of all family members, including IFI16, have been implicated in mediating oligonucleotide and oligosaccharide binding, protein-protein interactions and dimerization [40].

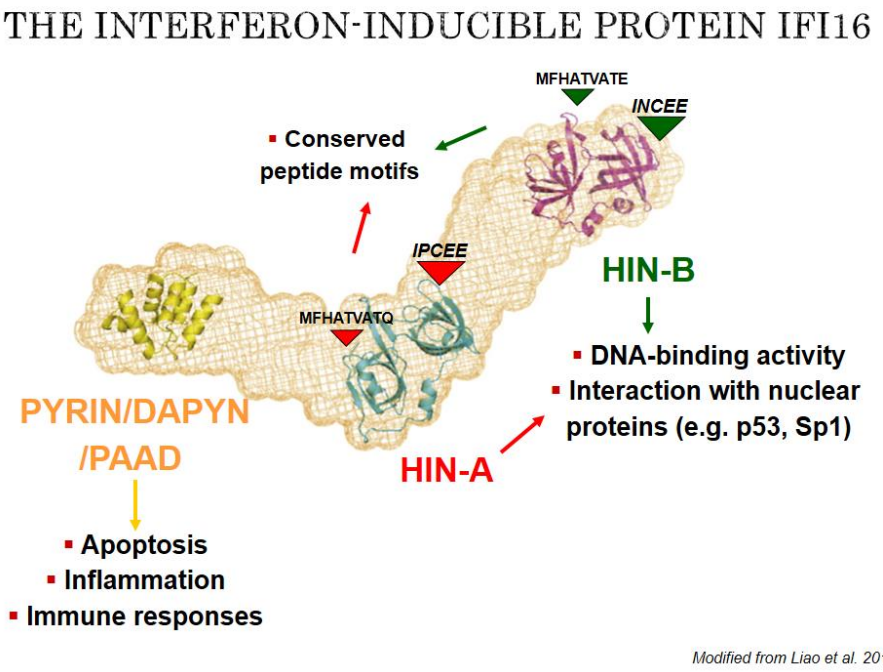

Figure 4: Predicted molecular arrangement of the Interferon Inducible 16 (IFI16) protein

For example, AIM2 binds dsDNA through its C-terminal oligonucleotide- or oligosaccharide binding domain (HIN200 domain), recruits ASC, and triggers inflammasome assembly and pro- IL-1b cleavage [41, 42]. More recently, it was demonstrated that following the stimulation of cells with transfected DNA, IFI16 binds to IFN-β stimulated viral DNA and recruits STING. Furthermore, small interfering RNA (siRNA) targeted against IFI16 inhibited DNA-induced, but not RNA-induced, activation of IRF3 and NF-kB, as well as IFN-β induction [43]. Altogether, these results demonstrate that PYD-HIN-200 proteins represent a new family of innate DNA sensors regulating the early steps of inflammation. The IFI16 nuclear phosphoprotein has been demonstrated to recognize foreign DNA and participates in the inhibition of cell cycle progression, modulation of differentiation, and cell survival [33].

Figure.5. Schematic diagram indicating the main signaling pathways triggered by IFI16 to regulate different cell functions

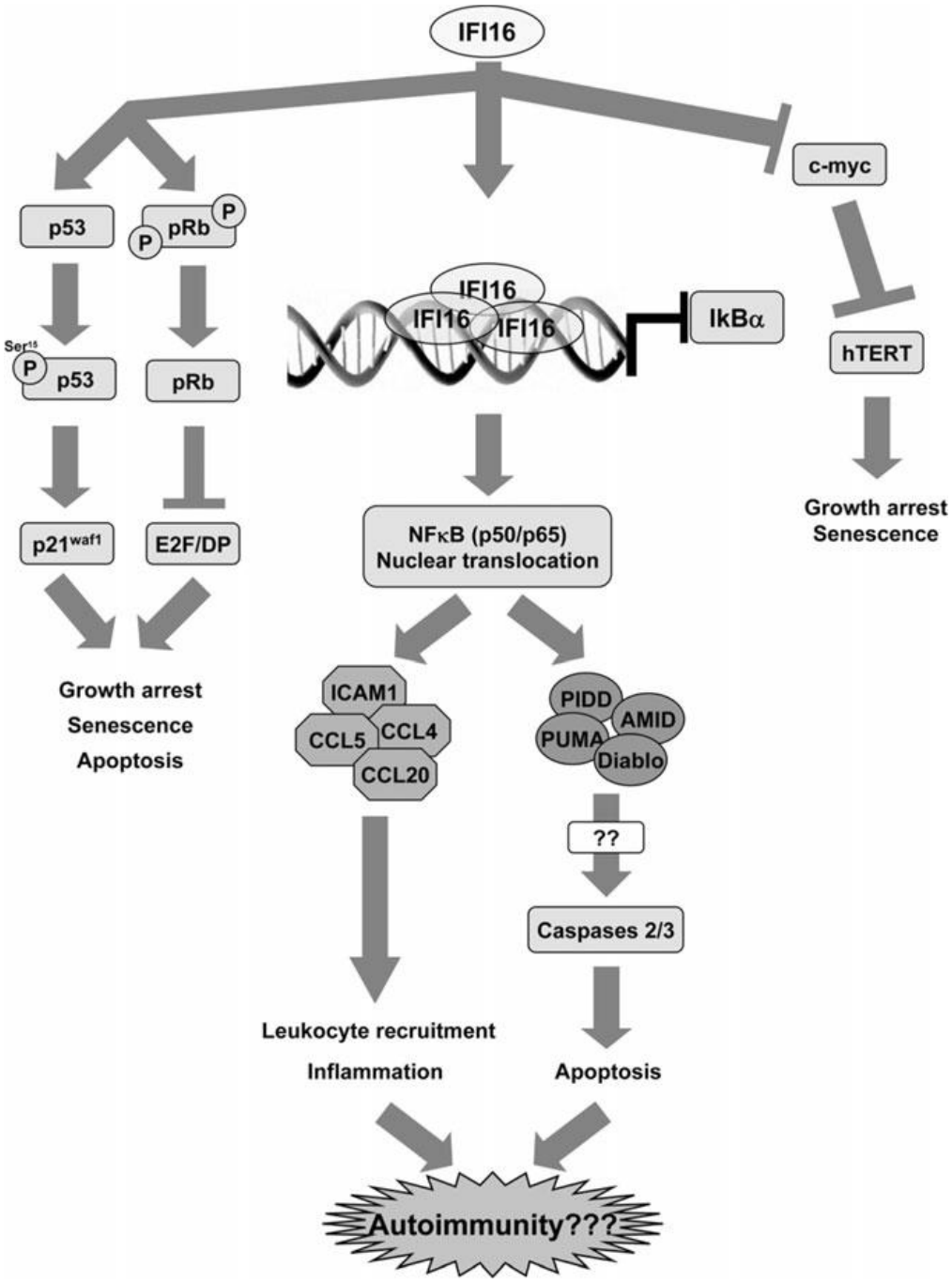

IFI16 was originally identified as a target of interferons (IFN-α/β and -γ), however additional triggers have recently been reported that include oxidative stress, cell density, and various pro-inflammatory cytokines [44]. IFI16 is expressed in hematopoietic cells and in vascular endothelial cells (EC) in blood and lymph vessels, suggesting a link between IFI16, angiogenesis and inflammation [3]. In the

skin, its expression is normally restricted to the basal proliferative layer, suggesting a possible role in the control of skin homeostasis. IFI16 has also been detected in normal salivary glands.

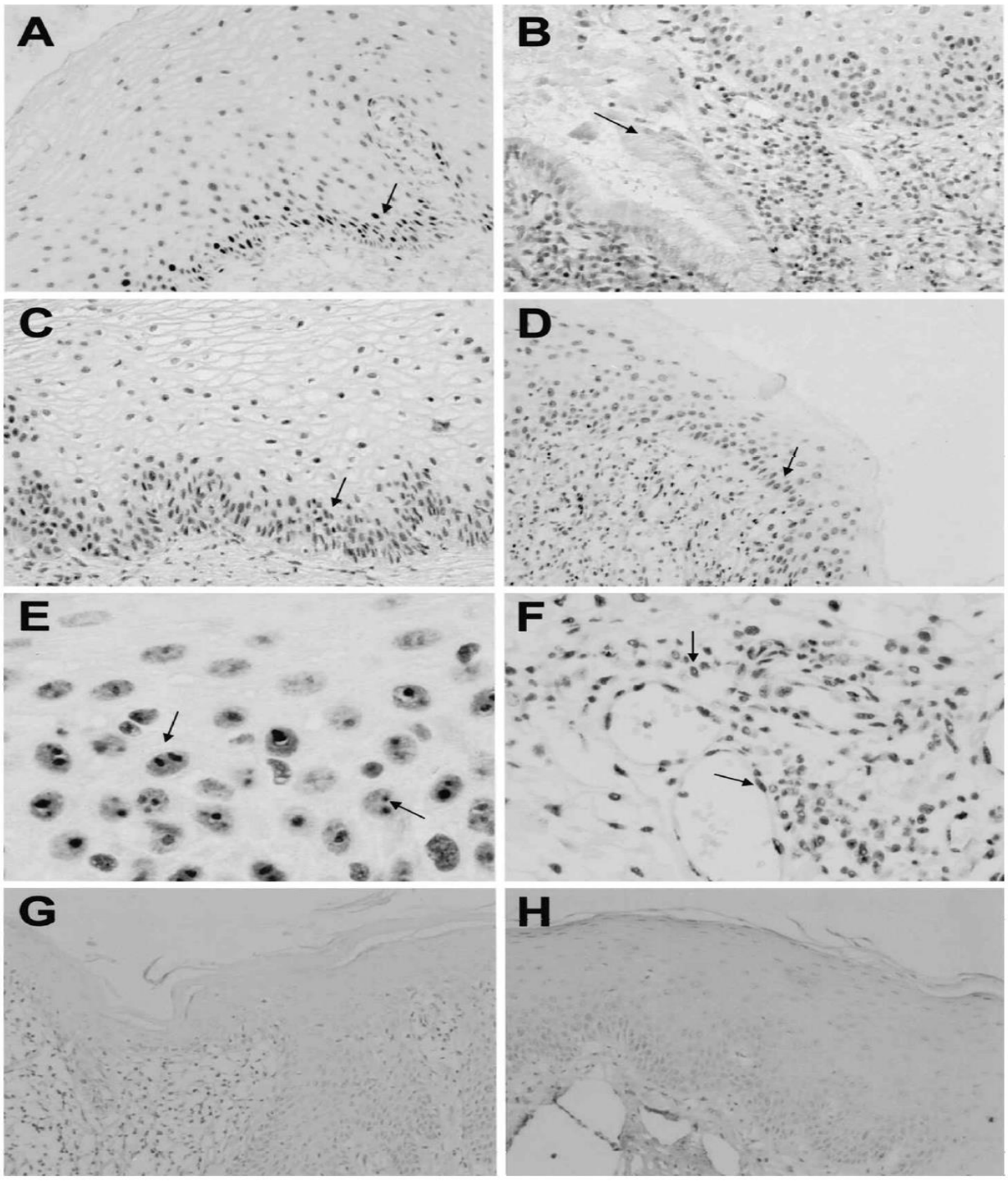

Figure 6. Immunohistochemical detection of IFI16 protein in normal human tissues. (**A**) Exocervix. (**B**) Exo-endocervix junction. The epithelial cells lining the exocervix are positive, but those lining the endocervix are not (arrow). Notice that the inflammatory cells strongly expressed IFI16. Nuclei of cells not expressing IFI16 are stained blue by counterstain. (**C**) Vocal cord epithelium. (**D**) Skin. (**E**) High-power field of IFI16-positive cells showing nucleolar staining (arrow). (**F**) Strong IFI16 immunoreactivity in stromal reactive (upper arrow) and endothelial cells (lower arrow). (**G**) Skin stained with preimmune serum. (**H**) Vocal cord epithelium stained with preimmune serum. Arrows in **A, C, D** indicate IFI16-positive cells. **A, B, C, D, G, H,** 310. **E,** 340. **F,** 320 [3].

Enhanced expression levels of IFI16 were found by the proposing group in the epidermis of SLE and SSc patients and in the dermal inflammatory infiltrate obtained from patient skin lesions, detected by immunohistochemistry [32]. While IFI16 expression is restricted to the basal layer in the normal epidermis from healthy subjects, it is greatly increased and ubiquitously expressed in all layers of the epidermis in the lesional skin from both SSc (either the limited [lc-] or the diffuse [dc-] cutaneous variant) and SLE patients. Furthermore, the dermal inflammatory infiltrate shows IFI16 positive staining, indicating that the protein is expressed at a high level in lymphocytes, reactive fibroblasts, and EC. This finding raises the possibility that local tissue expression of IFI16 (or even its de-localization) in epithelial and inflammatory cells can play a role in triggering an autoimmune response against this protein. In line with the potential role of IFI16 in these autoimmune diseases, lymphocytes as well as fibroblasts and EC can be targets for

autoimmune responses in SLE and SSc, while skin is one of the main tissue targets for the clinical manifestations in these patients.

Molecular studies performed in primary endothelial cells overexpressing IFI16 demonstrated that it may be involved in the early steps of inflammation by modulating endothelial cell function, such as expression of adhesion molecules and chemokine production, cell growth, and apoptosis. Moreover, as previously demonstrated that IFI16 expression is induced by proinflammatory cytokines in primary endothelial cells [32].

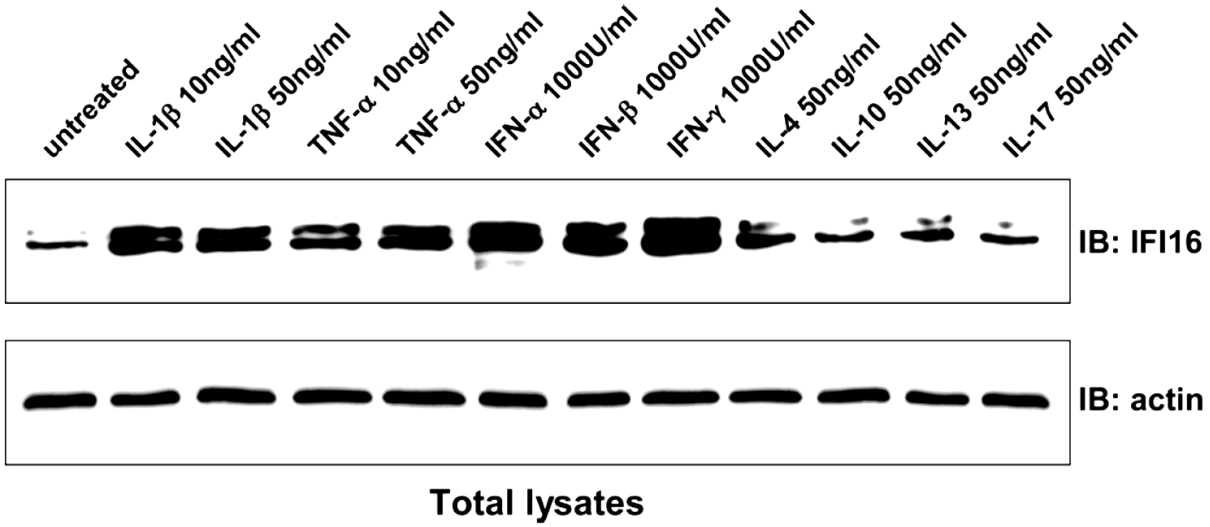

Figure 7: Modulation of IFI16 protein levels by cytokines in primary human endothelial cells.

On the other hand, overexpression of nuclear IFI16 protein seems to induce pro-inflammatory molecules in endothelial cells which indicates the cytokine promoting activity of endogenous nuclear IFI16 [45]. Such overexpressed IFI16 protein upregulates the production of adhesion molecules like ICAM1, VCAM1 and other chemokines like IL-8, MCP1, as shown in the Fig. 8.

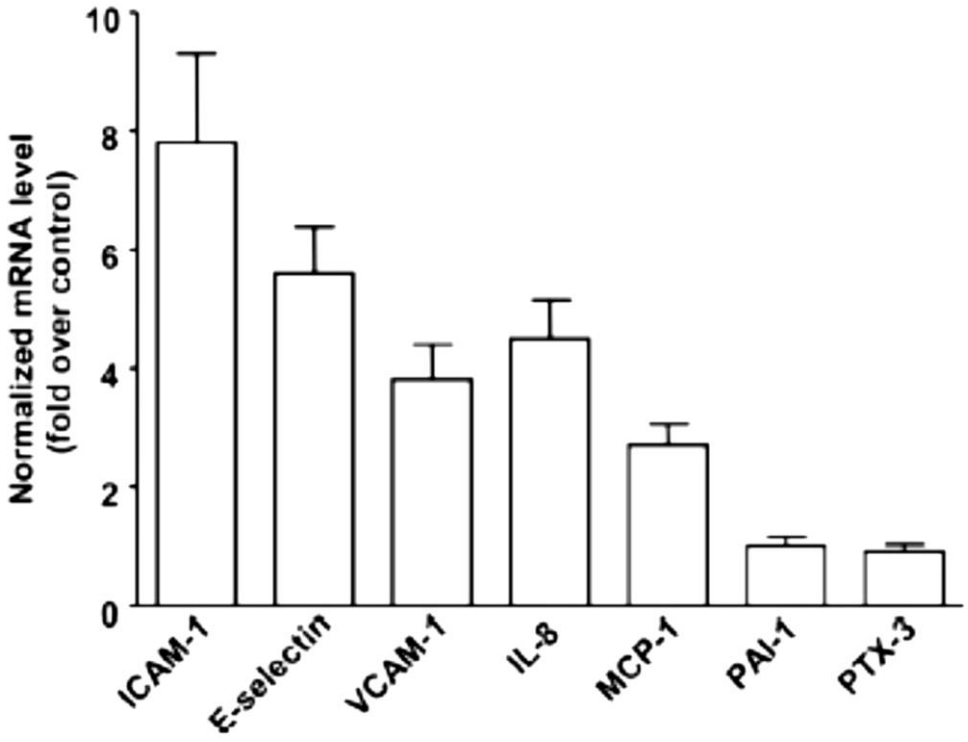

Figure 8: Real time PCR analysis of AdVIFI16-infected HUVEC

IFI16 has been much implicated on its role in inflammasome signaling. The group [43] demonstrates that IFI16 is critical for interferon-β responses upon exposure to intracellular cytoplasmic DNA and HSV-1 infection. Furthermore, IFI16 was shown to directly associate with IFN-β-inducing viral DNA motifs and the stimulator of interferon genes (STING). Early studies were unsuccessful in attempts to implicate IFI16 in the inflammasome. Specifically, an interaction between ASC and IFI16 was not found [46]. Light was shed on this in a study by [47], demonstrating that infection of endothelial cells with Kaposi sarcoma-associated herpesvirus (KSHV) led to the activation of an ASC-containing inflammasome, with a concomitant proteolytic processing of pro-IL-1β that was shown to be dependent on IFI16. In addition, the nuclear localization of pro-caspase-1 and ASC prior to infection was demonstrated. Cleaved caspase-1 (p20) and ASC were also shown to

be in the nucleus at early timepoints of infection followed by the movement of both to the cytoplasm at later times of infection with KSHV. Furthermore, by using short hairpin RNAs (shRNAs) targeting IFI16 or ASC, they demonstrated that both were required for KSHV induced processing of caspase-1 (Figure 9) [47]. IFI16 was found to be required for the induction of pro-IL-1β and IL-6 in response to HSV-1, highlighting a role for IFI16 in both transcriptional activation as well as the inflammasome [43].

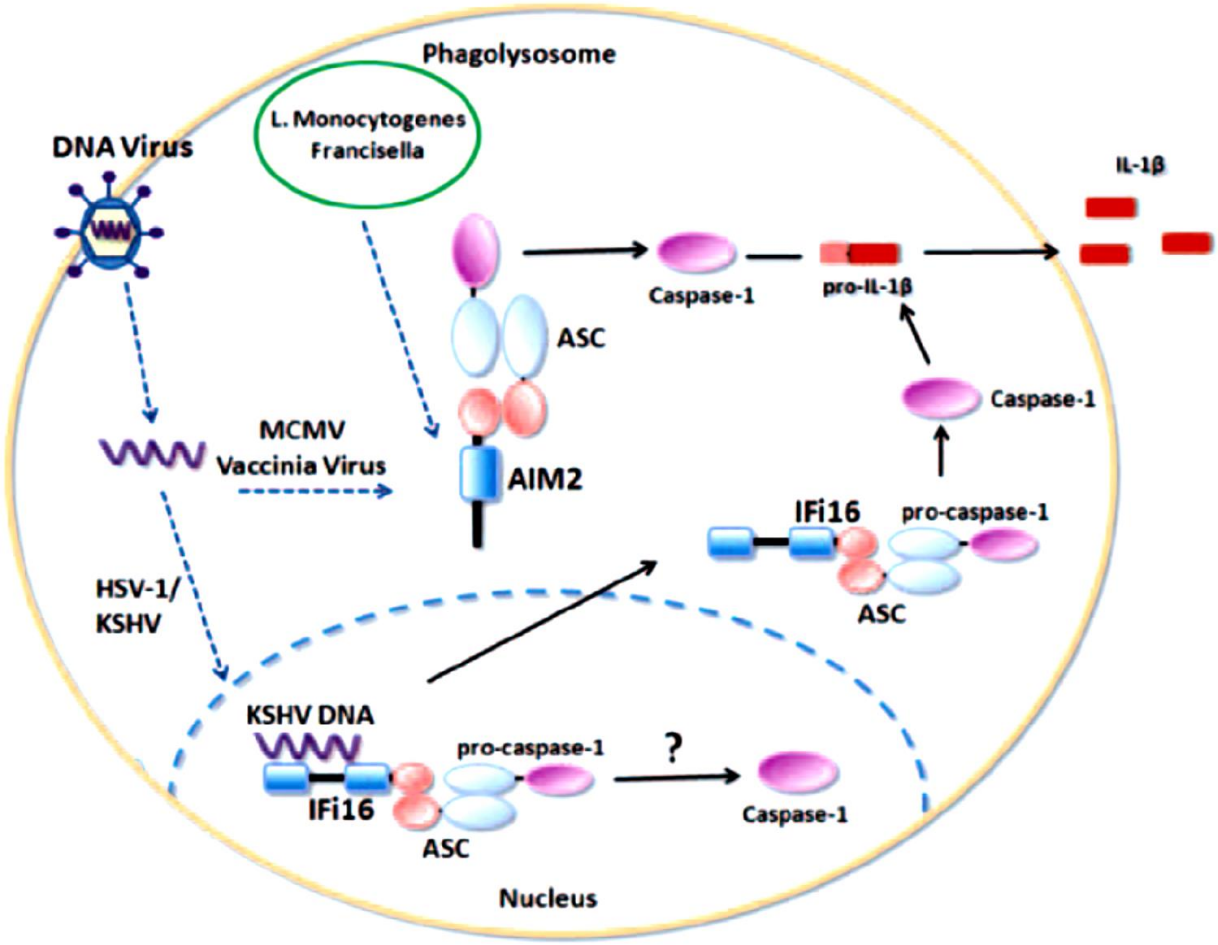

Figure 9: Schematic representation of AIM2 and IFI16 inflammasome activation [1]

UVB is a well-known stimulus capable of inducing apoptosis in vitro and in vivo, and it has been associated with lupus flares [48, 49]. Aberrant IFI16 expression in endothelial cells and epithelial cells from the skin, both of which exhibit the main clinical manifestations of autoimmune diseases, indicates that IFI16 may be involved in the early steps of inflammation by modulating endothelial and keratinocyte cell function. To verify whether the induction of autoimmunity against IFI16 could indeed involve the redistribution of this nuclear protein in keratinocytes following an apoptotic stimulus like UVB, an in vitro model was developed in the laboratory of the applicant consisting of keratinocyte monolayers and human skin explants to investigate the fate of IFI16 following their irradiation with UVB [2]. In parallel, IFI16 expression and localization were analyzed in diseased skin sections from SLE patients. The results obtained clearly demonstrated that IFI16, normally restricted in the nucleus, could be induced to appear in the cytoplasm under conditions of UVB-induced cell injury. This nucleus to cytoplasm translocation was also observed in skin explants exposed to UVB and in the skin lesions from SLE patients not exposed to UVB irradiation. In addition, IFI16 was found in the supernatants of UVB-exposed keratinocytes.

Figure 10. **IFI16 redistribution in ultraviolet (UV) B-irradiated human skin ex vivo**. After 24 h in culture medium, explants were UVB irradiated at 1000 J m^{-2} then harvested at 24 h (a) and 48 h (b) post-UVB treatment and processed for haematoxylin and eosin staining (H ⁄E) and immunohistochemical staining of IFI16 (blue); no counterstaining method was used. Arrows indicate pyknotic nuclei and hypereosinophilic cytoplasm (sunburn cells). Representative images were taken using 40· magnification. NT, not treated [2].

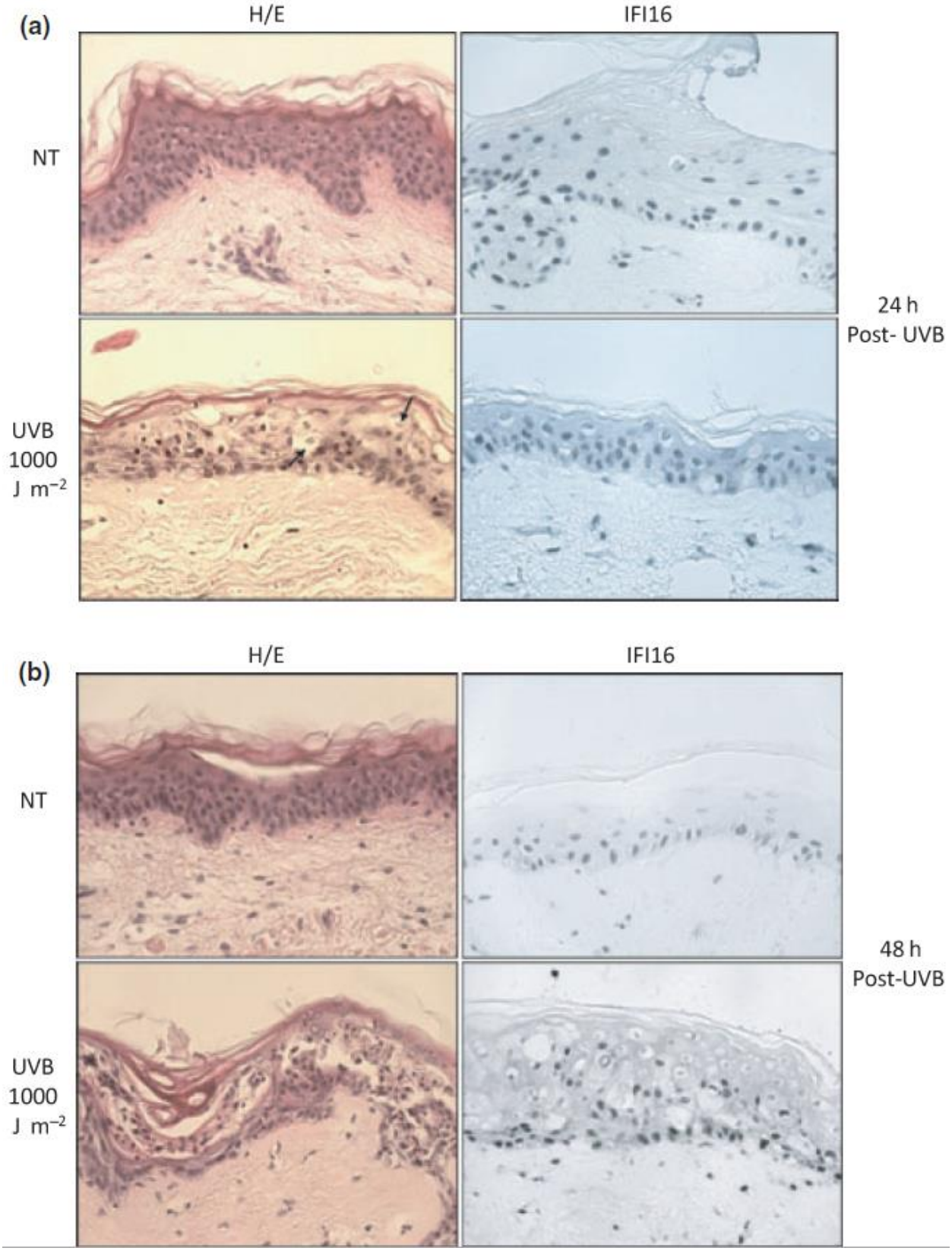
(a)
H/E
IFI16
NT
UVB
1000
J m−2
24 h
Post- UVB
(b)
H/E
IFI16
NT
UVB
1000
J m−2
48 h
Post-UVB

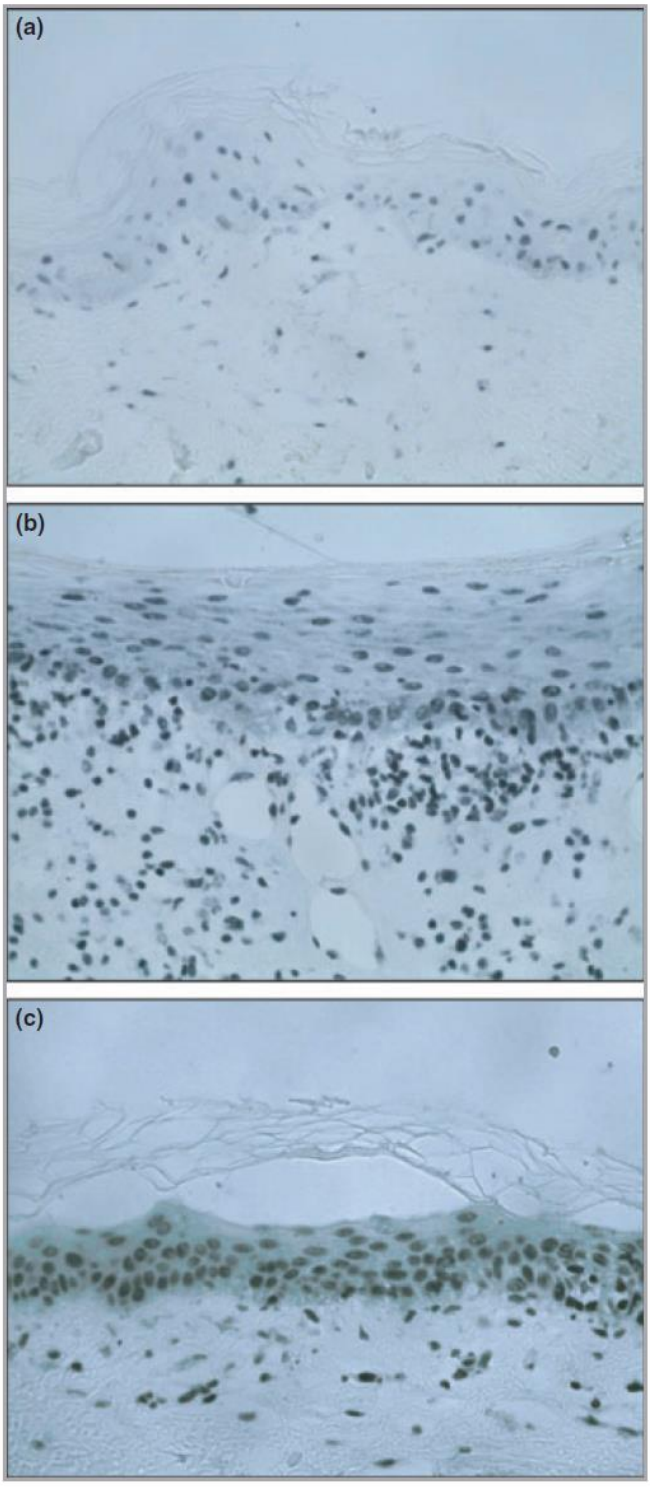

Figure 11. **Localization of IFI16 in systemic lupus erythematosus (SLE) skin lesions**. Sections of two representative SLE skin lesions stained with anti-IFI16 antibodies and visualized with SG substrate (blue; Vector Labs, Burlingame, CA, U.S.A.) are shown in panels (b) and (c). Normal skin processed in the same way is shown in panel (a) [2].

In conclusion, we hypothesize that IFI16 overexpression and its subsequent extranuclear appearance during the process of cell death contribute to the pathogenic mechanism through the following steps: i) induction of inflammatory

response in the target cells; ii) release into the extracellular milieu and induction of specific autoimmunity; and iii) triggering of proinflammatory activity via the release of extracellular free IFI16 protein.

2.5 IFI16 AS VIRAL RESTRICTION FACTOR FOR HCMV REPLICATION

IFI16 has been shown to bind to and function as a pattern recognition receptor (PRR) of virus-derived intracellular DNA, and trigger the expression of antiviral cytokines via the STING-TBK1-IRF3 signaling pathway [43, 47, 50-59]. Although many different functions have been ascribed to IFI16 (and to other proteins of the PYHIN family), its role as an antiviral restriction factor has not yet been fully described. Recent studies implicate the involvement of IFI16 in host defense against HCMV [60]. The evidence supporting such a role of IFI16 is as follows: (i) small interfering RNA (siRNA)-mediated depletion of IFI16 in primary human

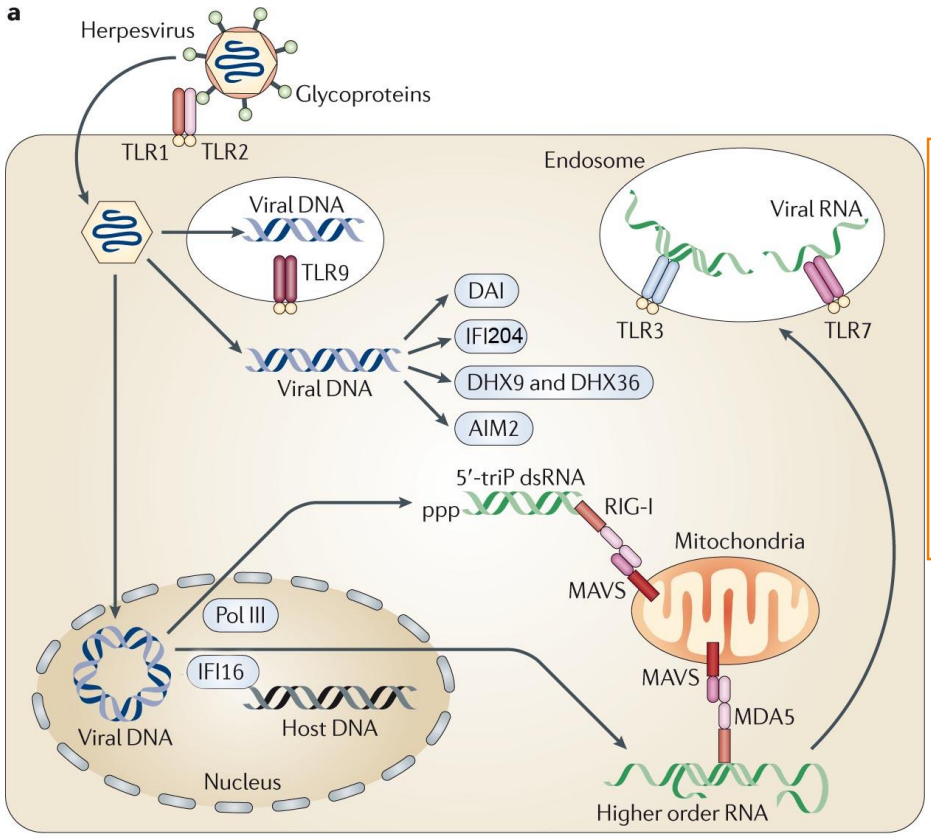

Figure 12: Innate/intrinsic immune recognition and activation by herpes viruses.

[5]

embryonic lung fibroblasts (HELF) significantly increases HCMV replication efficiency as a result of augmented viral DNA synthesis; (ii) similarly, viral plaque formation is enhanced in the presence of an exogenous dominant-negative IFI16 mutant that competes with the endogenous IFI16; (iii) overexpression of functional IFI16 in HCMV-infected HELFs decreases both virus yield and viral DNA copy number; and (iv) early and late, but not immediate-early viral mRNAs and proteins are strongly down-regulated under these same conditions, suggesting that IFI16 exerts its main antiviral effect at the level of viral genome synthesis. This unique defense mechanism distinguishes the activity of IFI16 from that described for ND10.

In more general terms, human viruses have to face powerful RF responses and thus have evolved a number of strategies to overcome RF attack. Viral antagonists can act through highly specialized mechanisms, such as coupling RFs to protein degradation pathways, causing their relocalization and thus down-regulating their functionality, or even by mimicking RF substrates [61]. In the case of HCMV, viral regulatory proteins (such as IE1p72, pp71, and others) mediate an efficient evasion from the antiviral state instituted by ND10, either by means of proteasomal degradation or by disrupting the host's subnuclear structure [62, 63].

In this study (second author manuscript attached), we investigated the mechanisms used by HCMV to evade IFI16 restriction activity. We observed that starting from 72-96 hours post-infection (hpi), nuclear levels of IFI16 protein started to decrease in the nucleus and gradually increased in the cytoplasm of infected cells where it relocalized to the virus assembly complex (AC), as shown by its co-localization with the viral structural proteins gB and pp65. Finally, through the use of immunogold electron microscopy and co-precipitation experiments, we

provide evidence indicating that IFI16 eventually transits into the maturing virions embedded in the outer tegument layer. In conclusion, these data suggest that in order to overcome the restriction activity of IFI16, HCMV may stimulate its subcellular relocalization from the nucleus to the viral AC, followed by its inclusion into mature virions.

3 AIMS OF THE RESEARCH

Collectively, present data and other findings suggest the following disease model: 1) IFI16 expression is enhanced in lesional tissues as a result of abnormal type I IFN production (either endogenously produced or exogenously administered) and/or other proinflammatory stimuli, including UVB; 2) IFI16 expression triggers proinflammatory activation of endothelial cells and keratinocytes; 3) sustained IFI16 overexpression impairs cell growth and viability; 4) IFI16 is then released as a consequence of increased cell death by apoptosis/necrosis; 5) the released IFI16 protein leads to a breakdown in tolerance to self-antigens and the injury of target cells (endothelial cells and keratinocytes); 6) circulating levels of free IFI16 directly damage endothelia (via the suppression of capillary formation), skin epithelia (via the suppression of stratified epithelium formation), and glandular epithelia (via the impairment of glandular physiology), thus amplifying the inflammatory process through local tissue destruction; 7) this loss of tolerance favors the generation of specific anti-IFI16 autoantibodies that may, paradoxically, exert protective activity by inhibiting the extracellular protein from binding to its specific receptors.

To prove this disease model, the proposed research project will be developed as follows:

Aim 1: In vivo studies to analyze the presence of IFI16 in the sera of systemic autoimmune patients and co-relate its occurrence with disease condition and other types of non-autoimmune diseases like non-SLE glomerulonephritis.

Aim 2: In vitro studies aimed at elucidating the molecular actions of extracellular IFI16 on different primary endothelial cell lines. These studies will be grouped into: i) definition of the mechanisms by which extracellular IFI16, released upon cell

death, interacts with target cells (endothelial and epithelial cells), and ii) the clarification of the IFI16 receptor-stimulated molecular pathways that lead to cell damage and death. The outcome of these experiments will help us to understand the pathogenesis of the vasculopathy and the skin lesions that accompany autoimmune diseases, such as SLE, SSc, and SjS.

4 MATERIALS AND METHODS

4.1 CELL CULTURES

Primary human umbilical vein endothelial cells (HUVECs), pooled from multiple donors, cryopreserved at the end of the primary culture [64], were grown on 0.2% gelatin (Sigma-Aldrich, Milan, Italy) coated base in the presence of endothelial growth medium (EGM-2, Lonza-Milan) containing 2% fetal bovine serum, human recombinant vascular endothelial growth factor (rVEGF), basic fibroblast growth factor, human epidermal growth factor, IGF-1, hydrocortisone, ascorbic acid, heparin, gentamycin, amphotericin B including 1% Penicillin-Streptomycin solution (Sigma-Aldrich, Milan, Italy) which we describe as complete EGM-2. Low passage human dermal fibroblasts, HDF (ATCC), mouse fibroblasts, 3T3 (ATCC), HeLa (ATCC) and HaCaT (ATCC) cells were grown in Dulbecco's modified Eagle's medium (DMEM) (Sigma-Aldrich, Milan, Italy) supplemented with 10% fetal bovine serum and 2% Penicillin-Streptomycin solution Unless specified, all cells were grown at 37°C and 5% CO2.

4.2 RECOMBINANT PROTEINS

The entire coding sequence of the b isoform of human IFI16 was subcloned into the pET30a expression vector (Novagen, Madison, WI) containing an N-terminal histidine tag. Protein Expression and affinity purification, followed by fast protein liquid chromatography (FPLC), were performed according to standard procedures. The purity of the proteins was assessed by 10% sodium dodecyl sulfate-polyacrylamide gel electrophoresis. The FPLC purified protein was then processed with Toxin Eraser™ Endotoxin Removal Kit (Genscript, USA), while the LPS concentration of the processed product was measured using Toxin Sensor™

Chromogenic LAL Endotoxin Assay Kit which was as low as 0.005 EU/ml. the final purified rIFI16 was stored at -80°C in endotoxin free vials. As negative controls in enzyme-linked immunosorbent assays (ELISA), the polypeptide encoded by the pET30a empty vector (control peptide) was expressed and purified according to the same protocol.

4.3 PATIENTS AND DETERMINATION OF HUMAN EXTRACELLULAR IFI16 BY CAPTURE ELISA

The study groups comprised patients suffering from Systemic Sclerosis, (n = 50), Systemic Lupus Erythematosus, (n = 100), Sjogren Syndrome, (n = 49), Rheumatoid Arthritis (n = 50) and Non-SLE Glomerulonephritis (n = 46). As controls, we investigated sera from 116 sex- and age-matched healthy subjects. Written informed consent was obtained from all subjects according to the Declaration of Helsinki and approval was obtained from local ethics committees of corresponding hospital.

For the determination of circulating extracellular IFI16, a capture ELISA was employed. Briefly, polystyrene micro-well plates (Nunc-Immuno MaxiSorp; Nunc, Roskilde, Denmark) were coated with a home-made polyclonal rabbit-anti-IFI16 antibody (478-729 aa). Subsequently, plates were washed and free binding sites then saturated with PBS / 0.05% Tween / 3% BSA. After blocking, sera were added to plates in duplicate. Purified 6His-IFI16 protein was used as the standard and BSA served as the negative control. The samples were washed, monoclonal mouse anti-IFI16 antibody (Santa Cruz, sc-8023) added, and then incubated for 1h at room temperature. After washing, horseradish peroxidase-conjugated anti-mouse antibody (GE Healthcare Europe GmbH, Milan, Italy) was added. Following the addition of the substrate (TMB; KPL, Gaithersburg, MD, USA), absorbance was

measured at 450nm using a microplate reader (TECAN, Mannedorf, Switzerland). Concentrations of extracellular IFI16 were determined using a standard curve for which increasing concentrations of purified 6His-IFI16 were used.

4.4 Cell Viability Assay

Cells were seeded at a density of 1×10^4/well in a 96-well culture plate. After 24 hours, cells were treated with different doses (10, 25 or 50µg/ml) of recombinant IFI16 protein (IFI16), mock-treated using the same volume of vehicle as each IFI16 dose (Mock), or left untreated (NT). Where indicated, different doses (1.75µgr or 3.5µgr) of antibody against IFI16 were added. Forty-eight hours after treatment, cell viability was determined using the 3-(4,5-dimethylthiazol-2-yl)-2,5-diphenyltetrazolium bromide (MTT) (Sigma-Aldrich, Milan, Italy) method, as previously described [65].

4.5 Tube morphogenesis assay

HUVEC were seeded in complete medium in 60-mm culture dishes coated with 0.2% gelatin (Sigma-Aldrich, Milan, Italy) and were treated for 48h with different doses (10 or 25µg/ml) of recombinant IFI16 protein (IFI16). As negative controls, cells were treated with the same volumes of vehicle (Mock) used for each IFI16 dose or left untreated (NT). Where indicated, different doses (1.75µgr or 3.5µgr) of antibody against IFI16 were added. Tube morphogenesis assay was performed as described in [66]. Briefly, a 24-microwell plate, pre-chilled at -20°C, was coated with 250µl/well of Matrigel Basement Membrane (5mg/ml; Becton and Dickinson, Milan, Italy) and then incubated at 37°C for 30 min until solidified. HUVEC (8×10^4 cells/500µl per well) were seeded onto the matrix and allowed to

incubate at 37°C in 5% CO_2. Plates were photographed after 6h using a Leica inverted microscope.

4.6 Migration Assay

Twenty-four well transwell inserts with an 8µm pore size (Corning B.V. Life Sciences, Amsterdam, The Netherlands) were coated with a thin layer of gelatin (0.2%). HUVECs cultured in EGM-2 with 2% FBS and pre-treated with different concentrations of IFI16 recombinant protein or mock- or untreated for 48 hours were washed twice with PBS, trypsinized and plated into the upper chambers (4×105 cells) resuspended in 200µl of EBM-2 (Lonza, Italy), 0.1% BSA (Sigma-Aldrich, Milan, Italy) plus IFI16 recombinant protein or mock solution (the same amounts as in the 48h pre-treatment). The lower chambers were filled with 600µl EGM2 containing VEGF and bFGF (as chemo-attractants) (Sigma-Aldrich, Milan, Italy), 2% FBS, and IFI16 recombinant protein or mock solution (the same amounts as in the upper chamber). The chambers were incubated for 5h at 37°C in a humidified atmosphere containing 5% CO2. After incubation, cells on the upper side of the filter were removed. The cells that had migrated to the lower side of the filter were washed twice with PBS, fixed with 2.5% glutaraldehyde (Sigma-Aldrich, Milan, Italy) for 20 min at room temperature, and stained with 0.5ml crystal violet (0.1% in 20% methyl alcohol solution) (Sigma-Aldrich, Milan, Italy). After washes, color was developed in 10% acetic acid and read in duplicate at 540nm on a microplate reader (Victor 3; Perkin-Elmer, Boston, MA).

4.7 rIFI16-FITC membrane binding and Confocal Microscopy

HUVEC were seeded in 24-well plate in the presence of glass cover-slip and were grown overnight in presence of 1 µg/ml tunicamycin (Sigma-Aldrich, Milan,

Italy) in EGM-2 medium with 2% FBS and antibiotics. The cells were washed twice with cold PBS and incubated with increasing concentrations (10nM, 20nM, 30nM) of FITC labeled rIFI16 (FluoReporter® FITC Protein Labeling Kit by Invitrogen) for 90 minutes at 4°C. Later the cells were washed twice with cold PBS and were fixed using 2% para-formaldehyde solution for 4 minutes. The PBS wash was repeated thrice and the coverslips were mounted on glass slides using ProLong® Gold Antifade Reagent by Invitrogen. The slides were observed using Leica Confocal Microscope at 490nm excitation wavelength for FITC in one channel while trans-illuminated light in the other.

4.8 Co-Culturing and Immunofluorescence

Co-culturing was performed with HeLa cells and HUVEC, as described in Koristka S. et.al [67]. 105 HeLa cells were seeded in 24 well-plate coated with 0.2% Gelatin in the presence of glass cover-slip and grown over-night in DMEM with 10% FCS at 37°C, 5% CO2. The cells were washed, suspended in PBS and lethally irradiated with UV-B lamp (HD 9021; Delta Ohm S.r.l., Padova, Italy). The dosage of 1000 Wm2 was counted using a UVB irradiance meter cosine corrector with spectral range of 280–319 nm (LP 9021 RAD; Delta Ohm). Followed by this, 5×104 HUVEC were added in the same well, grown in EGM-2 with 2% FCS until ready. Immunofluorescence was performed after 24hr, 36hr and 48hr using a home-made anti-IFI16 polyclonal as primary antibody and Alexa488- anti-rabbit (GE Healthcare) as secondary antibody. The cells were then fixed with 2% para-formaldehyde (Sigma-Aldrich, Milan, Italy), permeabilized with 0.2% Triton X-100 (Sigma-Aldrich, Milan, Italy) and nuclear stained with 1µg/ml propidium iodide (Sigma-Aldrich, Milan, Italy). The coverslips were mounted on glass slides using ProLong® Gold

Antifade Reagent by Invitrogen and the cells were observed by Leica confocal microscope.

4.9 RADIO-IODINATION OF RIFI16 AND BINDING ASSAYS

Iodination Beads were purchased from Thermo Fischer Scientific Inc. (Rockford, IL, USA) and used according to manufacturer's instructions. Briefly, two dry beads were washed with rIFI16 elution buffer (50mM HEPES pH 7.5; 1M NaCl) (Sigma-Aldrich, Milan, Italy), soaked dry and was incubated for 5 minutes with the solution of carrier-free 2mCi Na125I (Perkin Elmer Italia, Milan, Italy) and diluted in elution buffer. Later 200µg of rIFI16 was added and incubated for 15 minutes. The labeling reaction was passed through Zeba Spin Desalting Columns (Thermo Fischer Scientific Inc.) to remove excess $Na^{125}I$ or unincorporated ^{125}I from the iodinated protein. The concentration of the final radioiodinated [^{125}I]-rIFI16 was calculated using the following formula, where 'C' is the cpm counted, 'V' is volume of solution counted in ml and 'Y' is the specific activity of the radioligand in cpm/fmol.

Concentration of [^{125}I]-rIFI16 in (pM) = ['C'cpm / 'Y'cpm/fmol] / 'V'ml.

Binding assay was performed as described in [68, 69], 105 cells/well were seeded and attached in a 24-well plate with. Once ready, the medium was removed and the cells were washed with PBS. Further they were re-suspended with increasing concentrations of [^{125}I]-rIFI16 (1-32nM) within different wells in the presence of 200nM unlabeled rIFI16 for Non-Specific Binding. Separately, other wells were re-suspended with [^{125}I]-rIFI16 (1-32nM) without any unlabeled rIFI16 for total binding. The incubation was performed at 4°C for 90 minutes. Later, the cells were washed with PBS to remove any loosely bound ligand and were then suspended in warm 1% SDS (Sigma-Aldrich, Milan, Italy) for 5 minutes. The SDS lysate of the cells was then measured on Cobra II Series Auto-Gamma Counter. All

the experiments were carried out in triplicates and the data was analyzed using non-linear regression equations from GraphPad Prism with 95% confidence intervals.

4.10 Competition and Inhibition of [^{125}I]-rIFI16 binding

For binding competition experiments, cells were seeded into 96-well plates at a density of 10^4 cells/well. The medium was removed and cells were washed with PBS. HUVEC were then incubated at 4°C for 90 minutes with unlabeled rIFI16 (10-1000nM) in the presence of 10nM [^{125}I]-rIFI16. Binding inhibition was carried out overnight by incubating 10nM [^{125}I]-rIFI16 with varying concentrations (10-1000nM) of anti-IFI16 polyclonal N-terminal (1-205 aa) or C-terminal (478-729 aa) antibodies at 4°C. This mixture was then added to 10^4 HUVEC and incubated for 90 minutes at 4°C. The loosely bound ligand was removed by washing twice with PBS, and cells were then detached using warm 1% SDS and the levels of [^{125}I]-rIFI16-binding to HUVEC assessed using a Cobra II Series Auto-Gamma Counter. The data were analyzed using non-linear regression equations in GraphPad Prism under 95% confidence intervals.

4.11 Nf-κB Immunofluorescence

Immunofluorescence was performed after 0 hr, 24 hr and 48 hr of rIFI16 treatment using 1:1000 Nf-κB p65 monoclonal antibody (F-6) sc-8008 (Santa Cruz Biotechnology, Inc., USA) as primary and 1:500 Alexa488-anti-mouse (GE Healthcare) as secondary antibody. Briefly, after treatment the cells were fixed with 2% paraformaldehyde (Sigma-Aldrich, Milan, Italy) for 20 min at 4°C, permeabilized with 0.5% Triton X-100 (Sigma-Aldrich, Italy) for 30 min at RT, incubated with primary antibody for 2 hr at 37°C in a moist chamber, incubated

with secondary antibody and nuclear stain 1:500 TO-PRO-3 (Life-Technologies, Italy) for 1 hr at RT. The glass cover slips were mounted using ProLong® Gold Antifade Reagent (Invitrogen, Italy) and observed under Leica DM-IRE2 Confocal Microscope.

4.12 rIFI16 TREATMENT AND QUANTITATIVE REAL-TIME PCR

In the first experiment, HUVEC were grown in 6-well plate with complete/incomplete EGM-2 and treated with 50 µg/ml concentration of endo-free rIFI16 [70] and vehicle/mock for 24 hrs and gene expression levels of different pro-inflammatory cytokines as listed in the (Table 1) was assessed with quantitative real-time PCR. In another set of experiment, HUVEC were treated with 50 µg/ml rIFI16 within a time-course of 0 hr, 4 hr, 12 hr, 24 hr, 48 hr and 72 hr and activity of highly modulated genes from the first experiment was assessed. After rIFI16 treatment, HUVEC were trypsinized and m-RNA was extracted using TRI Reagent® (Sigma-Aldrich, Italy) as described in manufacturer protocol. The resulting m-RNA was treated with DNase I Amplification Grade kit (Sigma-Aldrich, Italy) as instructed. Later, 1 µg of m-RNA was used as a template first strand c-DNA synthesis using ImProm-II™ Reverse Transcription System (Promega, Italy) and C1000 Thermal Cycler (Bio-Rad, Italy) with annealing temperature 25°C for 5 min, followed by extension at 42°C for up to one hour. The reverse transcriptase was heat inactivated at 70°C for 15 min, while the final c-DNA preparation was quantified and stored at 4°C for immediate use. A random m-RNA sample was kept as RT^- (without reverse transcriptase) to assess the presence of contaminating genomic DNA in the preparation. The quantitative real-time PCR analyses were performed using CFX96 Real-Time PCR Detection System (Bio-Rad, Italy) with SsoAdvanced™ Universal SYBR® Green Supermix (Bio-Rad, Italy) and amplification conditions as

instructed in manufacturer protocol, upto 40 cycles of PCR. Primer sequences are summarized in Table 1. The Ct values for each gene were normalized to the Ct values for GAPDH using the Ct equation. The level of target RNA, normalized to the endogenous reference and relative to the mock treated and untreated cells, was calculated by the comparative Ct method using the $2^{-\delta\delta Ct}$ equation.

Table 1: List of SYBR Green RT-PCR primers for pro-inflammatory genes

Cytokines	Forward Primer	Reverse Primer
IL-1α	CCGTTTTGACGACGCACTTG	TTTGGCCATCTTGACTTCTTTGC
IL-1β	ACGAATCTCCGACCACCACT	CCATGGCCACAACAACTGAC
IL-2	GTAACCTCAACTCCTGCCACAA	TGTTTCAGTTCTGTGGCCTTCT
IL-4	TGCTGCCTCCAAGAACACAAC	GGTTCCTGTCGAGCCGTTTC
IL-6	GACCCAACCACAAATGCCA	GTCATGTCCTGCAGCCACTG
IL-8	CTGGCCGTGGCTCTCTTG	CCTTGGCAAAACTGCACCTT
IL-10	GGCGCTGTCATCGATTTCTTC	GTTTCTCAAGGGGCTGGGTC
IL-12p35	GCTCCAGAAGGCCAGACAAA	GGCCAGGCAACTCCCATTAG
IL-12p40	GCCCAGAGCAAGATGTGTCA	CACCATTTCTCCAGGGGCAT
IL-17A	AGACCTCATTGGTGTCACTGC	CTCTCAGGGTCCTCATTGCG
IL-18	TGCAGTCTACACAGCTTCGG	TCCAGGTTTTCATCATCTTCAGCTA
IL-33	CAAAGAAGTTTGCCCCATGT	AAGGCAAAGCACTCCACAGT
CCL2	CTCTGCCGCCCTTCTGTG	TGCATCTGGCTGAGCGAG
CCL3	AGCTGACTACTTTGAGACGAGCA	CGGCTTCGCTTGGTTAGGA
CCL4	CTGCTCTCCAGCGCTCTCA	GTAAGAAAAGCAGCAGGCGG
CCL5	GACACCACACCCTGCTGCT	TACTCCTTGATGTGGGCACG
CCL7	GCACTTCTGTGTCTGCTGCT	CAGCCTCTGCTTAGGGATTTT
CCL8	GCCCTCCAAGATGAAGGTTT	TCACGTTAAAGCAGCAGGTG
CCL20	TCCTGGCTGCTTTGATGTCA	TCAAAGTTGCTTGCTGCTTCTG
TLR1	CTGGTATCTCAGGATGGTGTGC	TTGGAGTTCTTCTAAGGGTATGTTCC

TLR2	GGCCAGCAAATTACCTGTGTG	AGGCGGACATCCTGAACCT
TLR3	TCCCAAGCCTTCAACGACTG	TGGTGAAGGAGAGCTATCCACA
TLR4	CTGCAATGGATCAAGGACCA	TTATCTGAAGGTGTTGCACATTCC
TLR5	TCGAGCCCCTACAAGGGAA	CACTGAGACTCTGCTATACAAGCTA
TLR7	TTACCTGGATGGAAACCAGCTAC	TCAAGGCTGAGAAGCTGTAAGCTA
TLR8	GAGAGCCGAGACAAAAACGTTC	TGTCGATGATGGCCAATCC
TLR9	TGGTGTTGAAGGACAGTTCTCTC	CACTCGGAGGTTTCCCAGC
TLR10	GAAAGGTTCCCGCAGACTTG	TGGAGTTGAAAAAGGAGGTTATAG
ICAM1	GCACATTGGTTGGCTATCTTCT	GCCCGAAGCGTTTACTTTGA
VCAM1	TTCCTCAGATTGGTGACTCCG	AAAACTCACAGGGCTCAGGGTCAG
VEGF	ATCTGCATGGTGATGTTGGA	GGGCAGAATCATCACGAAGT
IRF3	CCGACCTTCCATCGTAGGAG	AATCAGATCTTCCCCCGGCA
MyD88	CCACCCTTGATGACCCCTAGGACAAAC	GTCTGTTCTAGTTGCCGGATCATCTCCTGCAC
TNF-alpha	ATACTGACCCACGGCTCCA	GTTCGAGAAGATGATCTGACTGCC
TGF-beta1	CCCAGCATCTGCAAAGCTC	GTCAATGTACAGCTGCCGCA
GM-CSF	CATGTGAATGCCATCCAGGA	CAGGCCCACATTCTCTCACTT
GAPDH	CGGAGTCAACGGATTTGGTCGTATTGG	GCTCCTGGAAGATGGTGATGGGATTTCC

4.13 TRANSIENT TRANSFECTION AND LUCIFERASE ASSAY

The low passage (3-4) HUVECs were plated at approximately 2×10^5 cells per well in 6-well culture plates and incubated overnight for next day 80% confluence. Effectene Transfection Reagent (Qiagen, Italy) was optimized for 75% transfection efficiency, maintaining normal biological activity of HUVEC. Briefly, total 0.4 µg of plasmid DNA was diluted to 100 µl of EB buffer while the Enhancer and Effectene reagent was used as 4 µl and 5 µl respectively, by following the preparation conditions as directed by the manufacturer. Cells were incubated with the

transfection reagent diluted in serum/antibiotics free incomplete EGM-2 upto maximum 4 hr at 37°C with 5% CO_2. Later cells were incubated overnight with incomplete EGM-2 including 2% FCS and antibiotics, following which rIFI16, 50 µg/ml was added to the culture for next 48 hr before measurement of luciferase activity. For each transfection, the cells were co-transfected with 0.05 µg of pRL-TK (Promega) and either of 0.3 µg of pGL2-IL8-wild type, 0.3 µg of pGL2-IL8-ΔNf-κB, 0.3 µg of pGL2-IL8-ΔAP1 luciferase reporter plasmid or 0.3 µg control vector (pmaxGFP™ Vector). All plasmids were purified using the Toxin Eraser™ Endotoxin Removal Kit (Genscript, USA). Protein extracts were prepared and luciferase activity was measured using the Dual-Luciferase® Reporter Assay System (Promega, Italy) at the Victor X4 Multilabel Plate Reader (Perkin Elmer, Italy).

4.14 STATISTICAL ANALYSIS

All statistical tests were performed using GraphPad Prism version 5.00 for Windows (GraphPad, La Jolla, CA, USA). Positivity cut-off values for anti-IFI16 antibodies were calculated as the 95^{th} percentile for the control population and the Kruskal-Wallis test was used to measure associations. To test the effects of recombinant IFI16 protein (rIFI16) on biological functions of primary endothelial cells one-way analysis of variance (ANOVA) with Bonferroni adjustment for multiple comparisons was used. Significant upregulation of m-RNA expression was evaluated through paired t-test.

5 RESULTS

5.1 SERUM LEVELS OF IFI16 PROTEIN ARE INCREASED IN PATIENTS WITH SYSTEMIC AUTOIMMUNE DISEASES

Sera were harvested from patients suffering from systemic autoimmune diseases characterized by endothelial dysfunction, including SSc, SLE, SjS, and RA. IFI16 serum levels were quantified using an in-house sandwich ELISA and compared with age- and sex-matched healthy controls. All absorbance levels were in the range of assay linearity. With the cut-off value set to the 95th percentile of the control population (27ng/ml), mean IFI16 levels were significantly increased in patients with SSc, SLE, RA, and SjS compared to the control group (4.7ng/ml) (SSc: 25.4ng/ml, $p<0.001$; SLE: 23.5ng/ml, $p<0.001$; RA: 222ng/ml, $p<0.001$; SjS: 88.2ng/ml, $p<0.001$). Of note, the sera from RA patients displayed the highest levels of circulating free protein. IFI16 levels above the 95th percentile for control subjects were observed in 34% of SSc, 37% of SLE, 47% of SjS, and 56% of RA patients (Figure 13). By contrast, IFI16 levels in non-SLE GN patients did not show any significant difference in comparison with healthy controls. Since the objective of this part of the study was limited to demonstrate the presence of circulating IFI16 in patients' sera for justifying the rest of the in vitro studies, correlation with clinico-pathological parameters was behind the aim of these studies and was not performed.

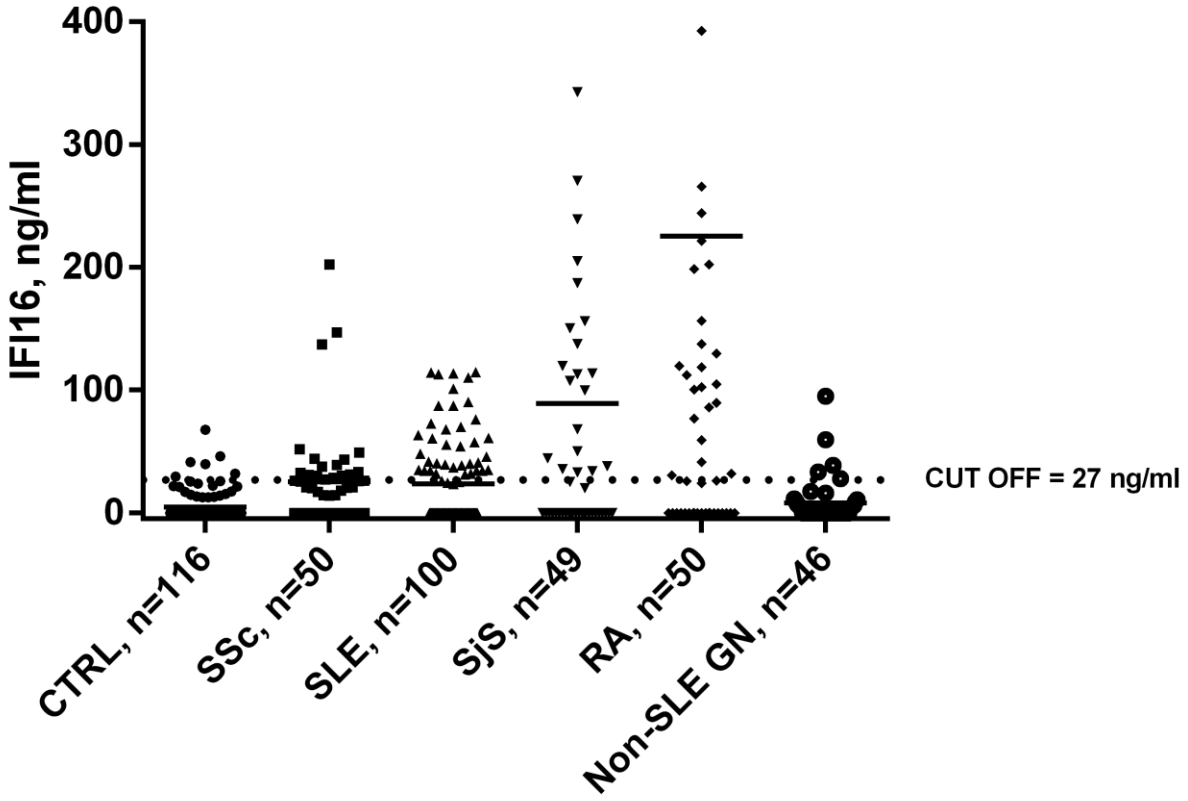

Figure 13. IFI16 protein levels in patients' and controls' sera determined using an in-house capture ELISA. Each dot represents the concentration of IFI16 protein (expressed in ng/ml on a linear scale) in each individual subject: patients suffering from Systemic Sclerosis (SSc, n=50), Systemic Lupus Erythematosus (SLE, n=100), Sjogren's Syndrome (SjS, n= 49), Rheumatoid Arthritis (RA, n=50), and non-SLE glomerulonephritis (non-SLE GN n=46) were investigated together with healthy controls (CTRL, n=116). The horizontal bars represent the median values. Values over the dotted line indicate the percentage of subjects with IFI16 protein levels above the cut-off value (27ng/ml) calculated as the 95th percentile of the control population. Statistical significance: *** $p < 0.001$ *vs*. controls (Kruskall-Wallis test).

5.2 EFFECTS OF EXTRACELLULAR IFI16 ON DIFFERENT FUNCTIONS OF PRIMARY ENDOTHELIAL CELLS

Abnormalities in angiogenesis are frequently present in systemic autoimmune diseases and may lead to tissue damage and premature vascular disease [71]. To verify whether extracellular IFI16 was also involved in this pathogenic process, HUVEC were treated with increasing concentrations of recombinant IFI16 protein (rIFI16) (10, 25 or 50µg/ml), mock-treated with the same volumes of vehicle (Mock), or left untreated (NT) and then assessed for cell viability at 48 hours incubation time by MTT assay. As shown in Figure 14A, the addition of endotoxin-free rIFI16 protein did not reduce the amount of viable adherent cells when compared to mock or untreated cells at the concentration of 10 and 25µg/ml, respectively. At the highest concentration used (50µg/ml), a slight reduction in cell viability was observed, and consequently the following studies were conducted with the lower doses.

Next, to test whether the addition of rIFI16 to culture media altered other biological parameters of endothelial cells, HUVEC were treated as described for the assessment of cell viability (MTT assay) and then analyzed for their tubule morphogenesis and chemotactic activities. As shown in Figure 10B, exogenous administration of 25µg/ml rIFI16 severely limited tubulogenesis, with most cells generating incomplete tubules or aggregating into clumps. The extent of angiogenesis was quantified by counting the intact capillary-like tubules called as Lumens, which showed 75% decrease in its numerical value, as well as the number of interconnecting branch points showing 77% decrease. (Figure 14B). These effects were less pronounced when a lower dose of 10µg/ml rIFI16 was used with 22% and 15% decrease respectively. In contrast, untreated or mock-treated HUVEC

plated onto matrigel supported the formation of an extensive interconnecting polygonal capillary-like network.

Next, we evaluated the effects of rIFI16 on the migration phase of angiogenesis in a transwell migration assay routinely used to study cell migration in response to specific stimuli. HUVECs untreated, mock-treated, or incubated with rIFI16 (10 or 25µg/ml) for 48h were transferred into transwell migration chambers. As shown in Fig. 10C, only a small population of HUVECs cultured in the presence of 25µg/ml rIFI16 were able to migrate through the chamber (30% of migration), whereas mock-treatment resulted in considerable migration (95% and 87% for 10µg/ml and 25µg/ml, respectively).

Taken together, these results demonstrate the capability of extracellular rIFI16 to impair physiological functions of endothelial cells, such as the differentiation phases responsible for tube morphogenesis and migration.

Figure 14. Extracellular IFI16 affects various biological functions of primary endothelial cells. HUVEC were treated with different doses of recombinant IFI16 protein (rIFI16), the same volumes of vehicle (Mock), or left untreated (NT) for 48h. (A) Viability analysis (MTT assay); the viability of control preparations (NT) was set to 100%. (B) Capillary-like tube formation assay (Matrigel). For a quantitative assessment of angiogenesis, the number of lumens and branch points was assessed (upper panels); representative images of three independent experiments are reported (lower panels). (C) Migration analysis (Transwell assay) results are reported as the percentage of migrated cells *vs*. untreated HUVECs. Values represent the mean±SD of 3 independent experiments, (**p<0.01, ***p<0.001; one-way ANOVA followed by Bonferroni's multiple comparison test).

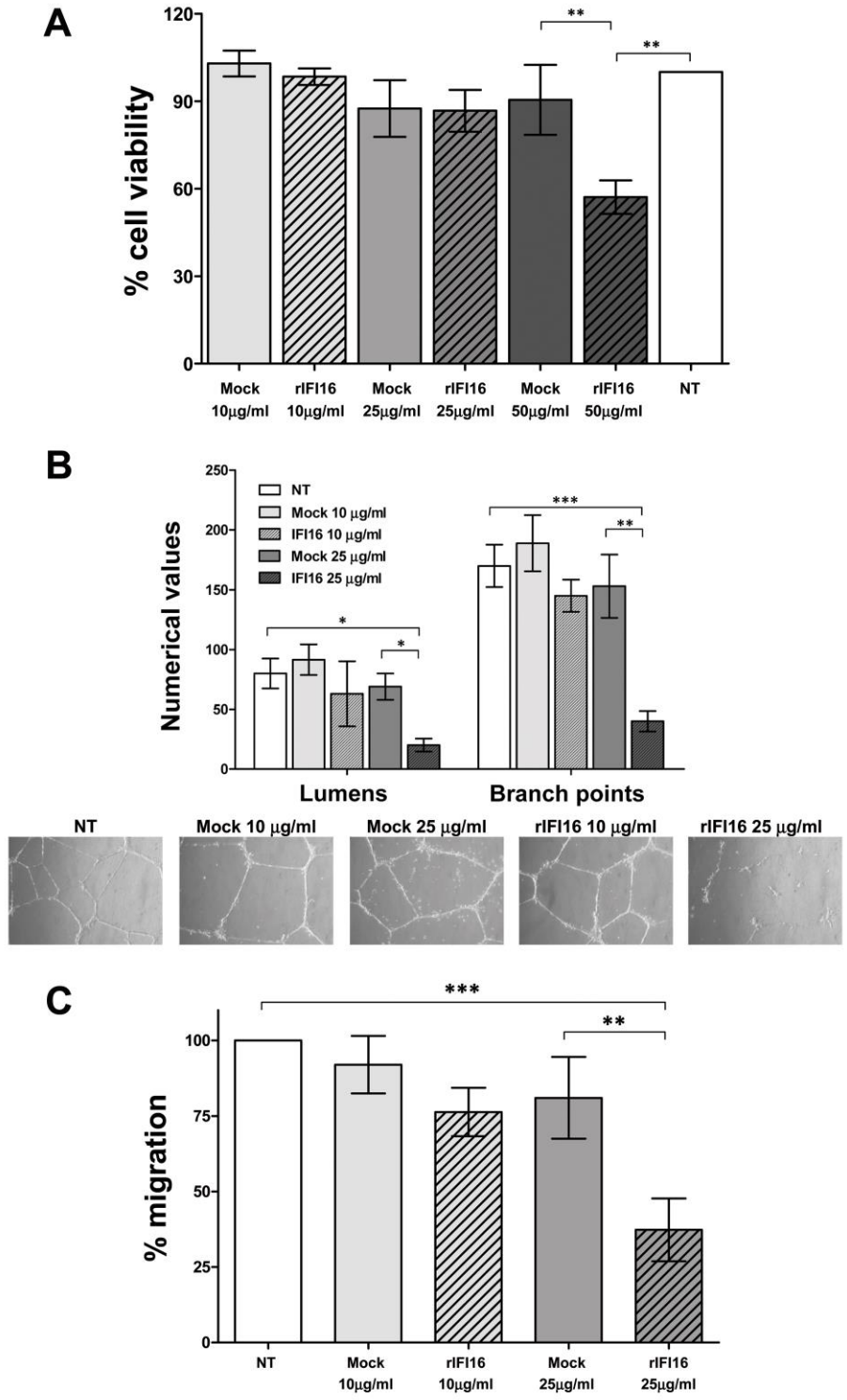
A
% cell viability
120
90
60
30
0
**
**
Mock 10µg/ml
rIFI16 10µg/ml
Mock 25µg/ml
rIFI16 25µg/ml
Mock 50µg/ml
rIFI16 50µg/ml
NT
B
Numerical values
250
200
150
100
50
0
NT
Mock 10 µg/ml
IFI16 10 µg/ml
Mock 25 µg/ml
IFI16 25 µg/ml
*
*
***
**
Lumens
Branch points
NT
Mock 10 µg/ml
Mock 25 µg/ml
rIFI16 10 µg/ml
rIFI16 25 µg/ml
C
% migration
100
75
50
25
0
***
**
NT
Mock 10µg/ml
rIFI16 10µg/ml
Mock 25µg/ml
rIFI16 25µg/ml

5.3 ANTI-N-TERMINUS IFI16 ANTIBODIES NEUTRALIZE THE CYTOTOXIC ACTIVITY OF IFI16

To demonstrate that the effects exerted by IFI16 protein on target cells were specific and not a consequence of cell cytotoxicity, HUVEC were treated with 25µg/ml rIFI16 in the presence or absence of specific rabbit polyclonal antibodies recognizing the N-terminal or the C-terminal domain of IFI16 protein. HUVEC incubated with rIFI16 in the presence of normal rabbit IgG were used as the positive control. As described in the previous section, rIFI16 severely affected the capability of endothelial cells to generate microtubules as well as their transwell migration activity, while the same effects were observed in presence of normal rabbit IgG (Figure 15A and 15B). In contrast, the presence of anti-N-terminus antibodies reduced the Lumens by 16%, Branch Points by 5% and migration by 1% while anti-C-terminus antibodies reduced the Lumens by 60%, Branch Points by 32% and migration by 49%. This indicates the role of anti-N-terminus antibody in inhibiting the activities of IFI16 toward endothelial cells, restoring the tube formation and migratory activities. Altogether, these results suggest that the IFI16 activity is specific and that the functional domain resides at the N-terminus, where the PYD domain is localized.

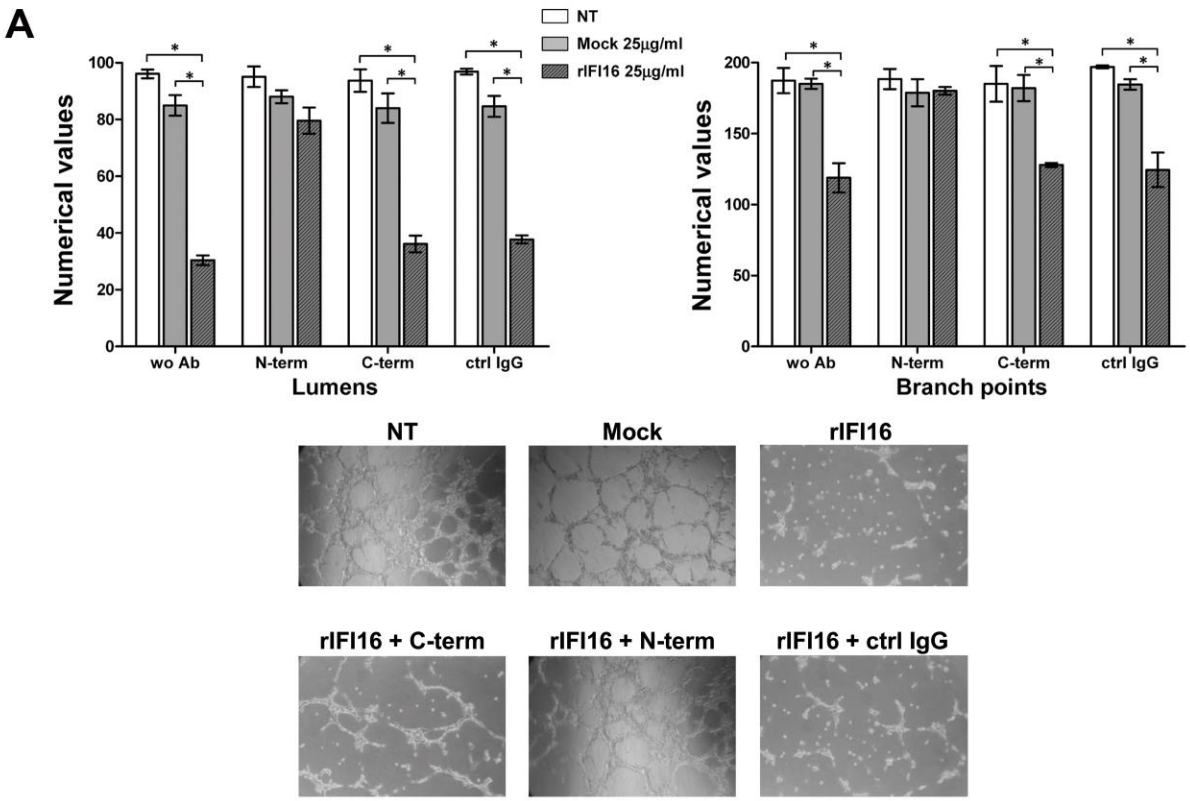
A
NT
Mock 25µg/ml
rIFI16 25µg/ml
Numerical values
Lumens
wo Ab
N-term
C-term
ctrl IgG
Branch points
NT
Mock
rIFI16
rIFI16 + C-term
rIFI16 + N-term
rIFI16 + ctrl IgG

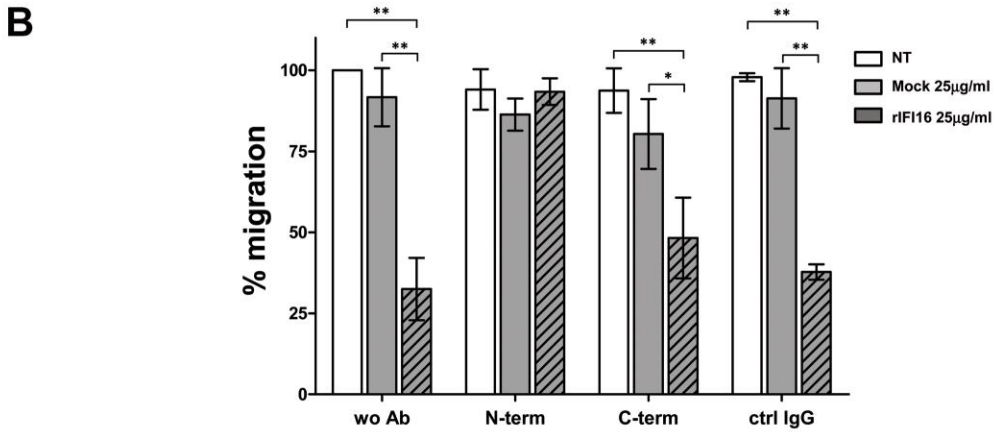
B
% migration
NT
Mock 25µg/ml
rIFI16 25µg/ml
wo Ab
N-term
C-term
ctrl IgG

Figure 15. Anti-IFI16 antibodies restore the biological activities of extracellular IFI16. HUVEC were treated for 48h with different doses of recombinant IFI16 protein (rIFI16), the same volumes of vehicle (Mock), or left untreated (NT), alone or in combination with antibodies against IFI16**.** (A) Capillary-like tube formation assay (Matrigel). For a quantitative assessment of angiogenesis, the number of lumens and branch points was assessed (upper panels); representative images of three independent experiments are reported (lower panels). (B) Migration analysis (Transwell assay) results are reported as the percentage of migrated cells *vs*. untreated HUVECs. Values represent the mean±SD of 3 independent experiments (**p<0.01, ***p<0.001, one-way ANOVA followed by Bonferroni's multiple comparison test).

5.4 BINDING OF EXTRACELLULAR IFI16 ON THE PLASMA MEMBRANE OF HUVEC

The finding that extracellular IFI16 impairs endothelial cell functions, including tube morphogenesis and transwell migration indicates a possible alarmin function as recently demonstrated for Danger and Pathogen-associated molecular pattern molecules collectively called as DAMPs, PAMPs such as autoantigen HMGB-1 [72, 73]. Thus to find evidence in this direction it was important to evaluate the binding interaction of IFI16 on the plasma membrane of HUVEC. A series of binding experiments were conducted to verify the presence of high-affinity binding sites in the membranes of the target cells. In the previous section, it has been described that 25 μg/ml (300 nM) rIFI16 concentration is non-toxic to HUVEC, while they can still perform biological functions. Thus HUVEC were incubated with lowest concentrations (10nM, 20nM, and 30nM) of FITC-labeled rIFI16 to avoid toxicity or apoptosis and the binding was visualized by confocal microscopy. As shown in Figure 16A, binding of FITC-labeled rIFI16 was detected at least concentration of 10nM, increased at 20nM, and saturated at 30nM. To avoid the non-specific binding of rIFI16 with sugar residues on plasma membrane, HUVEC were grown in presence of tunicamycin which inhibits N-glycosylation of proteins. By contrast to above findings, human fibroblasts were negative for FITC-labeled rIFI16 at all the rIFI16 concentrations investigated (data not shown).

Furthermore, to demonstrate that the binding of rIFI16 is of physiological relevance, co-culturing experiments were organized in such a way that UV-B irradiated cells release endogenous IFI16 [2] which in turn binds to neighboring HUVEC in the same system. As shown in Figure 16B, after 24 h HUVEC were observed to be surface bound with endogenous IFI16 released from HeLa cells, while by 36 h this bound IFI16 entered the cytoplasm and by 48 h it almost

disappeared. When fibroblasts were used instead of HUVEC, the binding was not observed, while also when HUVEC were cultured with normal HeLa cells, surface presence of IFI16 was not detected (data not shown).

Figure 16. Plasma membrane binding of IFI16 to HUVEC. (A) Cells were left untreated (a, negative control) or incubated with increasing concentrations of FITC-labeled recombinant IFI16 (b, 10nM rIFI16-FITC; c, 20nM rIFI16-FITC; d, 30nM rIFI16-FITC). Binding was detected by confocal microscopy using an excitation wavelength of 490nm for FITC in one channel and trans-illuminated light in the other. Representative images of three independent experiments are shown. (B) Endogenous IFI16 released by irradiated HeLa cells binds neighboring HUVEC. UV-B irradiated HeLa cells were co-cultured with HUVEC and after 24h, 36h and 48h, dead cell debris were removed and immunofluorescence was performed on the remaining live HUVEC using a home-made anti-IFI16 polyclonal as primary antibody and Alexa-488- anti-rabbit as secondary antibody. The cells were then fixed, permeabilized, nuclear-stained using propidium iodide and analyzed by confocal microscopy. Fibroblasts were employed as negative control. Representative images of three independent experiments are shown.

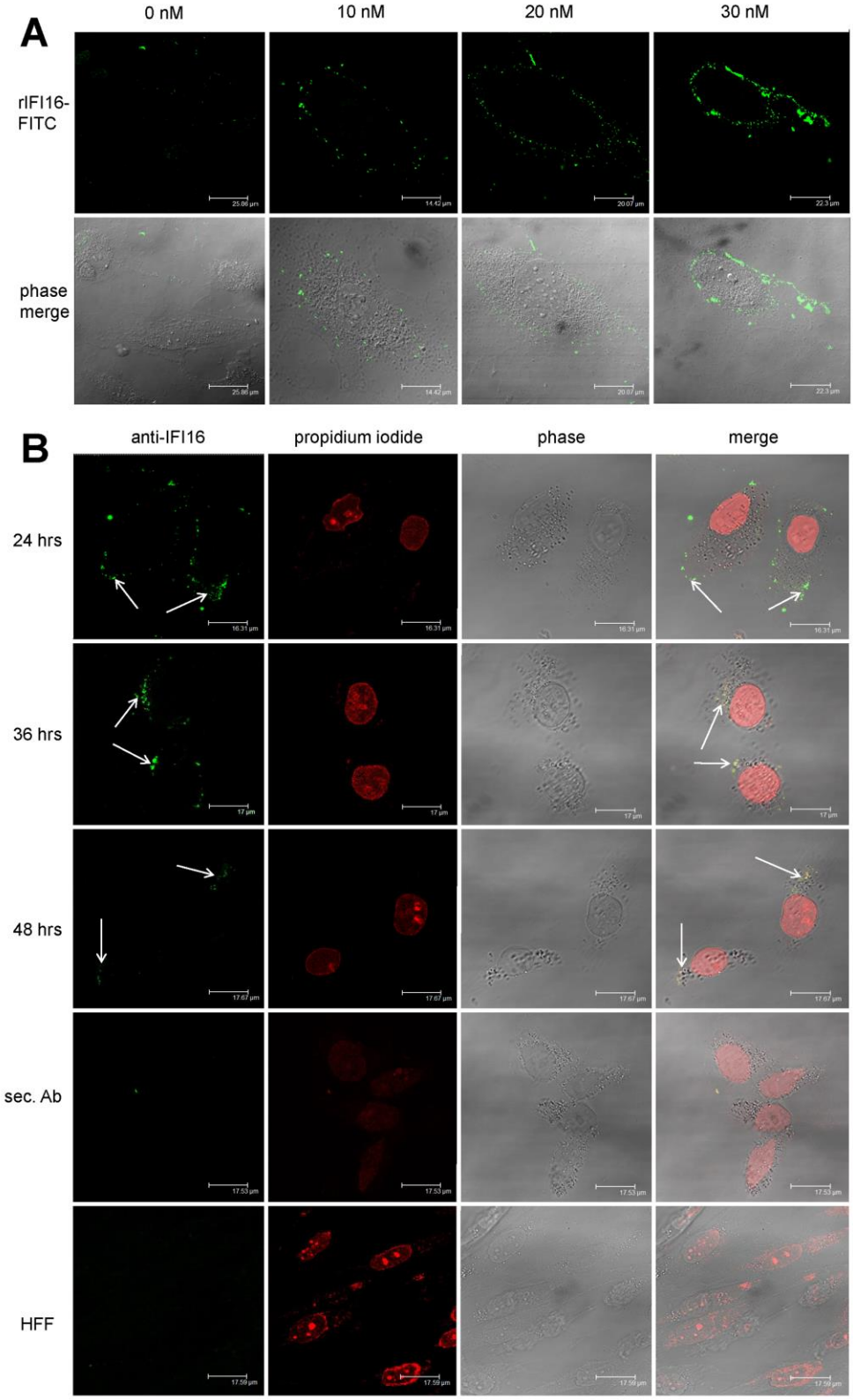
A
0 nM
10 nM
20 nM
30 nM
rIFI16-FITC
phase
merge
B
anti-IFI16
propidium iodide
phase
merge
24 hrs
36 hrs
48 hrs
sec. Ab
HFF

5.5 KINETICS OF RIFI16 BINDING ON DIFFERENT CELL LINES

To get some insights into the binding characteristics of IFI16 to different cell lines, binding kinetics experiments using radioiodinated rIFI16 were performed. Specific binding was calculated as the difference between total and non-specific binding. As shown in Figure 17A, the specific binding of [^{125}I]-rIFI16 to its binding site on HUVEC is saturable and has a dissociation constant (Kd) equal to 2.7nM; 71.55 to 83.84fmol of [^{125}I]-rIFI16 was estimated to saturate the binding sites on 10^5 HUVEC, thus the maximal number of binding sites (B_{max}) could be estimated to be in the range of 250,000 to 450,000 binding sites/cell. Furthermore, the binding of [^{125}I]-rIFI16 on HUVEC was displaced by 10- to 100-fold of unlabeled rIFI16, demonstrating its competitive nature (Figure 17B). The inhibition constant (K_i) was calculated to be 14.43nM and the half maximal inhibitory concentration (IC_{50}) was 67.88nM. Similar results were obtained for HeLa and HaCaT cell lines, which also indicated saturable and competitive nature towards rIFI16 binding. As a negative control, human dermal fibroblasts (HDF) and murine fibroblasts (3T3) were accessed for specific and competitive binding of [^{125}I]-rIFI16 in parallel with HUVEC (Figure 17A and 17B). Both HDF and 3T3 were found to exhibit non-saturable rIFI16 binding, indicating the lack of any specific IFI16 binding sites. Moreover, the binding of rIFI16 on these cells was non-competitive in nature (Figure 17B). Also as reported in Figure 17C, different cell lines shown variable affinities towards IFI16 binding.

Figure 17. Binding Kinetics of [^{125}I]-rIFI16 on HUVEC, HDF, and 3T3 cells. (A) Specific binding of [^{125}I]-rIFI16 on the plasma membrane of HUVEC, HeLa, HACAT, HDF, and 3T3 cells. (B) Competitive binding of [^{125}I]-rIFI16 on HUVEC, HeLa, HaCaT, HDF, and 3T3 cells. (C) The binding affinity (Kd), total bound ligand (B_{max}) and the estimated number of binding sites per cell for different cell lines. The experiment was carried out in triplicates and data was analyzed using non-linear regression equations from GraphPad Prism with 95% confidence intervals. All the experiments have been repeated at least three times and one representative is reported.

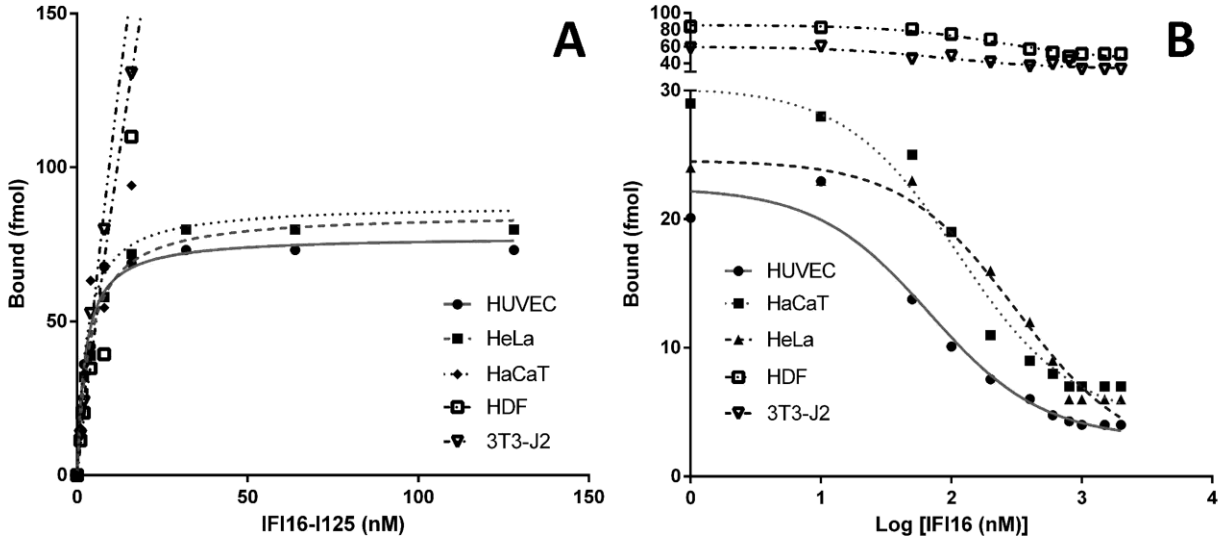

C

Cell Line	Kd	Bmax	Number of binding sites/cell
HUVEC	2.7 nM	77.7 fmol	2.5-5 × 10^5
HeLa	3.7 nM	85.3 fmol	2-4 × 10^5
HaCaT	2.7 nM	87.7 fmol	2-4 × 10^5

5.6 [^{125}I]-rIFI16 BINDING INHIBITION BY ANTI-IFI16 POLYCLONAL ANTIBODIES

To evaluate the binding properties of rIFI16 to its receptor with respect to epitope mapping, we performed a binding inhibition assay using radioiodinated rIFI16 in the presence of increasing concentrations of antibodies recognizing the IFI16 N-terminal domain. As depicted in Figure 18, a gradual decrease in the bound [^{125}I]-rIFI16 was observed with increasing concentrations of antibody (from 10 to 1000nM). Conversely, the anti-IFI16 antibody recognizing the C-terminal domain (478-729 aa) was not able to inhibit the binding of [^{125}I]-rIFI16 to its receptor. Together with the results from the functional assays, these observations provide evidence indicating that the N-terminal region of rIFI16 is required for its binding to the novel membrane receptor on HUVEC and is responsible for its signal transduction capacity.

Figure 18. Binding inhibition of [^{125}I]-rIFI16 using anti-IFI16 polyclonal antibodies. Antibody inhibition curve of HUVEC using anti-rIFI16 N-terminal (1-205 aa) polyclonal antibodies (dashed) and C-term polyclonal antibodies (dot-dashed). Competitive binding of rIFI16 and [^{125}I]-rIFI16 to HUVEC (plain) was used as the control condition. The experiment was carried out in triplicates and data was analyzed using non-linear regression equations from GraphPad Prism with 95% confidence intervals. All the experiments have been repeated at least three times and one representative is reported.

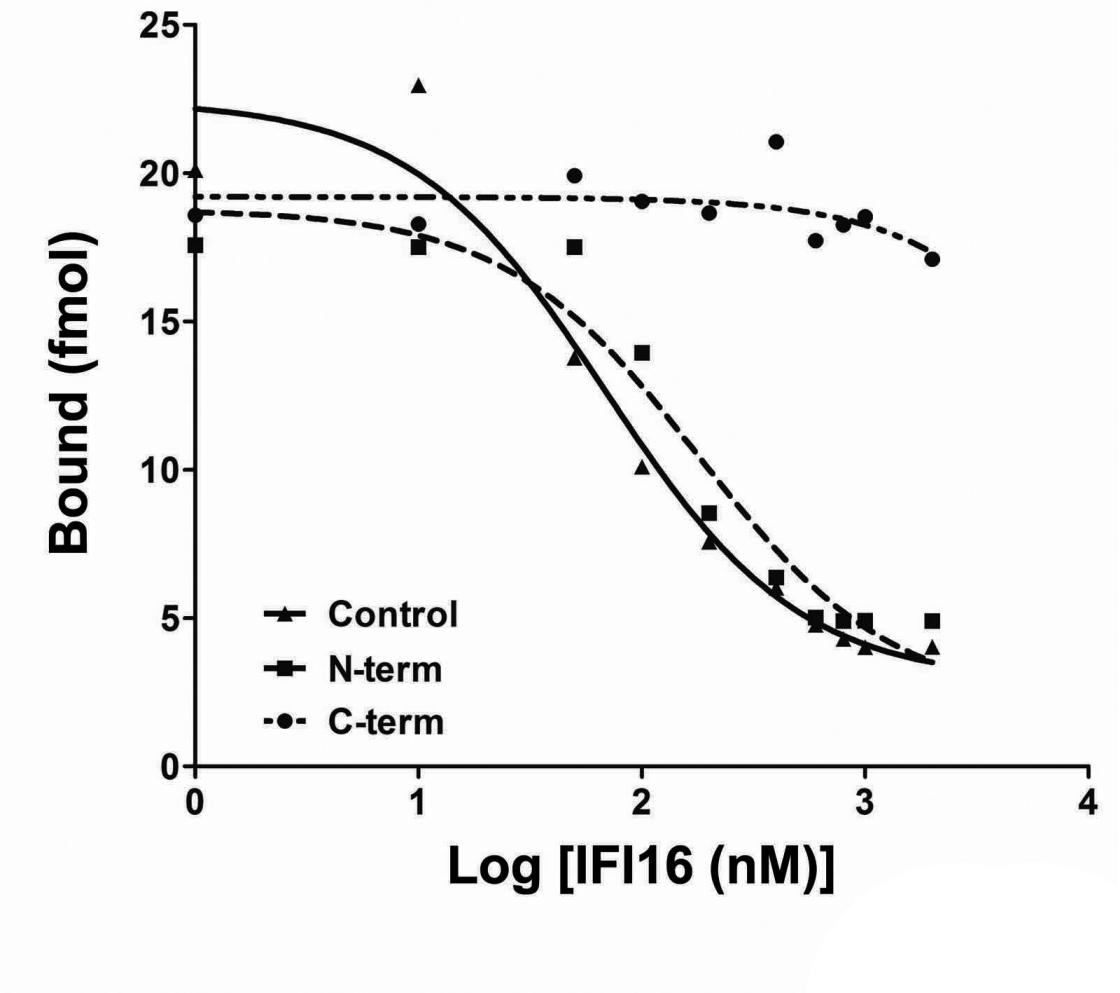

5.7 TIME-DEPENDENT NUCLEAR TRANSLOCATION OF NF-κB IN RIFI16 TREATED HUVEC

The activation of Nf-κB is an important event in the propagation of inflammation, since Nf-κB transcriptionally regulate the production of different pro-inflammatory cytokines. Since, rIFI16 treatment produced detrimental changes in the HUVEC, as demonstrated in, we tested the pro-inflammatory activity of endo-free rIFI16 by observing the nuclear translocation of p65 sub-unit of Nf-κB. Using a simple immunofluorescence assay we determine the time-dependent activity of p65 in the cytoplasm of HUVEC, after rIFI16 treatment. As shown in Fig.

19, the p65 sub-unit, without rIFI16 treatment was located abundantly in the cytoplasm of HUVEC, which after 24 hr treatment time-point starts to migrate inside the nucleus. By 48 hr, most of the cells were having complete p65 sub-unit translocated into the nucleus, confirming the activation of Nf-κB. The results were further confirmed by EMSA.

Figure 19. Time dependant Nf-κB nuclear translocation

HUVEC (-VEGF) treated with rIFI16 (10 µg/ml) for 0hr, 24hr and 48hr. Immunofluorescence was performed using 1:1000 anti-p65 polyclonal antibody (santacruz biotech) and 1:500 TO-PRO-3 (Life Technologies) as nuclear counter stain.

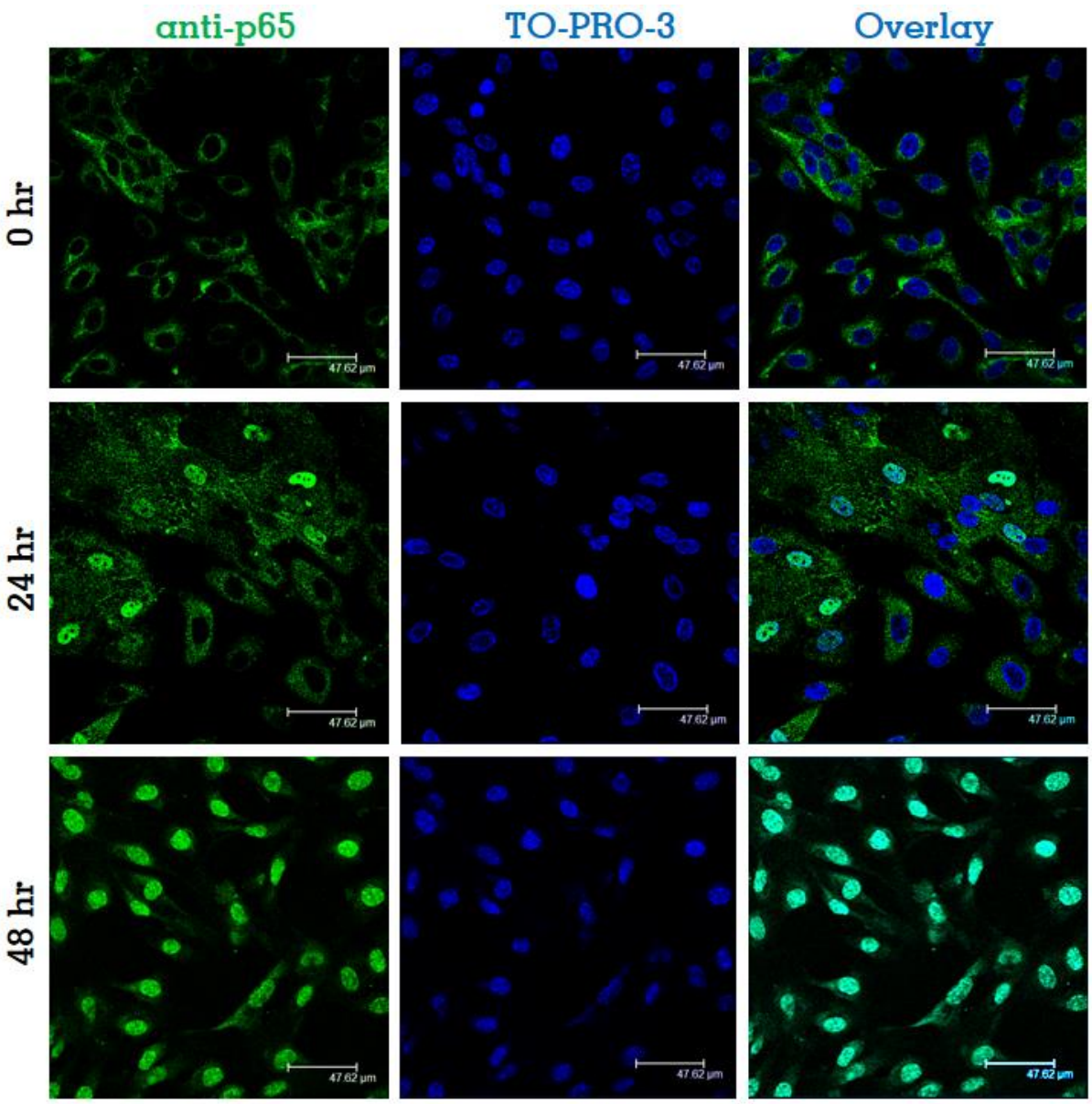
anti-p65
TO-PRO-3
Overlay
0 hr
24 hr
48 hr
47.62 µm

5.8 m-RNA Expression of Pro-Inflammatory Cytokines after rIFI16 treatment

The presence of extracellular IFI16 in the sera of autoimmune patients is a highly significant discovery which lead to strengthen our understanding on the leakage of endogenous molecules during cell death/apoptosis. It was thus necessary to evaluate the molecular activity of IFI16 protein when present in free form outside the cells. We treated endothelial cells with 50 μg/ml rIFI16 protein to understand the inflammatory properties of this protein. A broad range of pro-inflammatory cytokines upregulation was assessed 24 hr post rIFI16 treatment as shown in Fig. 20A. Normalized m-RNA expression levels were then compared with untreated controls and the results were statistically analyzed by paired t-test. The expression levels of IL-8, CCL2, CCL5, CCL20, TLR3, TLR4, TLR9, ICAM1, VCAM1 and TNF-α were significantly upregulated, 24 hr post rIFI16 treatment as shown in Fig. 20B.

We further checked the time dependent expression of these cytokines to check the activation patterns at 0 hr, 4 hr, 12 hr, 24 hr, 48 hr and 72 hr. The m-RNA profile reveals the inflammatory stimulation by rIFI16 which could represent an early event during an autoimmune inflammation.

Figure 20A: m-RNA expression profile of pro-inflammatory cytokines, 24 hr post rIFI16 treatment

HUVEC treated with 50 μg/ml of rIFI16 for 24 hr were lysed and m-RNA was extracted, followed by ImProm-II c-DNA synthesis. RT-PCR was performed using Bio-Rad CFX96 instrument, using Bio-Rad Universal SYBR green master mix and amplification protocol as described by the manufacturer. The normalized expression of genes was calculated by $2^{-\delta\delta ct}$ equation and significant gene expression was analyzed by paired t-test comparison.

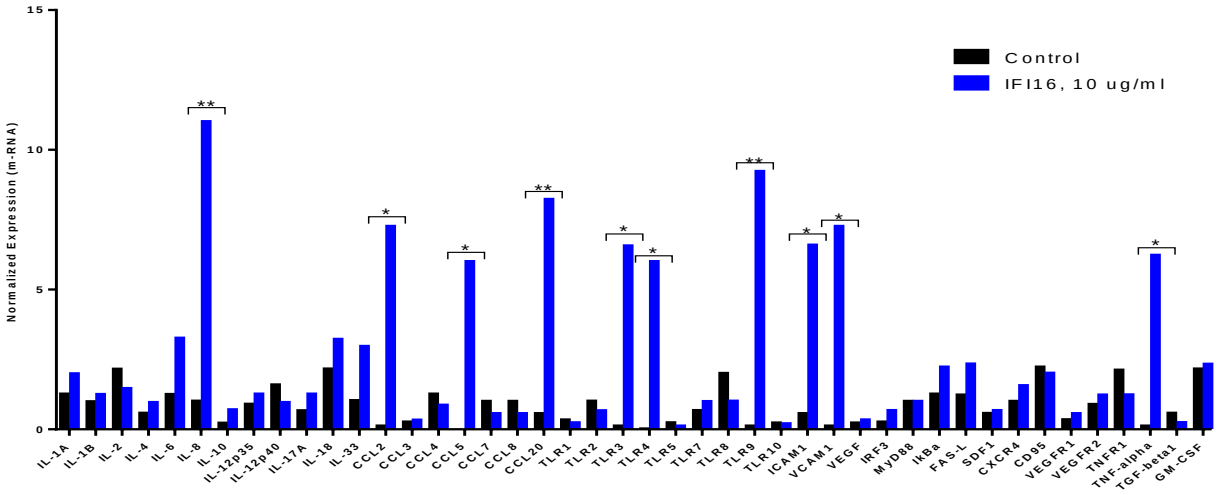

Figure 20B: Time-dependent m-RNA expression of IL-8, CCL2, CCL5, CCL20, TLR3, TLR4, TLR9, ICAM1, VCAM1, TNF-α

HUVEC treated with 50 μg/ml of rIFI16 for 0 hr, 4 hr, 12 hr, 24 hr, 48 hr and 72 hr were lysed and m-RNA was extracted, followed by ImProm-II c-DNA synthesis. RT-PCR was performed using Bio-Rad CFX96 instrument, using Bio-Rad Universal SYBR green master mix and amplification protocol as described by the manufacturer. The normalized expression of genes was calculated by $2^{-\delta\delta ct}$ equation and significant gene expression was analyzed by paired t-test comparision.

IL-8

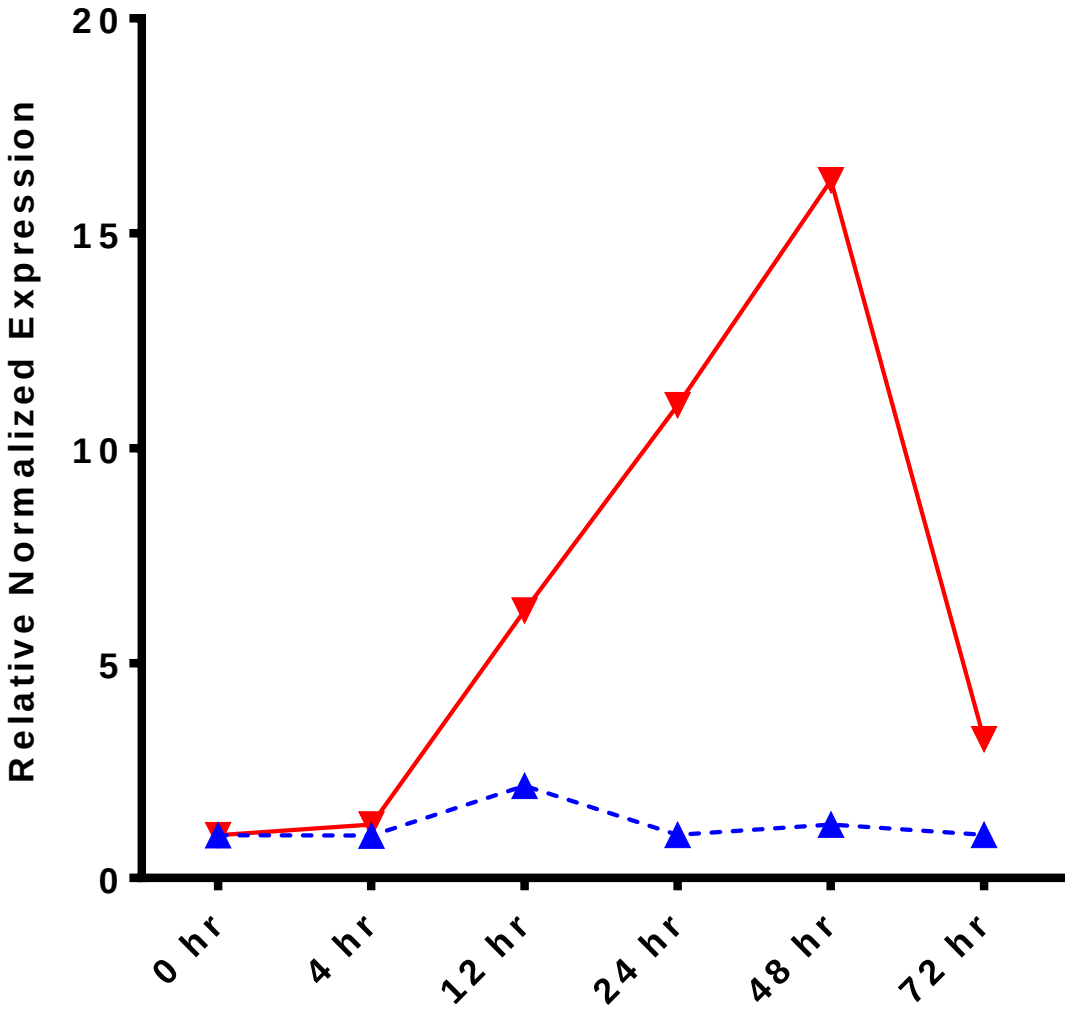
Relative Normalized Expression
20
15
10
5
0
0 hr
4 hr
12 hr
24 hr
48 hr
72 hr

C C L 2

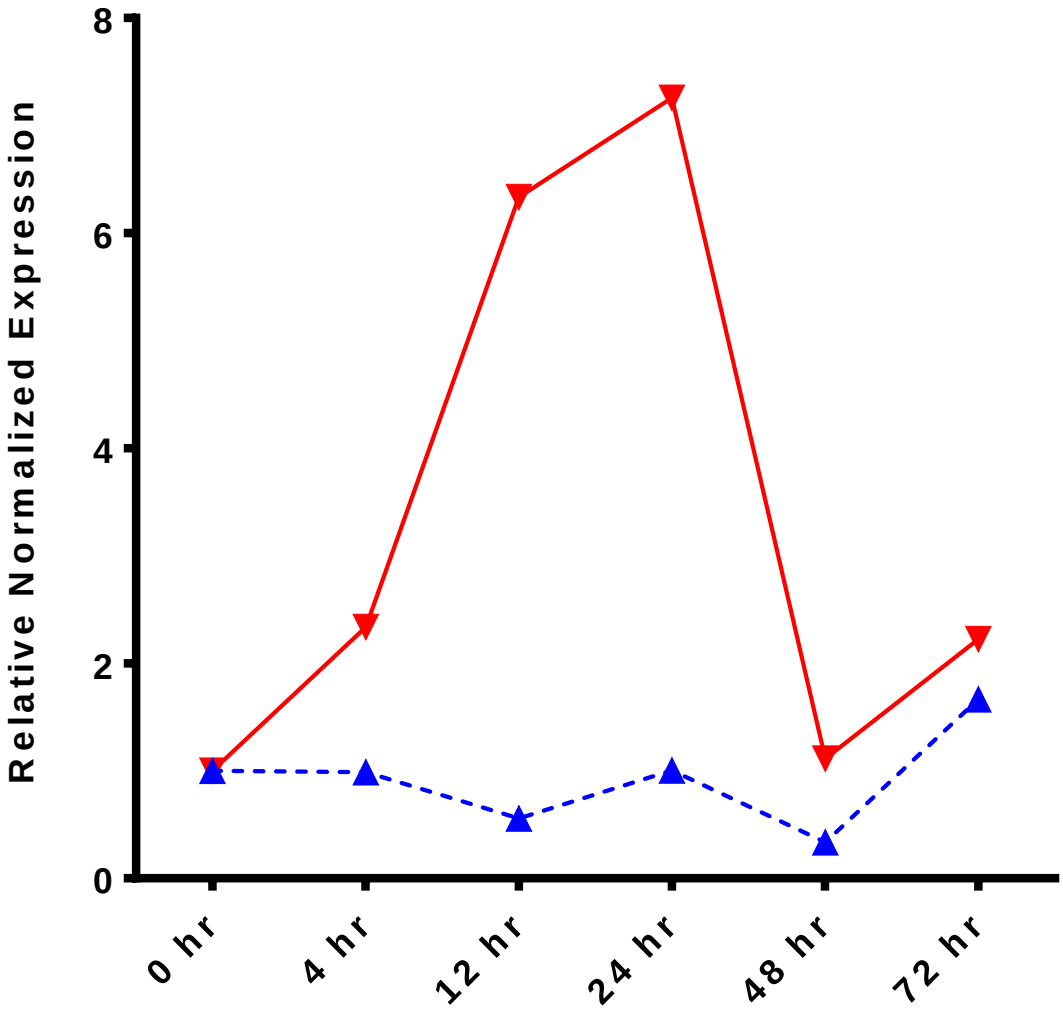
Relative Normalized Expression
8
6
4
2
0
0 hr
4 hr
12 hr
24 hr
48 hr
72 hr

C C L 5

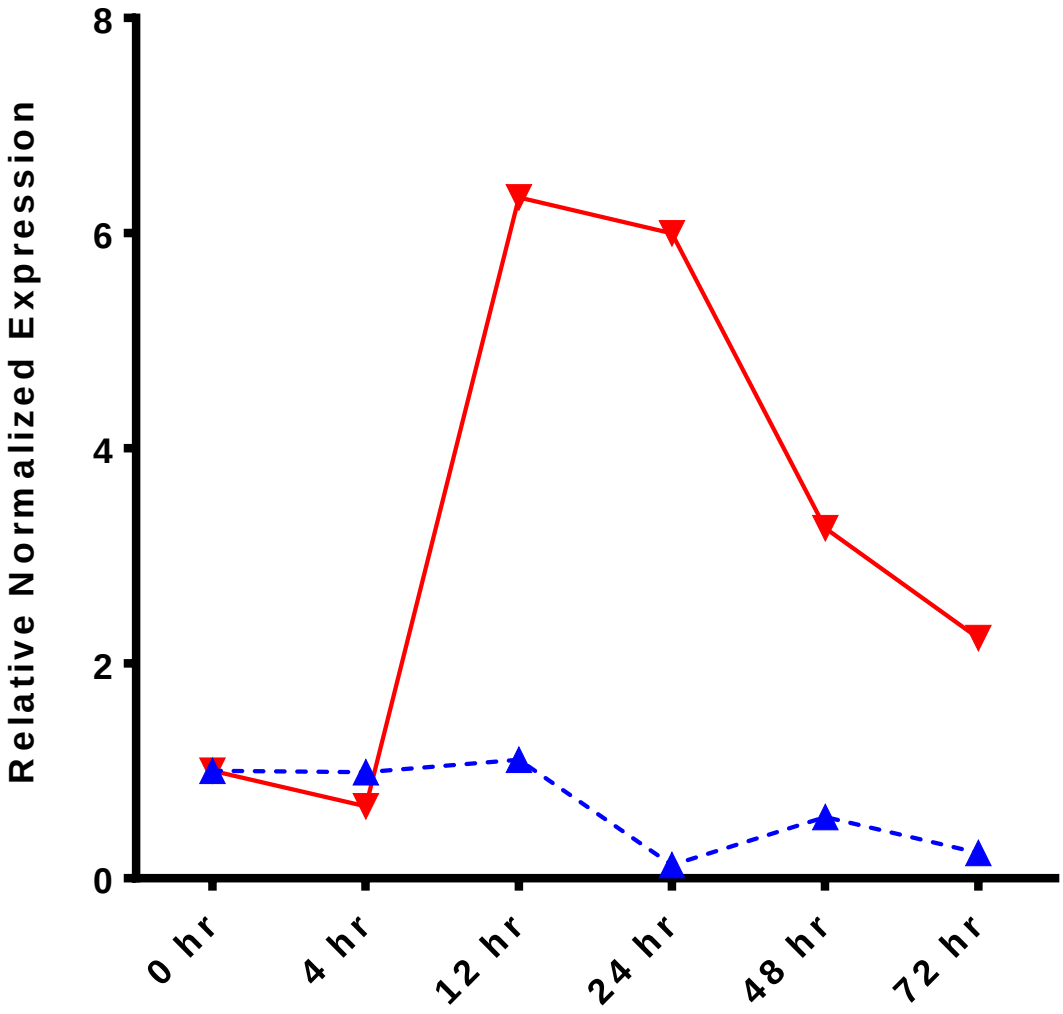
Relative Normalized Expression
8
6
4
2
0
0 hr
4 hr
12 hr
24 hr
48 hr
72 hr

CCL20

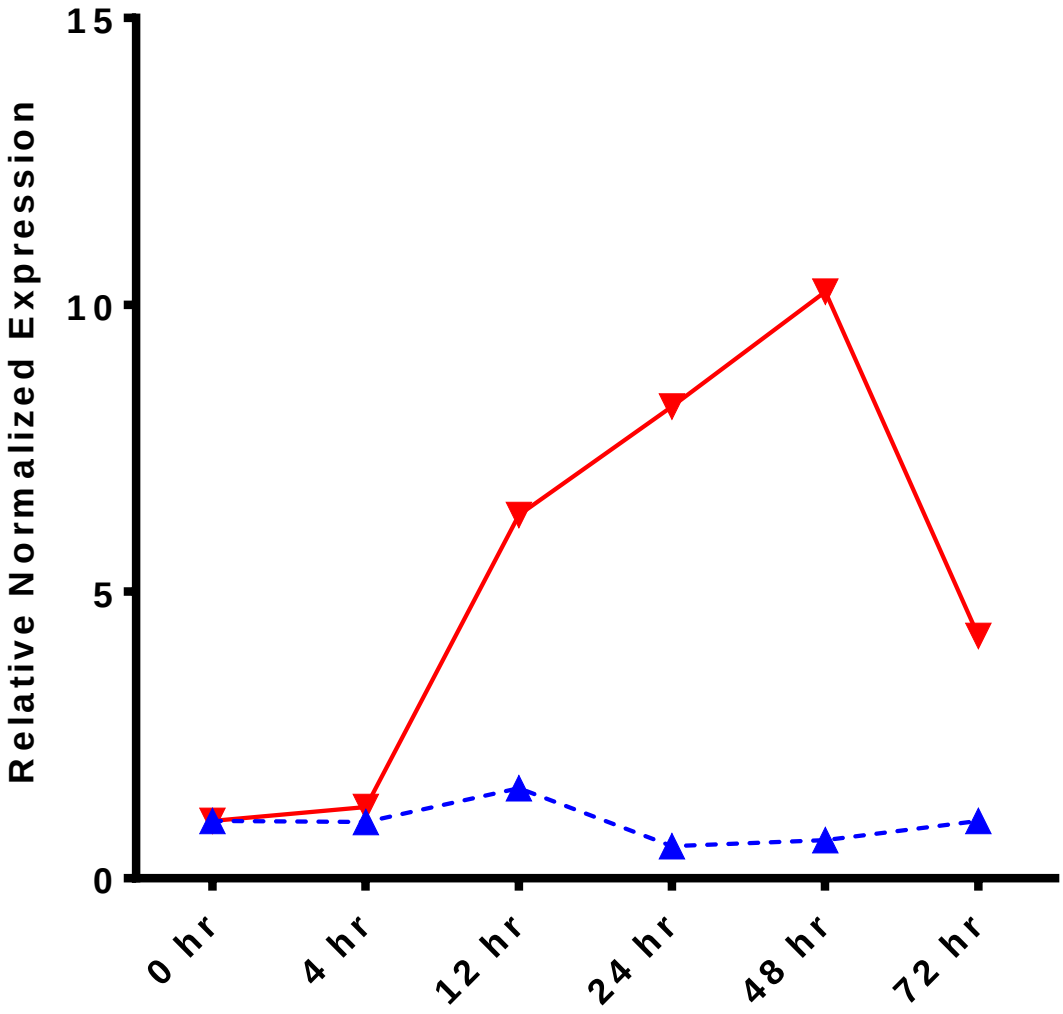
Relative Normalized Expression
15
10
5
0
0 hr
4 hr
12 hr
24 hr
48 hr
72 hr

TNF-alpha

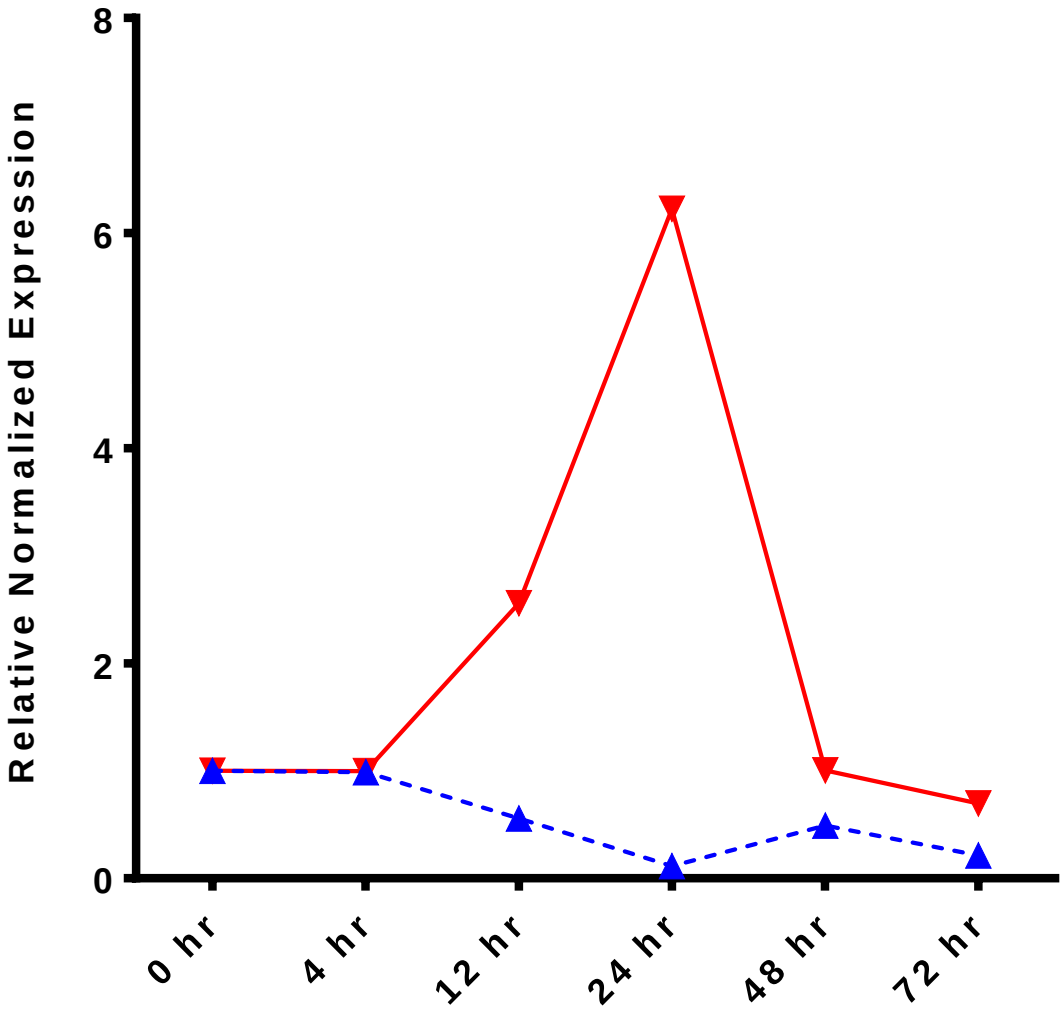
Relative Normalized Expression
8
6
4
2
0
0 hr
4 hr
12 hr
24 hr
48 hr
72 hr

TLR3

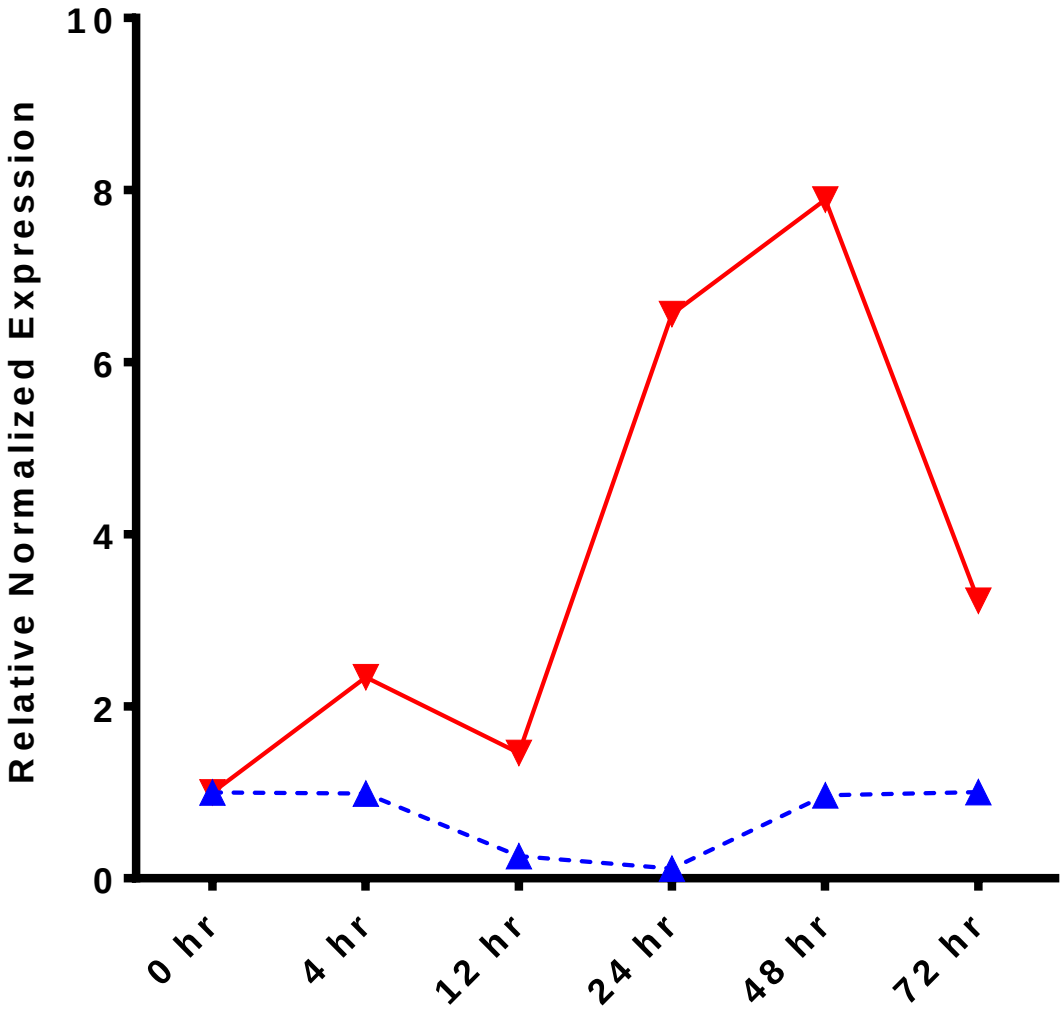
Relative Normalized Expression
10
8
6
4
2
0
0 hr
4 hr
12 hr
24 hr
48 hr
72 hr

TLR4

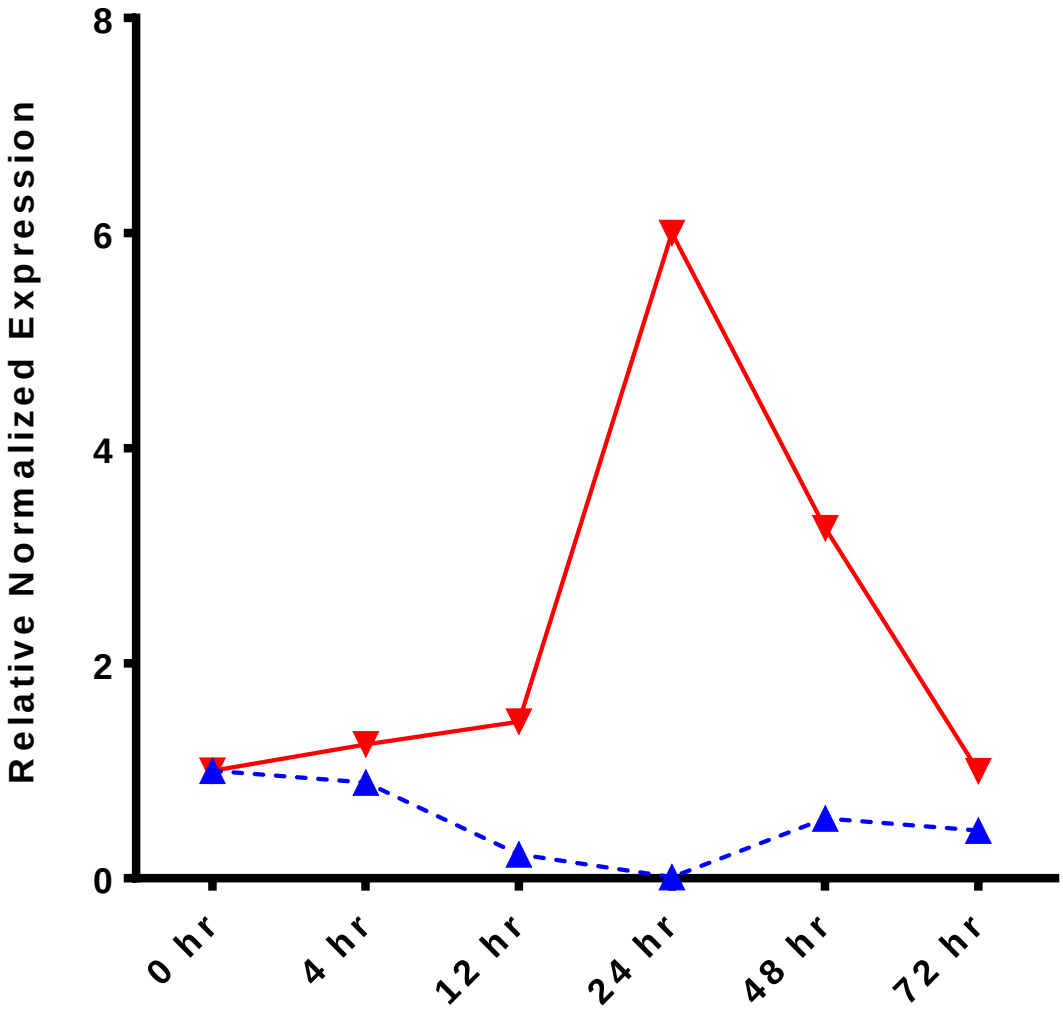
Relative Normalized Expression
8
6
4
2
0
0 hr
4 hr
12 hr
24 hr
48 hr
72 hr

TLR9

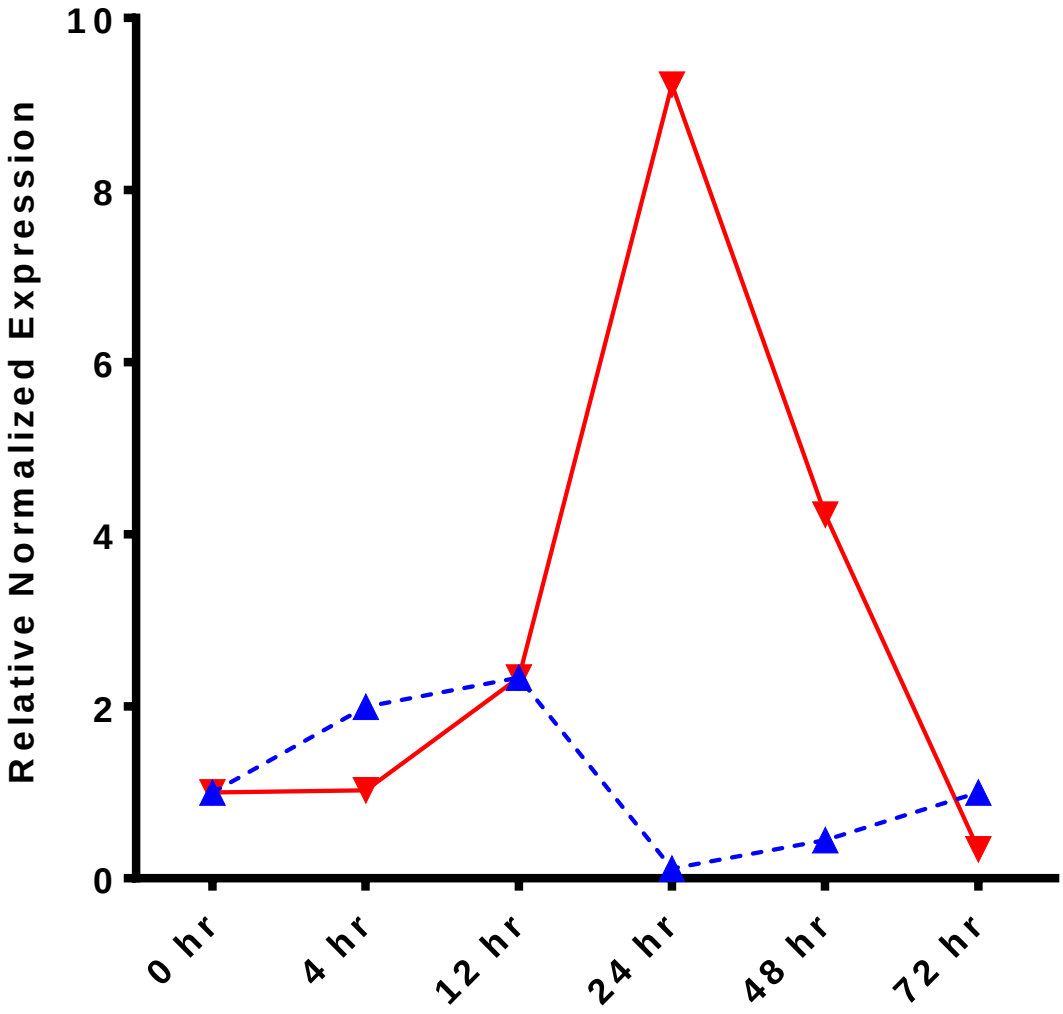
Relative Normalized Expression
10
8
6
4
2
0
0 hr
4 hr
12 hr
24 hr
48 hr
72 hr

ICAM1

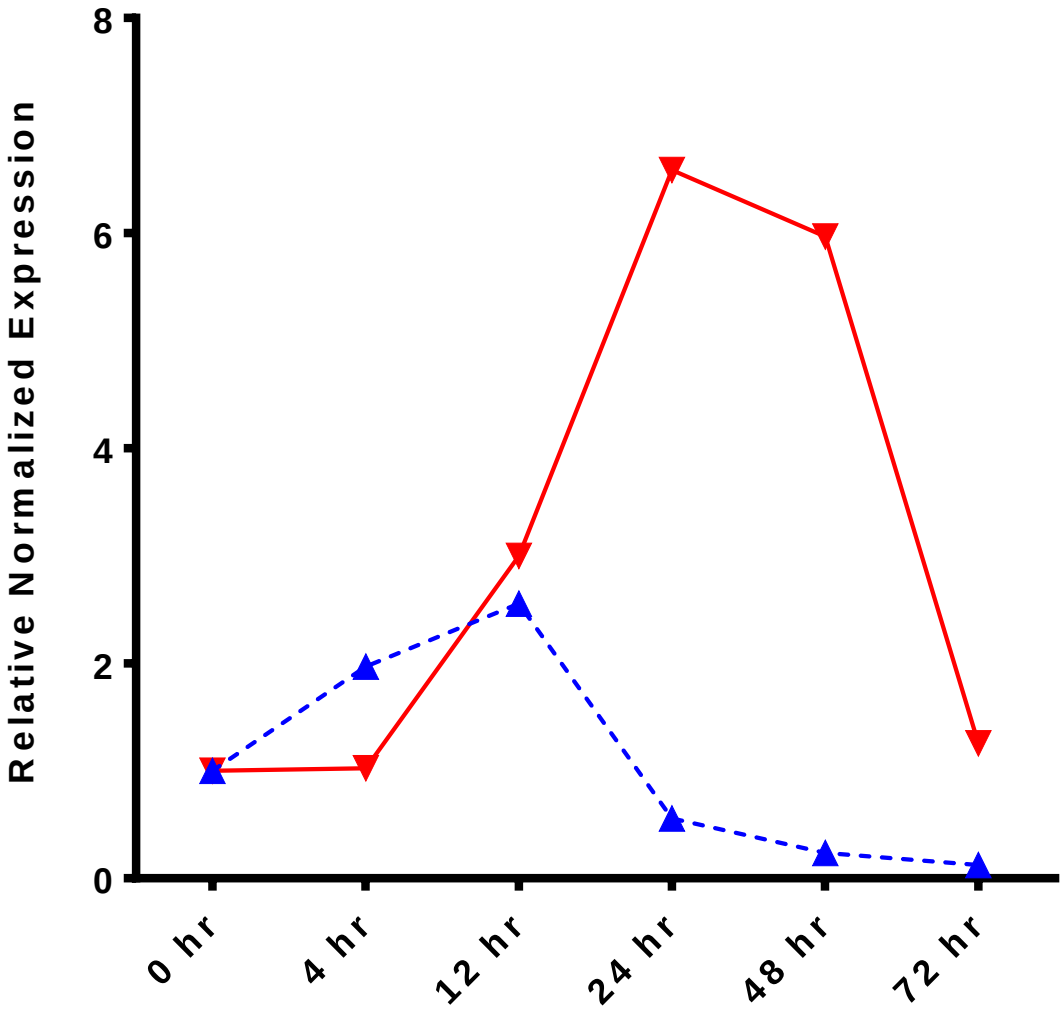
Relative Normalized Expression
8
6
4
2
0
0 hr
4 hr
12 hr
24 hr
48 hr
72 hr

VCAM1

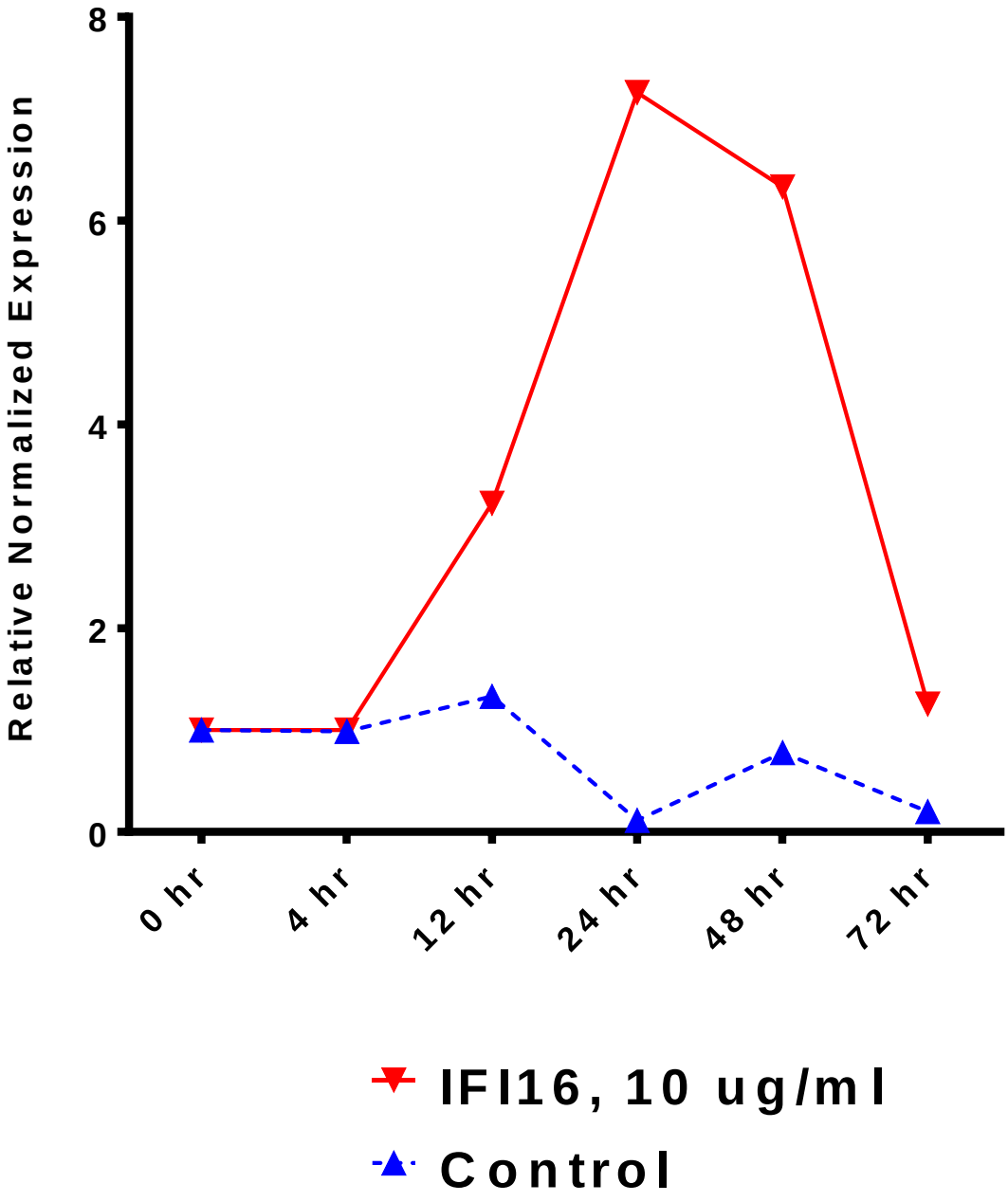
Relative Normalized Expression
8
6
4
2
0
0 hr
4 hr
12 hr
24 hr
48 hr
72 hr
IFI16, 10 ug/ml
Control

6 DISCUSSION

In this study, we demonstrate for the first time: i) the presence of significant levels of extracellular IFI16 protein in the sera of patients affected by systemic autoimmune diseases, including SSc, SjS, SLE and RA but not in non-SLE GN as compared to healthy controls, ii) that the extracellular IFI16 exerts biological effects on endothelial cells upon binding to a specific cell surface receptor and iii) extracellular IFI16 acts as an inflammatory stimuli for the production of different cytokines which could be the first steps of an autoimmune syndrome. These findings have important implications as they provide novel insights into the role of IFI16 in the pathogenesis of systemic autoimmune diseases. Various research groups, including ours, have shown that following transfection of virus-derived DNA [74, 75], or treatment with UVB [2], IFI16 delocalizes from the nucleus to the cytoplasm and is then eventually released into the extracellular milieu. Consistent with these observations, we now demonstrate the presence of circulating IFI16 protein in the sera of patients affected by systemic autoimmune diseases, but not in patients with non-autoimmune inflammatory diseases like non-SLE GN. Skin manifestations and vasculopathy are common components of a number of autoimmune diseases and represent a significant source of morbidity [76, 77]. Thus, to investigate the hypothesis that circulating IFI16 is able to exert harmful effects on target cells *in vivo*, an *in vitro* cell model consisting of primary endothelial cells (HUVEC) was used to test the activity of extracellular IFI16 on cell functions. These experiments clearly demonstrate that extracellular IFI16 affects some biological processes of endothelial cells, including tube morphogenesis and transwell migration. The specificity of these effects was assessed by the addition of anti-IFI16 antibodies which were able to neutralize the activity of the protein blocking its

inhibitory effects. Subsequently, the presence of IFI16 in the extracellular environment could also be the main reason behind the presence of anti-IFI16 autoantibodies in autoimmune patients' sera [78]. Together, these observations suggest the possible role of IFI16 in the clinical manifestation of autoimmune diseases, due to its presence in the extracellular environment. Since IFI16 can be released extracellularly which further reflect distinct extracellular biological activities, it is an indication of a novel alarmin function of this interferon inducible protein. Such stress-dependent shuttling, release, binding to cell surface was described in the past for autoantigen La/SS-B [79] and recently reviewed for HMGB1 protein [73] which upon release, binds to the cell surface receptors of neighboring cells. Thus as part of alarmin function, we further hypothesized that once released IFI16 protein must also bind neighboring cells to communicate the stress signal. In this direction, we assessed the affinity of IFI16 towards the plasma membrane of HUVEC. Confocal images visualized patterned binding of FITC labeled rIFI16 protein on the plasma membrane, which gave us the first preliminary evidence of the existence of an IFI16 interacting molecule which we suspect to be receptor-kind. Furthermore, we found experimental evidence that endogenous IFI16 protein released by dying cells bind neighboring cells. As a consequence of this binding, time-lapse studies proved its further entry into the cytoplasm. Moreover, such binding and transport of IFI16 was observed in different cell lines with different affinities. The experiments using radiolabeled IFI16 to investigate the binding kinetics of IFI16 in the HUVEC provide strong evidence supporting the presence of specific binding sites in the plasma membrane through which IFI16 exerts its cytotoxic activity. These binding sites were found to be saturable and competitive for IFI16, while the binding experiments in HUVEC indicate the

presence of approximately 250,000 to 450,000 binding sites per cell, with a dissociation constant (Kd) of 2.7nM. Similar binding characteristics were shown by different epithelial cell lines while a completely un-related cell line like fibroblasts demonstrated non-specific binding. This explains the specificity of IFI16 binding which is mostly restricted towards endothelium and epithelium. Neutralization experiments employing antibodies directed against different regions of the protein allowed us to demonstrate that the N-terminus, containing the PYD domain, is responsible for binding interaction. Consistent with this observation, the same antibodies were able to neutralize the biological activity of extracellular IFI16, as described earlier.

The activity of IFI16 is more similar to the DAMPs, for example HMGB1, which is released during cell death/necrosis/injury in the extracellular milieu. HMGB1 interacts with TLRs and RAGE to produce pro-inflammatory cytokines which further propagate the stress response and inflammation. We hypothesized the properties of IFI16 to be similar to such DAMPs. In relation to this hypothesis our quantitative PCR experiments demonstrate that IFI16 has cytokine stimulating activity which was proved by the overexpression of major chemokines such as IL-8, CCl2, CCL5 and CCL20. On the other hand TLRs such as TLR2, TLR4 and TLR9 were also observed to be modulated by IFI16 treatment on endothelial cells. These results suggest the specificity of IFI16 action on endothelial cells and other components of immune machinery. There could be a possibility of interacting TLRs in IFI16 mediated cytokine production and for the same our future experiments will be addressed to unravel the molecular mechanisms underlying IFI16 cytokine stimulating activity.

Overall the activity of IFI16 can be summarized as shown in the Figure. 20, which represent a model of an autoimmune syndrome with the involvement of IFI16.

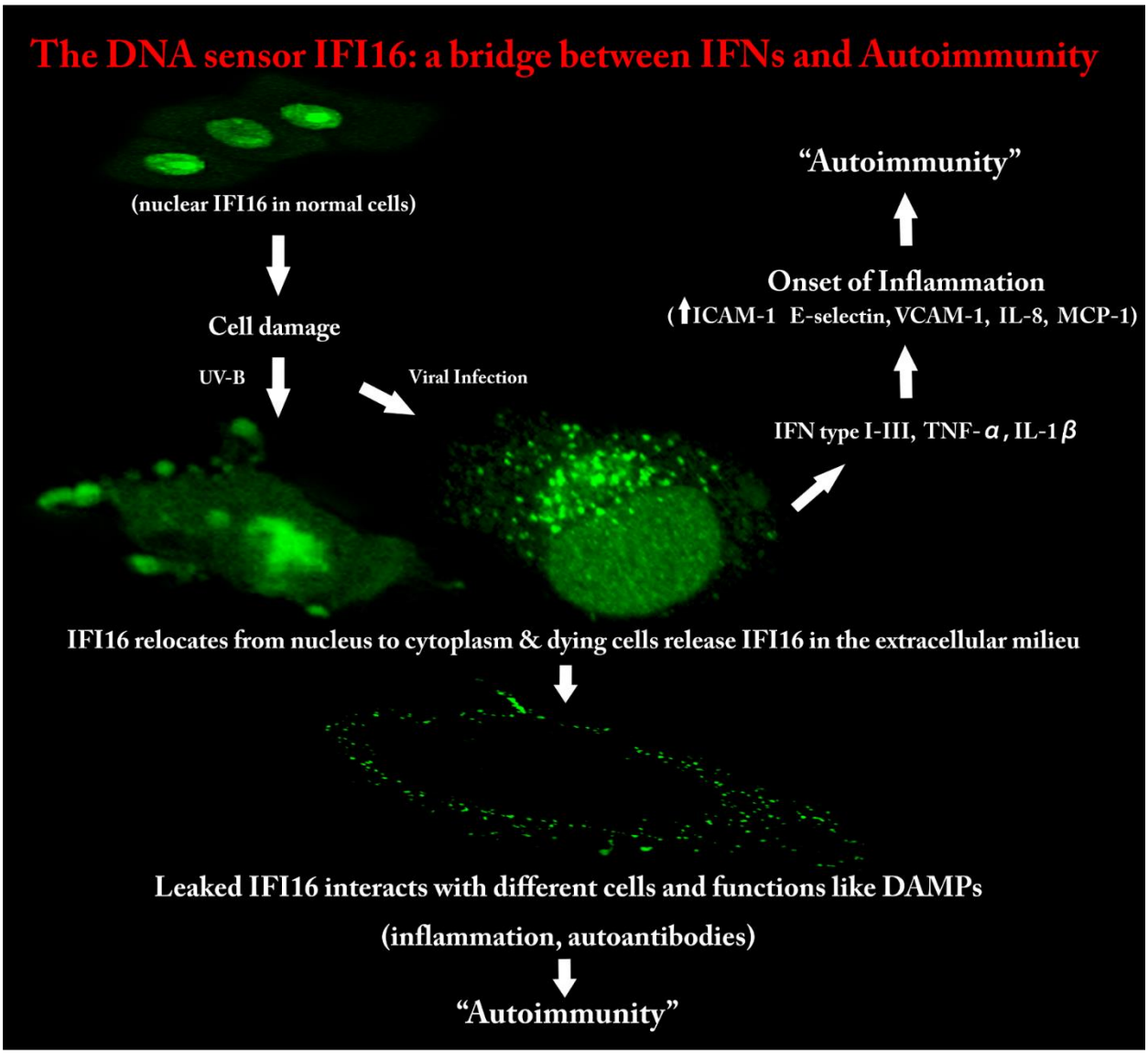

Figure 20: The involvement of IFI16 in the initiation and propagation of Autoimmunity

In summary, our results provide evidence for a novel alarmin function of IFI16 protein which is overexpressed upon inflammatory stimuli and then released in the extracellular environment. Once released, IFI16 binds to neighboring cells to Nf-κB dependent pathways for the production of different cytokines/chemokines which could propagate the stress signal causing damage. The presence of anti-IFI16 autoantibodies have been detected in many autoimmune diseases [32, 80-82], thus the release of IFI16 in the extracellular milieu and its cytokine stimulating activity represent a DAMP like behavior. We thus pronounce IFI16 as a novel DAMP like molecule which could be responsible for chronic stimulation of the immune system which marks the first step for the development of autoimmunity.

To shed some light into the viral restriction activity of IFI16 against HCMV, we recently demonstrated that the DNA sensor IFI16 restricts HCMV replication by down-regulating viral early and late but not immediate-early mRNAs and their protein expression [60]. In the attached manuscript (second author) we demonstrate that at an early time point during the in vitro infection of low-passage human embryonic lung fibroblasts (HELF), IFI16 binds to HCMV DNA. However, during a later phase following infection, IFI16 is mislocalized to the cytoplasmic virus assembly complex (AC), where it colocalizes with viral structural proteins. Indeed, upon its binding to pUL97, IFI16 undergoes phosphorylation and relocalizes to the cytoplasm of HCMV-infected cells. ESCRT (Endosomal Sorting Complex Required for Transport) machinery regulates the translocation of IFI16 into the virus AC by sorting and trafficking IFI16 into multivesicular bodies (MVB), as demonstrated by the interaction of IFI16 with two MVB markers: Vps4 and TGN46. Finally, IFI16 becomes incorporated into the newly assembled virions as demonstrated by Western blot analysis of purified virions and electron microscopy.

Together, these results suggest that HCMV has evolved mechanisms to mislocalize and hijack IFI16, trapping it within mature virions. However, the significance of this IFI16 trapping following nuclear mislocalization remains to be established.

7 BIBLIOGRAPHY

1. Dowling, J.K. and L.A. O'Neill, *Biochemical regulation of the inflammasome.* Crit Rev Biochem Mol Biol, 2012. **47**(5): p. 424-43.
2. Costa, S., et al., *Redistribution of the nuclear protein IFI16 into the cytoplasm of ultraviolet B-exposed keratinocytes as a mechanism of autoantigen processing.* Br J Dermatol, 2011. **164**(2): p. 282-90.
3. Gariglio, M., et al., *Immunohistochemical expression analysis of the human interferon-inducible gene IFI16, a member of the HIN200 family, not restricted to hematopoietic cells.* J Interferon Cytokine Res, 2002. **22**(7): p. 815-21.
4. Ermann, J. and C.G. Fathman, *Autoimmune diseases: genes, bugs and failed regulation.* Nat Immunol, 2001. **2**(9): p. 759-61.
5. Paludan, S.R., et al., *Recognition of herpesviruses by the innate immune system.* Nat Rev Immunol, 2011. **11**(2): p. 143-54.
6. Sinha, A.A., M.T. Lopez, and H.O. McDevitt, *Autoimmune diseases: the failure of self tolerance.* Science, 1990. **248**(4961): p. 1380-8.
7. Jacobson, D.L., et al., *Epidemiology and estimated population burden of selected autoimmune diseases in the United States.* Clin Immunol Immunopathol, 1997. **84**(3): p. 223-43.
8. Kong, J.S., S.S. Teuber, and M.E. Gershwin, *Potential adverse events with biologic response modifiers.* Autoimmun Rev, 2006. **5**(7): p. 471-85.
9. Borden, E.C., et al., *Interferons at age 50: past, current and future impact on biomedicine.* Nat Rev Drug Discov, 2007. **6**(12): p. 975-90.
10. Gualtierotti, R., et al., *Updating on the pathogenesis of systemic lupus erythematosus.* Autoimmun Rev, 2010. **10**(1): p. 3-7.

11. Waldman, M. and M.P. Madaio, *Pathogenic autoantibodies in lupus nephritis.* Lupus, 2005. **14**(1): p. 19-24.
12. Mok, C.C., *Biomarkers for lupus nephritis: a critical appraisal.* J Biomed Biotechnol, 2010. **2010**: p. 638413.
13. Hoffmann, M.H., et al., *Nucleic acid-associated autoantigens: pathogenic involvement and therapeutic potential.* J Autoimmun, 2010. **34**(3): p. J178-206.
14. Gu, Y.S., et al., *The immunobiology of systemic sclerosis.* Semin Arthritis Rheum, 2008. **38**(2): p. 132-60.
15. Abraham, D.J. and J. Varga, *Scleroderma: from cell and molecular mechanisms to disease models.* Trends Immunol, 2005. **26**(11): p. 587-95.
16. Tan, F.K., *Autoantibodies against PDGF receptor in scleroderma.* N Engl J Med, 2006. **354**(25): p. 2709-11.
17. Coelho, F.M., et al., *The chemokine receptors CXCR1/CXCR2 modulate antigen-induced arthritis by regulating adhesion of neutrophils to the synovial microvasculature.* Arthritis Rheum, 2008. **58**(8): p. 2329-37.
18. Dieude, P., *Rheumatic diseases: environment and genetics.* Joint Bone Spine, 2009. **76**(6): p. 602-7.
19. Dieguez-Gonzalez, R., et al., *Association of interferon regulatory factor 5 haplotypes, similar to that found in systemic lupus erythematosus, in a large subgroup of patients with rheumatoid arthritis.* Arthritis Rheum, 2008. **58**(5): p. 1264-74.
20. Orozco, G., et al., *Association of STAT4 with rheumatoid arthritis: a replication study in three European populations.* Arthritis Rheum, 2008. **58**(7): p. 1974-80.

21. Zervou, M.I., et al., *Association of a TRAF1 and a STAT4 gene polymorphism with increased risk for rheumatoid arthritis in a genetically homogeneous population.* Hum Immunol, 2008. **69**(9): p. 567-71.
22. Banchereau, J., V. Pascual, and A.K. Palucka, *Autoimmunity through cytokine-induced dendritic cell activation.* Immunity, 2004. **20**(5): p. 539-50.
23. Trinchieri, G. and A. Sher, *Cooperation of Toll-like receptor signals in innate immune defence.* Nat Rev Immunol, 2007. **7**(3): p. 179-90.
24. Biggioggero, M., L. Gabbriellini, and P.L. Meroni, *Type I interferon therapy and its role in autoimmunity.* Autoimmunity, 2010. **43**(3): p. 248-54.
25. Hall, J.C. and A. Rosen, *Type I interferons: crucial participants in disease amplification in autoimmunity.* Nat Rev Rheumatol, 2010. **6**(1): p. 40-9.
26. Obermoser, G. and V. Pascual, *The interferon-alpha signature of systemic lupus erythematosus.* Lupus, 2010. **19**(9): p. 1012-9.
27. Crow, M.K., *Type I interferon and autoimmune disease.* Autoimmunity, 2003. **36**(8): p. 445-6.
28. Crow, M.K., *Type I interferon in systemic lupus erythematosus.* Curr Top Microbiol Immunol, 2007. **316**: p. 359-86.
29. Nordmark, G., G.V. Alm, and L. Ronnblom, *Mechanisms of Disease: primary Sjogren's syndrome and the type I interferon system.* Nat Clin Pract Rheumatol, 2006. **2**(5): p. 262-9.
30. Kimoto, O., et al., *Activation of the interferon pathway in peripheral blood of patients with Sjogren's syndrome.* J Rheumatol, 2011. **38**(2): p. 310-6.
31. Eloranta, M.L., et al., *Type I interferon system activation and association with disease manifestations in systemic sclerosis.* Ann Rheum Dis, 2010. **69**(7): p. 1396-402.

32. Mondini, M., et al., *Role of the interferon-inducible gene IFI16 in the etiopathogenesis of systemic autoimmune disorders.* Ann N Y Acad Sci, 2007. **1110**: p. 47-56.
33. Gariglio, M., et al., *The multifaceted interferon-inducible p200 family proteins: from cell biology to human pathology.* J Interferon Cytokine Res, 2011. **31**(1): p. 159-72.
34. Bertin, J. and P.S. DiStefano, *The PYRIN domain: a novel motif found in apoptosis and inflammation proteins.* Cell Death Differ, 2000. **7**(12): p. 1273-4.
35. Park, H.H., et al., *The death domain superfamily in intracellular signaling of apoptosis and inflammation.* Annu Rev Immunol, 2007. **25**: p. 561-86.
36. Aglipay, J.A., et al., *A member of the Pyrin family, IFI16, is a novel BRCA1-associated protein involved in the p53-mediated apoptosis pathway.* Oncogene, 2003. **22**(55): p. 8931-8.
37. Choubey, D., et al., *Interferon-inducible p200-family proteins as novel sensors of cytoplasmic DNA: role in inflammation and autoimmunity.* J Interferon Cytokine Res, 2010. **30**(6): p. 371-80.
38. Mondini, M., et al., *The interferon-inducible HIN-200 gene family in apoptosis and inflammation: implication for autoimmunity.* Autoimmunity, 2010. **43**(3): p. 226-31.
39. Albrecht, M., D. Choubey, and T. Lengauer, *The HIN domain of IFI-200 proteins consists of two OB folds.* Biochem Biophys Res Commun, 2005. **327**(3): p. 679-87.
40. Yan, H., et al., *RPA nucleic acid-binding properties of IFI16-HIN200.* Biochim Biophys Acta, 2008. **1784**(7-8): p. 1087-97.

41. Krieg, A.M., *AIMing 2 defend against intracellular pathogens.* Nat Immunol, 2010. **11**(5): p. 367-9.
42. Krieg, A.M., *AIMing 2 detect foreign DNA.* Sci Signal, 2009. **2**(77): p. pe39.
43. Unterholzner, L., et al., *IFI16 is an innate immune sensor for intracellular DNA.* Nat Immunol, 2010. **11**(11): p. 997-1004.
44. Gugliesi, F., et al., *Up-regulation of the interferon-inducible IFI16 gene by oxidative stress triggers p53 transcriptional activity in endothelial cells.* J Leukoc Biol, 2005. **77**(5): p. 820-9.
45. Caposio, P., et al., *A novel role of the interferon-inducible protein IFI16 as inducer of proinflammatory molecules in endothelial cells.* J Biol Chem, 2007. **282**(46): p. 33515-29.
46. Hornung, V., et al., *AIM2 recognizes cytosolic dsDNA and forms a caspase-1-activating inflammasome with ASC.* Nature, 2009. **458**(7237): p. 514-8.
47. Kerur, N., et al., *IFI16 acts as a nuclear pathogen sensor to induce the inflammasome in response to Kaposi Sarcoma-associated herpesvirus infection.* Cell Host Microbe, 2011. **9**(5): p. 363-75.
48. Bijl, M., et al., *Inflammatory clearance of apoptotic cells after UVB challenge.* Autoimmunity, 2007. **40**(4): p. 244-8.
49. Bijl, M. and C.G. Kallenberg, *Ultraviolet light and cutaneous lupus.* Lupus, 2006. **15**(11): p. 724-7.
50. Ansari, M.A., et al., *Constitutive interferon-inducible protein 16-inflammasome activation during Epstein-Barr virus latency I, II, and III in B and epithelial cells.* J Virol, 2013. **87**(15): p. 8606-23.

51. Cristea, I.M., et al., *Human cytomegalovirus pUL83 stimulates activity of the viral immediate-early promoter through its interaction with the cellular IFI16 protein.* J Virol, 2010. **84**(15): p. 7803-14.

52. Cristea, I.M., et al., *Host factors associated with the Sindbis virus RNA-dependent RNA polymerase: role for G3BP1 and G3BP2 in virus replication.* J Virol, 2010. **84**(13): p. 6720-32.

53. Horan, K.A., et al., *Proteasomal degradation of herpes simplex virus capsids in macrophages releases DNA to the cytosol for recognition by DNA sensors.* J Immunol, 2013. **190**(5): p. 2311-9.

54. Johnson, K.E., L. Chikoti, and B. Chandran, *Herpes simplex virus 1 infection induces activation and subsequent inhibition of the IFI16 and NLRP3 inflammasomes.* J Virol, 2013. **87**(9): p. 5005-18.

55. Orzalli, M.H., N.A. DeLuca, and D.M. Knipe, *Nuclear IFI16 induction of IRF-3 signaling during herpesviral infection and degradation of IFI16 by the viral ICP0 protein.* Proc Natl Acad Sci U S A, 2012. **109**(44): p. E3008-17.

56. Singh, V.V., et al., *Decreased pattern recognition receptor signaling, interferon-signature, and bactericidal/permeability-increasing protein gene expression in cord blood of term low birth weight human newborns.* PLoS One, 2013. **8**(4): p. e62845.

57. Li, T., J. Chen, and I.M. Cristea, *Human cytomegalovirus tegument protein pUL83 inhibits IFI16-mediated DNA sensing for immune evasion.* Cell Host Microbe, 2013. **14**(5): p. 591-9.

58. Berg, R.K., et al., *T cells detect intracellular DNA but fail to induce type I IFN responses: implications for restriction of HIV replication.* PLoS One, 2014. **9**(1): p. e84513.

59. Monroe, K.M., et al., *IFI16 DNA sensor is required for death of lymphoid CD4 T cells abortively infected with HIV.* Science, 2014. **343**(6169): p. 428-32.
60. Gariano, G.R., et al., *The intracellular DNA sensor IFI16 gene acts as restriction factor for human cytomegalovirus replication.* PLoS Pathog, 2012. **8**(1): p. e1002498.
61. Duggal, N.K. and M. Emerman, *Evolutionary conflicts between viruses and restriction factors shape immunity.* Nat Rev Immunol, 2012. **12**(10): p. 687-95.
62. Tavalai, N. and T. Stamminger, *Intrinsic cellular defense mechanisms targeting human cytomegalovirus.* Virus Res, 2011. **157**(2): p. 128-33.
63. Saffert, R.T. and R.F. Kalejta, *Inactivating a cellular intrinsic immune defense mediated by Daxx is the mechanism through which the human cytomegalovirus pp71 protein stimulates viral immediate-early gene expression.* J Virol, 2006. **80**(8): p. 3863-71.
64. Baggetta, R., et al., *The interferon-inducible gene IFI16 secretome of endothelial cells drives the early steps of the inflammatory response.* Eur J Immunol, 2010. **40**(8): p. 2182-9.
65. Pauwels, R., et al., *Rapid and automated tetrazolium-based colorimetric assay for the detection of anti-HIV compounds.* J Virol Methods, 1988. **20**(4): p. 309-21.
66. Gugliesi, F., et al., *Tumor-derived endothelial cells evade apoptotic activity of the interferon-inducible IFI16 gene.* J Interferon Cytokine Res, 2011. **31**(8): p. 609-18.
67. Koristka, S., et al., *Retargeting of regulatory T cells to surface-inducible autoantigen La/SS-B.* J Autoimmun, 2013. **42**: p. 105-16.

68. Coleman, J.W. and R.C. Godfrey, *The number and affinity of IgE receptors on dispersed human lung mast cells.* Immunology, 1981. **44**(4): p. 859-63.

69. Imai, Y., et al., *Epidermal growth factor receptors and effect of epidermal growth factor on growth of human breast cancer cells in long-term tissue culture.* Cancer Res, 1982. **42**(11): p. 4394-8.

70. Gugliesi, F., et al., *Nuclear DNA sensor IFI16 as circulating protein in autoimmune diseases is a signal of damage that impairs endothelial cells through high-affinity membrane binding.* PLoS One, 2013. **8**(5): p. e63045.

71. Guiducci, S., et al., *Mechanisms of vascular damage in SSc--implications for vascular treatment strategies.* Rheumatology (Oxford), 2008. **47 Suppl 5**: p. v18-20.

72. Bianchi, M.E., *DAMPs, PAMPs and alarmins: all we need to know about danger.* J Leukoc Biol, 2007. **81**(1): p. 1-5.

73. Harris, H.E., U. Andersson, and D.S. Pisetsky, *HMGB1: a multifunctional alarmin driving autoimmune and inflammatory disease.* Nat Rev Rheumatol, 2012. **8**(4): p. 195-202.

74. Keating, S.E., M. Baran, and A.G. Bowie, *Cytosolic DNA sensors regulating type I interferon induction.* Trends Immunol, 2011. **32**(12): p. 574-81.

75. Unterholzner, L. and A.G. Bowie, *Innate DNA sensing moves to the nucleus.* Cell Host Microbe, 2011. **9**(5): p. 351-3.

76. Kaplan, M.J., *Endothelial damage and autoimmune diseases.* Autoimmunity, 2009. **42**(7): p. 561-2.

77. Rashtak, S. and M.R. Pittelkow, *Skin involvement in systemic autoimmune diseases.* Curr Dir Autoimmun, 2008. **10**: p. 344-58.

78. Caneparo, V., et al., *Anti-IFI16 antibodies and their relation to disease characteristics in systemic lupus erythematosus.* Lupus, 2013. **22**(6): p. 607-13.

79. Bachmann, M., T. Zaubitzer, and W.E. Muller, *The autoantigen La/SSB: detection on and uptake by mitotic cells.* Exp Cell Res, 1992. **201**(2): p. 387-98.

80. Rekvig, O.P., et al., *Autoantibodies in lupus: culprits or passive bystanders?* Autoimmun Rev, 2012. **11**(8): p. 596-603.

81. Mondini, M., et al., *A novel autoantigen to differentiate limited cutaneous systemic sclerosis from diffuse cutaneous systemic sclerosis: the interferon-inducible gene IFI16.* Arthritis Rheum, 2006. **54**(12): p. 3939-44.

82. Costa, S., et al., *Detection of anti-IFI16 antibodies by ELISA: clinical and serological associations in systemic sclerosis.* Rheumatology (Oxford), 2011. **50**(4): p. 674-81.

8 PUBLICATIONS

1. Gugliesi F*, **Bawadekar M***, De Andrea M, Dell'Oste V, Caneparo V, Gariglio M and Landolfo S. Nuclear DNA Sensor IFI16 as Circulating Protein in Autoimmune Diseases Is a Signal of Damage that Impairs Endothelial Cells through High-Affinity Membrane Binding. PLoS ONE, 2013, 8(5): e63045. doi:10.1371/journal.pone.0063045. (* Contributed Equally)

2. Dell'Oste V, Gatti D, Gugliesi F, De Andrea M, **Bawadekar M**, Lo Cigno I, Biolatti M, Vallino M, Marschall M, Gariglio M and Landolfo S. Early stage IFI16 cytoplasmic translocation and late stage entrapment into egressing virions during HCMV infection. (submitted)

OPEN ACCESS Freely available online

PLOS ONE

Nuclear DNA Sensor IFI16 as Circulating Protein in Autoimmune Diseases Is a Signal of Damage that Impairs Endothelial Cells through High-Affinity Membrane Binding

Francesca Gugliesi[1☯], Mandar Bawadekar[2,3☯], Marco De Andrea[1,2], Valentina Dell'Oste[1], Valeria Caneparo[2,3], Angela Tincani[4], Marisa Gariglio[2,3], Santo Landolfo[1]*

1 Department of Public Health and Pediatric Sciences, University of Turin, Medical School, Turin, Italy, **2** Department of Translational Medicine, University of Piemonte Orientale "Amedeo Avogadro", Medical School, Novara, Italy, **3** Interdisciplinary Research Center of Autoimmune Diseases, Department of Translational Medicine, University of Piemonte Orientale "Amedeo Avogadro", Medical School, Novara, Italy, **4** Rheumatology and Clinical Immunology, Spedali Civili and University of Brescia, Brescia, Italy

Abstract

IFI16, a nuclear pathogenic DNA sensor induced by several pro-inflammatory cytokines, is a multifaceted protein with various functions. It is also a target for autoantibodies as specific antibodies have been demonstrated in the sera of patients affected by systemic autoimmune diseases. Following transfection of virus-derived DNA, or treatment with UVB, IFI16 delocalizes from the nucleus to the cytoplasm and is then eventually released into the extracellular milieu. In this study, using an in-house capture enzyme-linked immunsorbent assay we demonstrate that significant levels of IFI16 protein can also exist as circulating form in the sera of autoimmune patients. We also show that the rIFI16 protein, when added in-vitro to endothelial cells, does not affect cell viability, but severely limits their tubulogenesis and transwell migration activities. These inhibitory effects are fully reversed in the presence of anti-IFI16 N-terminal antibodies, indicating that its extracellular activity resides within the N-terminus. It was further demonstrated that endogenous IFI16 released by apoptotic cells bind neighboring cells in a co-culture. Immunofluorescence assays revealed existence of high-affinity binding sites on the plasma membrane of endothelial cells. Free recombinant IFI16 binds these sites on HUVEC with dissociation constant of 2.7 nM, radioiodinated and unlabeled IFI16 compete for binding sites, with inhibition constant (K_i) of 14.43 nM and half maximal inhibitory concentration (IC_{50}) of 67.88 nM; these data allow us to estimate the presence of 250,000 to 450,000 specific binding sites per cell. Corroborating the results from functional assays, this binding could be completely inhibited using anti-IFI16 N-terminal antibody, but not with an antibody raised against the IFI16 C-terminal. Altogether, these data demonstrate that IFI16 may exist as circulating protein in the sera of autoimmune patients which binds endothelial cells causing damage, suggesting a new pathogenic and alarmin function through which this protein triggers the development of autoimmunity.

Citation: Gugliesi F, Bawadekar M, De Andrea M, Dell'Oste V, Caneparo V, et al. (2013) Nuclear DNA Sensor IFI16 as Circulating Protein in Autoimmune Diseases Is a Signal of Damage that Impairs Endothelial Cells through High-Affinity Membrane Binding. PLoS ONE 8(5): e63045. doi:10.1371/journal.pone.0063045

Editor: Michael P. Bachmann, Carl-Gustav Carus Technical University-Dresden, Germany

Received February 4, 2013; **Accepted** March 28, 2013; **Published** May 14, 2013

Funding: This study was supported by MIUR PRIN 2008 (Ministero dell'Istruzione, dell'Università e della Ricerca - Progetti di Ricerca di Interesse Nazionaleto) to SL, MG and AT, and research funding from the University of Turin 2011 to SL. VC acknowledges a grant for the Lagrange Project-CRT Foundation. MB is a recipient of an international PhD fellowship in Innovative Biomedical Technologies (IBT) funded by Cariplo Foundation-Milan, Italy. The funders had no role in study design, data collection and analysis, decision to publish, or preparation of the manuscript.

Competing Interests: The authors have declared that no competing interests exist.

* E-mail: santo.landolfo@unito.it

☯ These authors contributed equally to this work.

Introduction

A wealth of data now exists demonstrating the critical role of interferons (IFNs) in the pathogenesis and perpetuation of autoimmunity [1–5]. Genomic studies have revealed that type I IFN inducible genes are markedly overexpressed in the peripheral blood of patients with systemic autoimmune diseases including Systemic Lupus Erythematosus (SLE), Systemic Sclerosis (SSc), and Sjogren's Syndrome (SjS) [6–8]. In SLE patients, this so-called "IFN signature" is generally associated with active disease states, renal, and CNS involvement [9]. Together, these findings have led to the hypothesis that type I IFNs (IFN-α and IFN-β) may be the master cytokines responsible for the initiation and progression of the autoimmune process [10–12].

One family of IFN-inducible genes is the HIN200/Ifi200 gene family, which encodes evolutionary related human (IFI16, IFIX, MNDA, and AIM2) and murine (Ifi202a, Ifi202b, Ifi203, Ifi204, Ifi205/D3, and Ifi206) proteins. The common domain architecture of this protein family consists of one or two copies of the HIN domain (a 200 amino acid repeat) and an N-terminal PYD domain, also named PAAD, DAPIN, or Pyrin. The PYD domain, commonly found in death-family proteins, like Pyrin and ASC, is present in the N terminus of most HIN200 proteins, suggesting a role of these proteins in inflammation and apoptosis [13,14]. The

IFI16 protein is specifically expressed in vascular endothelial cells, keratinocytes, and hematopoietic cells [15] and has been recently shown to act as a foreign DNA sensor [16–19]. We have previously demonstrated that oxidative stress and various proinflammatory cytokines can also trigger IFI16 nuclear expression [20] and [21]. In addition, a role of IFI16 as an inducer of proinflammatory molecules (e.g. ICAM-1, RANTES, and CCL20) and apoptosis in endothelial cells has also been observed, supporting its role in the initial steps of the inflammatory processes that precede the onset of autoimmune syndromes [22–24]. IFI16 protein is also a target for autoantibodies. Anti-IFI16 autoantibodies have been demonstrated in the sera of patients affected by systemic autoimmune diseases including SLE, SSc, and SjS. [25–28]. To explain this observation, we hypothesized that its overexpression and extranuclear appearance during cell death contribute to its release into the extracellular milieu and eventually to the induction of specific autoantibodies. Consistent with this hypothesis, we have recently demonstrated *in vitro* that the IFI16 protein, normally detected in the nucleus of human keratinocytes, can be induced to appear in the cytoplasm under conditions of UV light-induced cell injury and then released in the culture media. A similar situation was also found in tissue sections of skin biopsies from patients with SLE. In this model, IFI16 expression was upregulated and mislocalized to the cytoplasm, suggesting that aberrant expression of IFI16 in epithelial and inflammatory cells can also play a role in triggering an autoimmune response *in vivo* [29]. However, since IFI16 was previously thought to be restricted to the intracellular environment, and in particular to the nucleus [13,30], all the recognized biological activities of IFI16, as well as their possible links with human pathologies, have only been considered in relation to this localization. Indeed, all the *in vitro* studies published to date have involved the overexpressing or down-regulation of IFI16 in different cell models, and the modulation of IFI16 has always been monitored intracellularly (i.e. using cell extracts or by directly analyzing the presence of IFI16 inside the cells, for instance using immunofluorescence techniques).

In the present study, using an in-house enzyme-linked immunosorbent assay (ELISA) we demonstrate the presence of detectable amounts of a circulating form of IFI16 in the sera from patients affected by autoimmune disorders. We also provide experimental evidence showing that the extracellular form of IFI16 is directly involved in specifically down-regulating the migratory activities and tube morphogenesis of endothelial cells. Moreover, we demonstrate the ability of IFI16 to bind to the plasma membrane of endothelial cells and, by means of binding kinetics analyses, we show for the first time, evidence of high affinity IFI16 binding sites on these cells. These data point to a new pathogenic mechanism through which IFI16 is triggering systemic autoimmune diseases.

Materials and Methods

Cell Cultures

Human umbilical vein endothelial cells (HUVECs), were grown in Endothelial cell growth medium-2 *(EGM-2)* (Lonza, Italy) with 2% Fetal Bovine Serum (Sigma-Aldrich, Milan, Italy) and supplemented with 1% Penicillin-Streptomycin solution (Sigma-Aldrich, Milan, Italy) as previously described [31]. Low passage human dermal fibroblasts, HDF (ATCC), mouse fibroblasts, 3T3 (ATCC), HeLa (ATCC) and HaCaT (ATCC) cells were grown in Dulbecco's modified Eagle's medium (*DMEM)* (Sigma-Aldrich, Milan, Italy) supplemented with 10% fetal bovine serum and 2% Penicillin-Streptomycin solution Unless specified, all cells were grown at 37°C and 5% CO_2.

Recombinant Proteins

The entire coding sequence of the b isoform of human IFI16 was subcloned into the pET30a expression vector (Novagen, Madison, WI) containing an N-terminal histidine tag. Protein Expression and affinity purification, followed by fast protein liquid chromatography (FPLC), were performed according to standard procedures. The purity of the proteins was assessed by 10% sodium dodecyl sulfate-polyacrylamide gel electrophoresis. As negative controls in enzyme-linked immunosorbent assays (ELISA), the polypeptide encoded by the pET30a empty vector (control peptide) was expressed and purified according to the same protocol.

Patients and Determination of Human Extracellular IFI16 by Capture ELISA

The study groups comprised patients suffering from Systemic Sclerosis, (n = 50), Systemic Lupus Erythematosus, (n = 100), Sjogren Syndrome, (n = 49), Rheumatoid Arthritis (n = 50) and Non-SLE Glomerulonephritis (n = 46). As controls, we investigated sera from 116 sex- and age-matched healthy subjects. Written informed consent was obtained from all subjects according to the Declaration of Helsinki and approval was obtained from local ethics committees of corresponding hospital.

For the determination of circulating extracellular IFI16, a capture ELISA was employed. Briefly, polystyrene micro-well plates (Nunc-Immuno MaxiSorp; Nunc, Roskilde, Denmark) were coated with a home-made polyclonal rabbit-anti-IFI16 antibody (478–729 aa). Subsequently, plates were washed and free binding sites then saturated with PBS/0.05% Tween/3% BSA. After blocking, sera were added to plates in duplicate. Purified 6His-IFI16 protein was used as the standard and BSA served as the negative control. The samples were washed, monoclonal mouse anti-IFI16 antibody (Santa Cruz, sc-8023) added, and then incubated for 1 h at room temperature. After washing, horseradish peroxidase-conjugated anti-mouse antibody (GE Healthcare Europe GmbH, Milan, Italy) was added. Following the addition of the substrate (TMB; KPL, Gaithersburg, MD, USA), absorbance was measured at 450 nm using a microplate reader (TECAN, Mannedorf, Switzerland). Concentrations of extracellular IFI16 were determined using a standard curve for which increasing concentrations of purified 6His-IFI16 were used.

Cell Viability Assay

Cells were seeded at a density of 1×10^4/well in a 96-well culture plate. After 24 hours, cells were treated with different doses (10, 25 or 50 μg/ml) of recombinant IFI16 protein (IFI16), mock-treated using the same volume of vehicle as each IFI16 dose (Mock), or left untreated (NT). Where indicated, different doses (1.75 μgr or 3.5 μgr) of antibody against IFI16 were added. Forty-eight hours after treatment, cell viability was determined using the 3-(4,5-dimethylthiazol-2-yl)-2,5-diphenyltetrazolium bromide (MTT) (Sigma-Aldrich, Milan, Italy) method, as previously described [32].

Tube Morphogenesis Assay

HUVEC were seeded in complete medium in 60-mm culture dishes coated with 0.2% gelatin (Sigma-Aldrich, Milan, Italy) and were treated for 48 h with different doses (10 or 25 μg/ml) of recombinant IFI16 protein (IFI16). As negative controls, cells were treated with the same volumes of vehicle (Mock) used for each IFI16 dose or left untreated (NT). Where indicated, different doses

(1.75 μgr or 3.5 μgr) of antibody against IFI16 were added. Tube morphogenesis assay was performed as described in [33]. Briefly, a 24-microwell plate, pre-chilled at −20°C, was coated with 250 μl/well of Matrigel Basement Membrane (5 mg/ml; Becton and Dickinson, Milan, Italy) and then incubated at 37°C for 30 min until solidified. HUVEC (8×10^4 cells/500 μl per well) were seeded onto the matrix and allowed to incubate at 37°C in 5% CO_2. Plates were photographed after 6 h using a Leica inverted microscope.

Migration Assay

Twenty-four well transwell inserts with an 8 μm pore size (Corning B.V. Life Sciences, Amsterdam, The Netherlands) were coated with a thin layer of gelatin (0.2%). HUVECs cultured in EGM-2 with 2% FBS and pre-treated with different concentrations of IFI16 recombinant protein or mock- or untreated for 48 hours were washed twice with PBS, trypsinized and plated into the upper chambers (4×10^5 cells) resuspended in 200 μl of EBM-2 (Lonza, Italy), 0.1% BSA (Sigma-Aldrich, Milan, Italy) plus IFI16 recombinant protein or mock solution (the same amounts as in the 48 h pre-treatment). The lower chambers were filled with 600 μl EGM2 containing VEGF and bFGF (as chemo-attractants) (Sigma-Aldrich, Milan, Italy), 2% FBS, and IFI16 recombinant protein or mock solution (the same amounts as in the upper chamber). The chambers were incubated for 5 h at 37°C in a humidified atmosphere containing 5% CO_2. After incubation, cells on the upper side of the filter were removed. The cells that had migrated to the lower side of the filter were washed twice with PBS, fixed with 2.5% glutaraldehyde (Sigma-Aldrich, Milan, Italy) for 20 min at room temperature, and stained with 0.5 ml crystal violet (0.1% in 20% methyl alcohol solution) (Sigma-Aldrich, Milan, Italy). After washes, color was developed in 10% acetic acid and read in duplicate at 540 nm on a microplate reader (Victor 3; Perkin-Elmer, Boston, MA).

rIFI16-FITC Membrane Binding and Confocal Microscopy

HUVEC were seeded in 24-well plate in the presence of glass cover-slip and were grown overnight in presence of 1 μg/ml tunicamycin (Sigma-Aldrich, Milan, Italy) in EGM-2 medium with 2% FBS and antibiotics. The cells were washed twice with cold PBS and incubated with increasing concentrations (10 nM, 20 nM, 30 nM) of FITC labeled rIFI16 (FluoReporter® FITC Protein Labeling Kit by Invitrogen) for 90 minutes at 4°C. Later the cells were washed twice with cold PBS and were fixed using 2% para-formaldehyde solution for 4 minutes. The PBS wash was repeated thrice and the coverslips were mounted on glass slides using ProLong® Gold Antifade Reagent by Invitrogen. The slides were observed using Leica Confocal Microscope at 490 nm excitation wavelength for FITC in one channel while trans-illuminated light in the other.

Co-Culturing and Immunofluorescence

Co-culturing was performed with HeLa cells and HUVEC, as described in Koristka S. et.al [34]. 10^5 HeLa cells were seeded in 24 well-plate coated with 0.2% Gelatin in the presence of glass cover-slip and grown over-night in DMEM with 10% FCS at 37°C, 5% CO_2. The cells were washed, suspended in PBS and lethally irradiated with UV-B lamp (HD 9021; Delta Ohm S.r.l., Padova, Italy). The dosage of 1000 Wm^2 was counted using a UVB irradiance meter cosine corrector with spectral range of 280–319 nm (LP 9021 RAD; Delta Ohm). Followed by this, 5×10^4 HUVEC were added in the same well, grown in EGM-2 with 2% FCS until ready. Immunofluorescence was performed after 24 hr, 36 hr and 48 hr using a home-made anti-IFI16 polyclonal as primary antibody and Alexa488- anti-rabbit (GE Healthcare) as secondary antibody. The cells were then fixed with 2% para-formaldehyde (Sigma-Aldrich, Milan, Italy), permeabilized with 0.2% Triton X-100 (Sigma-Aldrich, Milan, Italy) and nuclear stained with 1 μg/ml propidium iodide (Sigma-Aldrich, Milan, Italy). The coverslips were mounted on glass slides using ProLong® Gold Antifade Reagent by Invitrogen and the cells were observed by Leica confocal microscope.

Radioiodination of rIFI16 and Binding Assays

Iodination Beads were purchased from Thermo Fischer Scientific Inc. (Rockford, IL, USA) and used according to manufacturer's instructions. Briefly, two dry beads were washed with rIFI16 elution buffer (50 mM HEPES pH 7.5; 1 M NaCl) (Sigma-Aldrich, Milan, Italy), soaked dry and was incubated for 5 minutes with the solution of carrier-free 2 mCi $Na^{125}I$ (Perkin Elmer Italia, Milan, Italy) and diluted in elution buffer. Later 200 μg of rIFI16 was added and incubated for 15 minutes. The labeling reaction was passed through Zeba Spin Desalting Columns (Thermo Fischer Scientific Inc.) to remove excess $Na^{125}I$ or unincorporated ^{125}I from the iodinated protein. The concentration of the final radioiodinated [^{125}I]-rIFI16 was calculated using the following formula, where 'C' is the cpm counted, 'V' is volume of solution counted in ml and 'Y' is the specific activity of the radioligand in cpm/fmol.

Concentration of [^{125}I]-rIFI16 in (pM) = ['C'cpm/'Y'cpm/fmol]/'V'ml.

Binding assay was performed as described in [35,36], 10^5 cells/well were seeded and attached in a 24-well plate with. Once ready, the medium was removed and the cells were washed with PBS. Further they were re-suspended with increasing concentrations of [^{125}I]-rIFI16 (1–32 nM) within different wells in the presence of 200 nM unlabeled rIFI16 for Non-Specific Binding. Separately, other wells were re-suspended with [^{125}I]-rIFI16 (1–32 nM) without any unlabeled rIFI16 for total binding. The incubation was performed at 4°C for 90 minutes. Later, the cells were washed with PBS to remove any loosely bound ligand and were then suspended in warm 1% SDS (Sigma-Aldrich, Milan, Italy) for 5 minutes. The SDS lysate of the cells was then measured on Cobra II Series Auto-Gamma Counter. All the experiments were carried out in triplicates and the data was analyzed using non-linear regression equations from GraphPad Prism with 95% confidence intervals.

Competition and Inhibition of [^{125}I]-rIFI16 Binding

For binding competition experiments, cells were seeded into 96-well plates at a density of 10^4 cells/well. The medium was removed and cells were washed with PBS. HUVEC were then incubated at 4°C for 90 minutes with unlabeled rIFI16 (10–1000 nM) in the presence of 10 nM [^{125}I]-rIFI16. Binding inhibition was carried out overnight by incubating 10 nM [^{125}I]-rIFI16 with varying concentrations (10–1000 nM) of anti-IFI16 polyclonal N-terminal (1–205 aa) or C-terminal (478–729 aa) antibodies at 4°C. This mixture was then added to 10^4 HUVEC and incubated for 90 minutes at 4°C. The loosely bound ligand was removed by washing twice with PBS, and cells were then detached using warm 1% SDS and the levels of [125]-rIFI16-binding to HUVEC assessed using a Cobra II Series Auto-Gamma Counter. The data were analyzed using non-linear regression equations in GraphPad Prism under 95% confidence intervals.

Statistical Analysis

All statistical tests were performed using GraphPad Prism version 5.00 for Windows (GraphPad, La Jolla, CA, USA).

Positivity cut-off values for anti-IFI16 antibodies were calculated as the 95th percentile for the control population and the Kruskal-Wallis test was used to measure associations. To test the effects of recombinant IFI16 protein (rIFI16) on biological functions of primary endothelial cells one-way analysis of variance (ANOVA) with Bonferroni adjustment for multiple comparisons was used.

Results

Serum Levels of IFI16 Protein are Increased in Patients with Systemic Autoimmune Diseases

Sera were harvested from patients suffering from systemic autoimmune diseases characterized by endothelial dysfunction, including SSc, SLE, SjS, and RA. IFI16 serum levels were quantified using an in-house sandwich ELISA and compared with age- and sex-matched healthy controls. All absorbance levels were in the range of assay linearity. With the cut-off value set to the 95th percentile of the control population (27 ng/ml), mean IFI16 levels were significantly increased in patients with SSc, SLE, RA, and SjS compared to the control group (4.7 ng/ml) (SSc: 25.4 ng/ml, $p<0.001$; SLE: 23.5 ng/ml, $p<0.001$; RA: 222 ng/ml, $p<0.001$; SjS: 88.2 ng/ml, $p<0.001$). Of note, the sera from RA patients displayed the highest levels of circulating free protein. IFI16 levels above the 95th percentile for control subjects were observed in 34% of SSc, 37% of SLE, 47% of SjS, and 56% of RA patients (Figure 1). By contrast, IFI16 levels in non-SLE GN patients did not show any significant difference in comparison with healthy controls. Since the objective of this part of the study was limited to demonstrate the presence of circulating IFI16 in patients' sera for justifying the rest of the in vitro studies, correlation with clinicopathological parameters was behind the aim of these studies and was not performed.

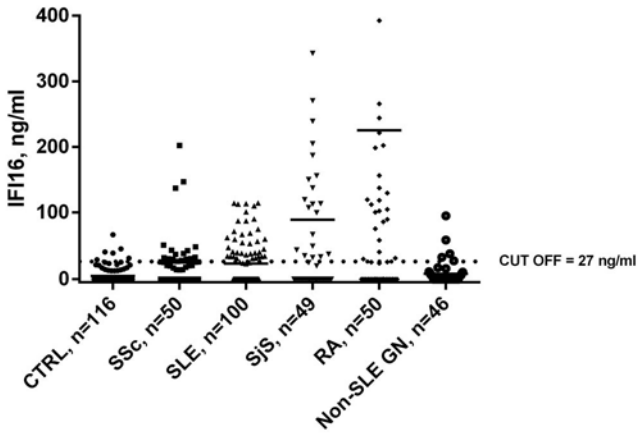

Figure 1. IFI16 protein levels in patients' and controls' sera determined using an in-house capture ELISA. Each dot represents the concentration of IFI16 protein (expressed in ng/ml on a linear scale) in each individual subject: patients suffering from Systemic Sclerosis (SSc, n = 50), Systemic Lupus Erythematosus (SLE, n = 100), Sjogren's Syndrome (SjS, n = 49), Rheumatoid Arthritis (RA, n = 50), and non-SLE glomerulonephritis (non-SLE GN n = 46) were investigated together with healthy controls (CTRL, n = 116). The horizontal bars represent the median values. Values over the dotted line indicate the percentage of subjects with IFI16 protein levels above the cut-off value (27 ng/ml) calculated as the 95th percentile of the control population. Statistical significance: *** $p<0.001$ *vs.* controls (Kruskall-Wallis test).
doi:10.1371/journal.pone.0063045.g001

Effects of Extracellular IFI16 on Different Functions of Primary Endothelial Cells

Abnormalities in angiogenesis are frequently present in systemic autoimmune diseases and may lead to tissue damage and premature vascular disease [37]. To verify whether extracellular IFI16 was also involved in this pathogenic process, HUVEC were treated with increasing concentrations of recombinant IFI16 protein (rIFI16) (10, 25 or 50 μg/ml), mock-treated with the same volumes of vehicle (Mock), or left untreated (NT) and then assessed for cell viability at 48 hours incubation time by MTT assay. As shown in Figure 2A, the addition of endotoxin-free rIFI16 protein did not reduce the amount of viable adherent cells when compared to mock or untreated cells at the concentration of 10 and 25 μg/ml, respectively. At the highest concentration used (50 μg/ml), a slight reduction in cell viability was observed, and consequently the following studies were conducted with the lower doses.

Next, to test whether the addition of rIFI16 to culture media altered other biological parameters of endothelial cells, HUVEC were treated as described for the assessment of cell viability (MTT assay) and then analyzed for their tubule morphogenesis and chemotactic activities. As shown in Figure 2B, exogenous administration of 25 μg/ml rIFI16 severely limited tubulogenesis, with most cells generating incomplete tubules or aggregating into clumps. The extent of angiogenesis was quantified by counting the intact capillary-like tubules called as Lumens, which showed 75% decrease in its numerical value, as well as the number of interconnecting branch points showing 77% decrease. (Figure 2B). These effects were less pronounced when a lower dose of 10 μg/ml rIFI16 was used with 22% and 15% decrease respectively. In contrast, untreated or mock-treated HUVEC plated onto matrigel supported the formation of an extensive interconnecting polygonal capillary-like network.

Next, we evaluated the effects of rIFI16 on the migration phase of angiogenesis in a transwell migration assay routinely used to study cell migration in response to specific stimuli. HUVECs untreated, mock-treated, or incubated with rIFI16 (10 or 25 μg/ml) for 48 h were transferred into transwell migration chambers. As shown in Fig. 2C, only a small population of HUVECs cultured in the presence of 25 μg/ml rIFI16 were able to migrate through the chamber (30% of migration), whereas mock-treatment resulted in considerable migration (95% and 87% for 10 μg/ml and 25 μg/ml, respectively).

Taken together, these results demonstrate the capability of extracellular rIFI16 to impair physiological functions of endothelial cells, such as the differentiation phases responsible for tube morphogenesis and migration.

Anti-N-terminus IFI16 Antibodies Neutralize the Cytotoxic Activity of IFI16

To demonstrate that the effects exerted by IFI16 protein on target cells were specific and not a consequence of cell cytotoxicity, HUVEC were treated with 25 μg/ml rIFI16 in the presence or absence of specific rabbit polyclonal antibodies recognizing the N-terminal or the C-terminal domain of IFI16 protein. HUVEC incubated with rIFI16 in the presence of normal rabbit IgG were used as the positive control. As described in the previous section, rIFI16 severely affected the capability of endothelial cells to generate microtubules as well as their transwell migration activity, while the same effects were observed in presence of normal rabbit IgG (Figure 3A and 3B). In contrast, the presence of anti-N-terminus antibodies reduced the Lumens by 16%, Branch Points by 5% and migration by 1% while anti-C-terminus antibodies reduced the Lumens by 60%, Branch Points by 32% and

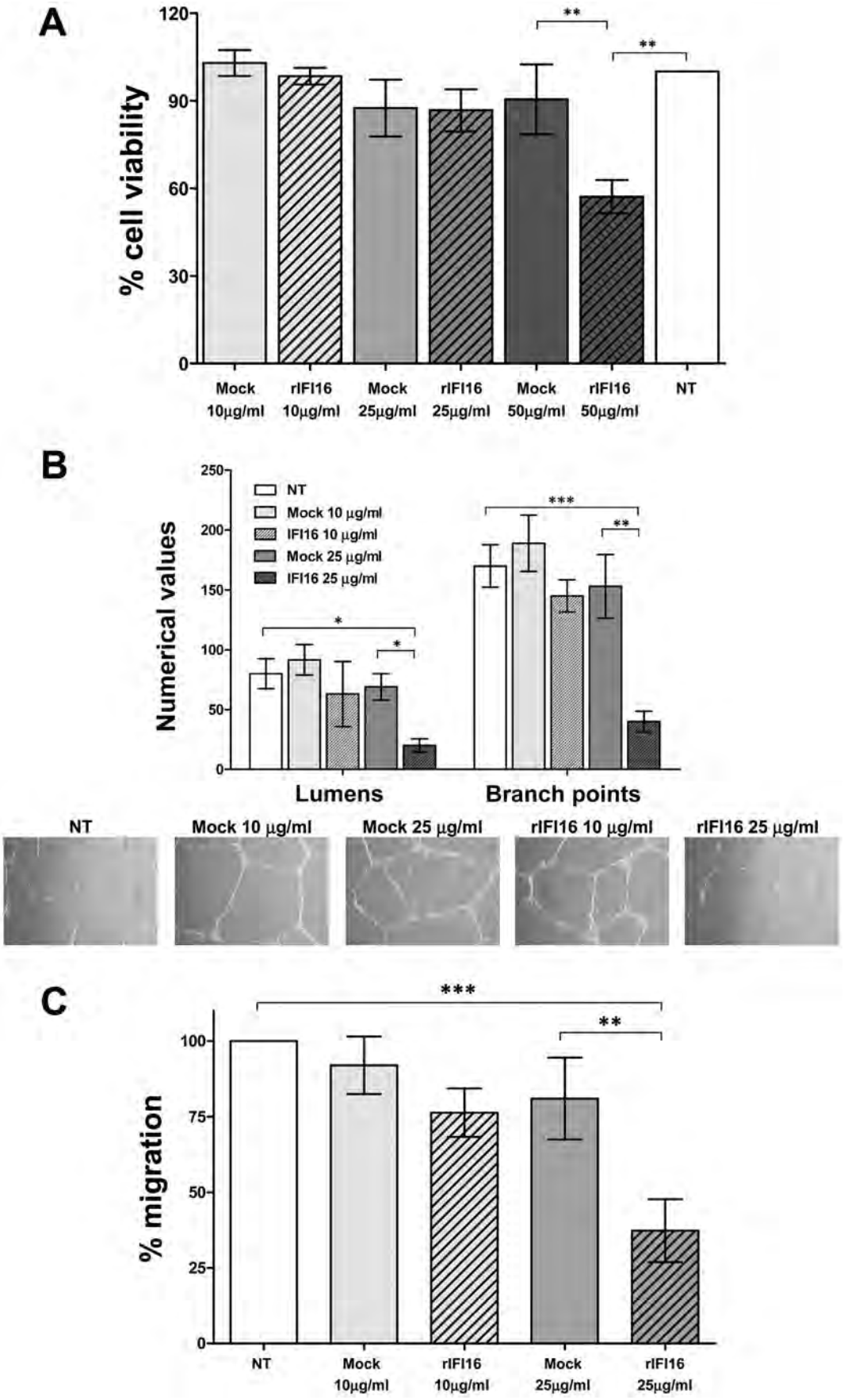
A
% cell viability
120
90
60
30
0
**
**
Mock 10μg/ml
rIFI16 10μg/ml
Mock 25μg/ml
rIFI16 25μg/ml
Mock 50μg/ml
rIFI16 50μg/ml
NT
B
Numerical values
250
200
150
100
50
0
NT
Mock 10 μg/ml
IFI16 10 μg/ml
Mock 25 μg/ml
IFI16 25 μg/ml
*
*
***
**
Lumens
Branch points
NT
Mock 10 μg/ml
Mock 25 μg/ml
rIFI16 10 μg/ml
rIFI16 25 μg/ml
C
% migration
100
75
50
25
0
***
**
NT
Mock 10μg/ml
rIFI16 10μg/ml
Mock 25μg/ml
rIFI16 25μg/ml

Figure 2. Extracellular IFI16 affects various biological functions of primary endothelial cells. HUVEC were treated with different doses of recombinant IFI16 protein (rIFI16), the same volumes of vehicle (Mock), or left untreated (NT) for 48 h. (A) Viability analysis (MTT assay); the viability of control preparations (NT) was set to 100%. (B) Capillary-like tube formation assay (Matrigel). For a quantitative assessment of angiogenesis, the number of lumens and branch points was assessed (upper panels); representative images of three independent experiments are reported (lower panels). (C) Migration analysis (Transwell assay) results are reported as the percentage of migrated cells *vs.* untreated HUVECs. Values represent the mean±SD of 3 independent experiments, (**p<0.01, ***p<0.001; one-way ANOVA followed by Bonferroni's multiple comparison test).
doi:10.1371/journal.pone.0063045.g002

migration by 49%. This indicates the role of anti-N-terminus antibody in inhibiting the activities of IFI16 toward endothelial cells, restoring the tube formation and migratory activities. Altogether, these results suggest that the IFI16 activity is specific and that the functional domain resides at the N-terminus, where the PYD domain is localized.

Binding of Extracellular IFI16 on the Plasma Membrane of HUVEC

The finding that extracellular IFI16 impairs endothelial cell functions, including tube morphogenesis and transwell migration indicates a possible alarmin function as recently demonstrated for Danger and Pathogen-associated molecular pattern molecules collectively called as DAMPs, PAMPs such as autoantigen HMGB-1 [38,39]. Thus to find evidence in this direction it was important to evaluate the binding interaction of IFI16 on the plasma membrane of HUVEC. A series of binding experiments were conducted to verify the presence of high-affinity binding sites in the membranes of the target cells. In the previous section, it has been described that 25 μg/ml (300 nM) rIFI16 concentration is non-toxic to HUVEC, while they can still perform biological functions. Thus HUVEC were incubated with lowest concentrations (10 nM, 20 nM, and 30 nM) of FITC-labeled rIFI16 to avoid toxicity or apoptosis and the binding was visualized by confocal microscopy. As shown in Figure 4A, binding of FITC-labeled rIFI16 was detected at least concentration of 10 nM, increased at 20 nM, and saturated at 30 nM. To avoid the non-specific binding of rIFI16 with sugar residues on plasma membrane, HUVEC were grown in presence of tunicamycin which inhibits N-glycosylation of proteins. By contrast to above findings, human fibroblasts were negative for FITC-labeled rIFI16 at all the rIFI16 concentrations investigated (data not shown).

Furthermore, to demonstrate that the binding of rIFI16 is of physiological relevance, co-culturing experiments were organized in such a way that UV-B irradiated cells release endogenous IFI16 [29] which in turn binds to neighboring HUVEC in the same system. As shown in Figure 4B, after 24 h HUVEC were observed to be surface bound with endogenous IFI16 released from HeLa cells, while by 36 h this bound IFI16 entered the cytoplasm and by 48 h it almost disappeared. When fibroblasts were used instead of HUVEC, the binding was not observed, while also when HUVEC were cultured with normal HeLa cells, surface presence of IFI16 was not detected (data not shown).

Kinetics of rIFI16 Binding on Different Cell Lines

To get some insights into the binding characteristics of IFI16 to different cell lines, binding kinetics experiments using radioiodinated rIFI16 were performed. Specific binding was calculated as the difference between total and non-specific binding. As shown in Figure 5A, the specific binding of [^{125}I]-rIFI16 to its binding site on HUVEC is saturable and has a dissociation constant (Kd) equal to 2.7 nM; 71.55 to 83.84 fmol of [^{125}I]-rIFI16 was estimated to saturate the binding sites on 10^5 HUVEC, thus the maximal number of binding sites (B_{max}) could be estimated to be in the range of 250,000 to 450,000 binding sites/cell. Furthermore, the binding of [^{125}I]-rIFI16 on HUVEC was displaced by 10- to 100-fold of unlabeled rIFI16, demonstrating its competitive nature (Figure 5B). The inhibition constant (K_i) was calculated to be 14.43 nM and the half maximal inhibitory concentration (IC_{50}) was 67.88 nM. Similar results were obtained for HeLa and HaCaT cell lines, which also indicated saturable and competitive nature towards rIFI16 binding. As a negative control, human dermal fibroblasts (HDF) and murine fibroblasts (3T3) were accessed for specific and competitive binding of [^{125}I]-rIFI16 in parallel with HUVEC (Figure 5A and 5B). Both HDF and 3T3 were found to exhibit non-saturable rIFI16 binding, indicating the lack of any specific IFI16 binding sites. Moreover, the binding of rIFI16 on these cells was non-competitive in nature (Figure 5B). Also as reported in Figure 5C, different cell lines shown variable affinities towards IFI16 binding.

[^{125}I]-rIFI16 Binding Inhibition by Anti-IFI16 Polyclonal Antibodies

To evaluate the binding properties of rIFI16 to its receptor with respect to epitope mapping, we performed a binding inhibition assay using radioiodinated rIFI16 in the presence of increasing concentrations of antibodies recognizing the IFI16 N-terminal domain. As depicted in Figure 6, a gradual decrease in the bound [^{125}I]-rIFI16 was observed with increasing concentrations of antibody (from 10 to 1000 nM). Conversely, the anti-IFI16 antibody recognizing the C-terminal domain (478–729 aa) was not able to inhibit the binding of [^{125}I]-rIFI16 to its receptor. Together with the results from the functional assays, these observations provide evidence indicating that the N-terminal region of rIFI16 is required for its binding to the novel membrane receptor on HUVEC and is responsible for its signal transduction capacity.

Discussion

In the present study, we demonstrate for the first time: i) the presence of significant levels of extracellular IFI16 protein in the sera of patients affected by systemic autoimmune diseases, including SSc, SjS, SLE and RA but not in non-SLE GN as compared to healthy controls, and ii) that the extracellular IFI16 exerts biological effects on endothelial cells upon binding to a specific cell surface receptor. These findings have important implications as they provide novel insights into the role of IFI16 in the pathogenesis of systemic autoimmune diseases. Various research groups, including ours, have shown that following transfection of virus-derived DNA [19,40], or treatment with UVB [29], IFI16 delocalizes from the nucleus to the cytoplasm and is then eventually released into the extracellular milieu. Consistent with these observations, we now demonstrate the presence of circulating IFI16 protein in the sera of patients affected by systemic autoimmune diseases, but not in patients with non-autoimmune inflammatory diseases like non-SLE GN. Skin manifestations and vasculopathy are common components of a number of autoimmune diseases and represent a significant source of morbidity [41,42]. Thus, to investigate the hypothesis that circulating IFI16 is able to exert harmful effects on target cells *in vivo*, an *in vitro* cell model consisting of primary endothelial cells

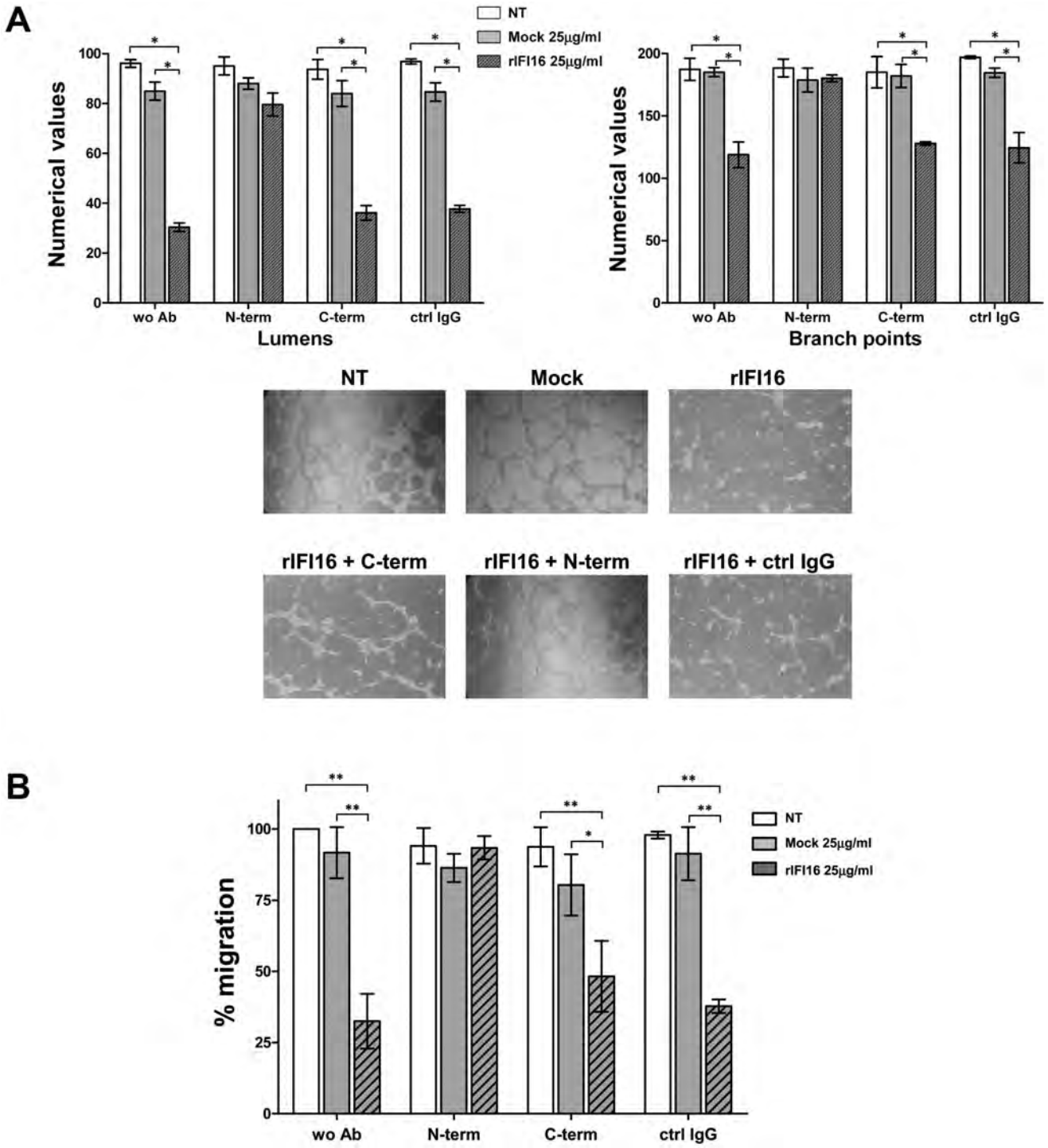

Figure 3. Anti-IFI16 antibodies restore the biological activities of extracellular IFI16. HUVEC were treated for 48 h with different doses of recombinant IFI16 protein (rIFI16), the same volumes of vehicle (Mock), or left untreated (NT), alone or in combination with antibodies against IFI16. (A) Capillary-like tube formation assay (Matrigel). For a quantitative assessment of angiogenesis, the number of lumens and branch points was assessed (upper panels); representative images of three independent experiments are reported (lower panels). (B) Migration analysis (Transwell assay) results are reported as the percentage of migrated cells *vs*. untreated HUVECs. Values represent the mean±SD of 3 independent experiments (**p<0.01, ***p<0.001, one-way ANOVA followed by Bonferroni's multiple comparison test).
doi:10.1371/journal.pone.0063045.g003

(HUVEC) was used to test the activity of extracellular IFI16 on cell functions. These experiments clearly demonstrate that extracellular IFI16 affects some biological processes of endothelial cells, including tube morphogenesis and transwell migration. The specificity of these effects was assessed by the addition of anti-IFI16 antibodies which were able to neutralize the activity of the protein blocking its inhibitory effects. Subsequently, the presence of IFI16 in the extracellular environment could also be the main

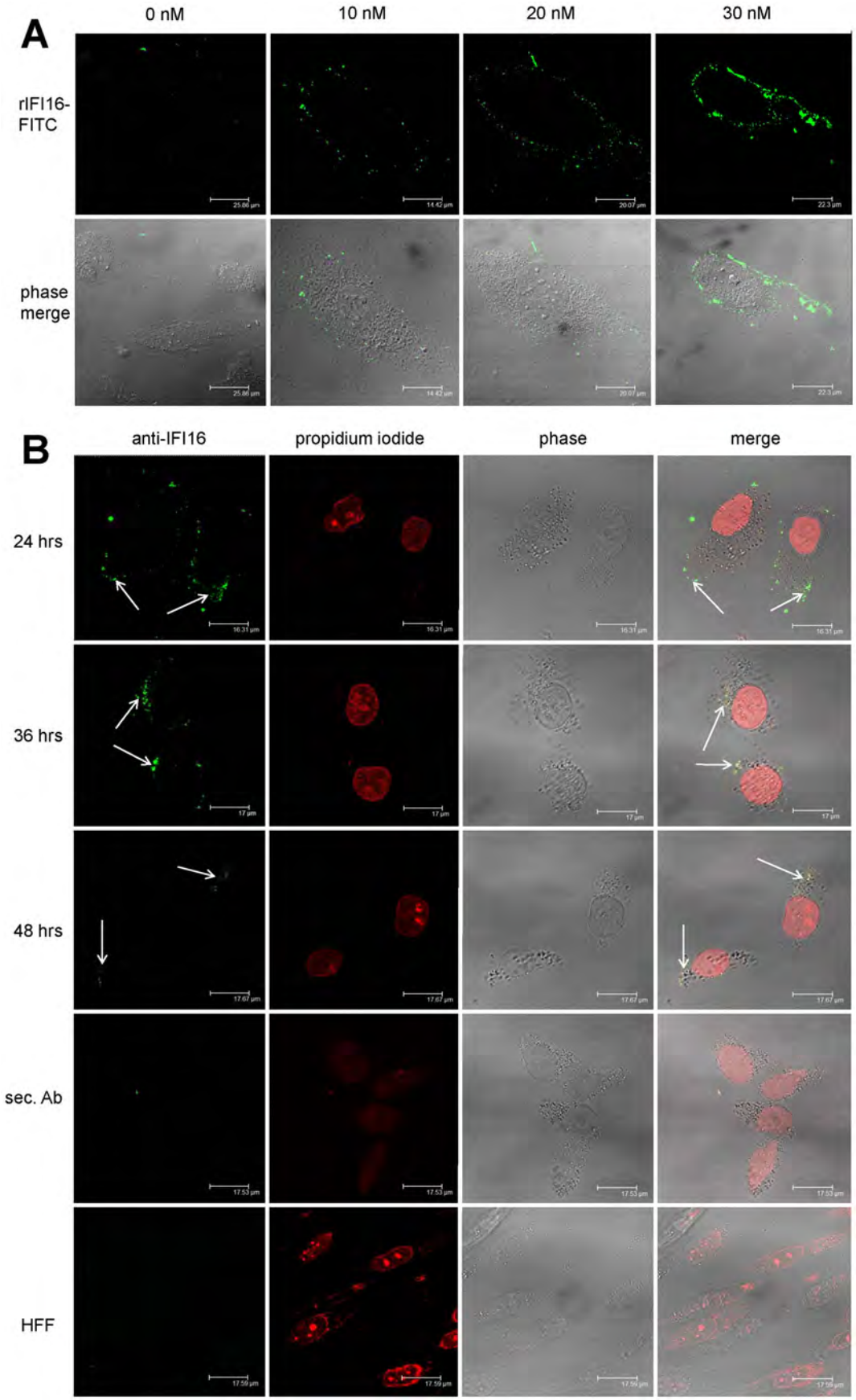
A
0 nM
10 nM
20 nM
30 nM
rIFI16-FITC
phase merge
B
anti-IFI16
propidium iodide
phase
merge
24 hrs
36 hrs
48 hrs
sec. Ab
HFF

Figure 4. Plasma membrane binding of IFI16 to HUVEC. (A) Cells were left untreated (a, negative control) or incubated with increasing concentrations of FITC-labeled recombinant IFI16 (b, 10 nM rIFI16-FITC; c, 20 nM rIFI16-FITC; d, 30 nM rIFI16-FITC). Binding was detected by confocal microscopy using an excitation wavelength of 490 nm for FITC in one channel and trans-illuminated light in the other. Representative images of three independent experiments are shown. (B) Endogenous IFI16 released by irradiated HeLa cells binds neighboring HUVEC. UV-B irradiated HeLa cells were co-cultured with HUVEC and after 24 h, 36 h and 48 h, dead cell debris were removed and immunofluorescence was performed on the remaining live HUVEC using a home-made anti-IFI16 polyclonal as primary antibody and Alexa-488- anti-rabbit as secondary antibody. The cells were then fixed, permeabilized, nuclear-stained using propidium iodide and analyzed by confocal microscopy. Fibroblasts were employed as negative control. Representative images of three independent experiments are shown.
doi:10.1371/journal.pone.0063045.g004

reason behind the presence of anti-IFI16 autoantibodies in autoimmune patients' sera. (Caneparo et al. Lupus 2013, accepted) Together, these observations suggest the possible role of IFI16 in the clinical manifestation of autoimmune diseases, due to its presence in the extracellular environment. Since IFI16 can be released extracellularly which further reflect distinct extracellular biological activities, it is an indication of a novel alarmin function of this interferon inducible protein. Such stress-dependent shuttling, release, binding to cell surface was described in the past for autoantigen La/SS-B [43] and recently reviewed for HMGB1 protein [39] which upon release, binds to the cell surface receptors of neighboring cells. Thus as part of alarmin function, we further hypothesized that once released IFI16 protein must also bind neighboring cells to communicate the stress signal. In this direction, we assessed the affinity of IFI16 towards the plasma membrane of HUVEC. Confocal images visualized patterned binding of FITC labeled rIFI16 protein on the plasma membrane, which gave us the first preliminary evidence of the existence of an IFI16 interacting molecule which we suspect to be receptor-kind. Furthermore, we found experimental evidence that endogenous IFI16 protein released by dying cells bind neighboring cells. As a consequence of this binding, time-lapse studies proved its further entry into the cytoplasm. Moreover, such binding and transport of IFI16 was observed in different cell lines with different affinities. The experiments using radiolabeled IFI16 to investigate the binding kinetics of IFI16 in the HUVEC provide strong evidence supporting the presence of specific binding sites in the plasma membrane through which IFI16 exerts its cytotoxic activity. These binding sites were found to be saturable and competitive for IFI16, while the binding experiments in HUVEC indicate the presence of approximately 250,000 to 450,000 binding sites per cell, with a dissociation constant (Kd) of 2.7 nM. Similar binding character-

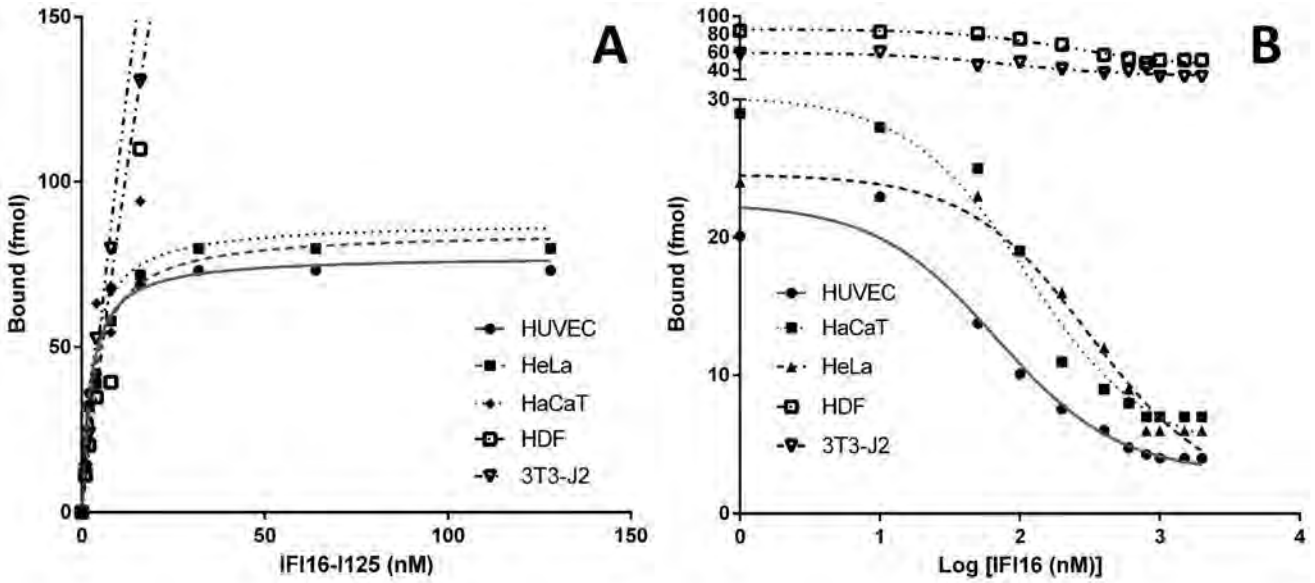

C

Cell Line	Kd	Bmax	Number of binding sites/cell
HUVEC	2.7 nM	77.7 fmol	2.5-5 × 10^5
HeLa	3.7 nM	85.3 fmol	2-4 × 10^5
HaCaT	2.7 nM	87.7 fmol	2-4 × 10^5

Figure 5. Binding Kinetics of [^{125}I]-rIFI16 on HUVEC, HDF, and 3T3 cells. (A) Specific binding of [^{125}I]-rIFI16 on the plasma membrane of HUVEC, HeLa, HACAT, HDF, and 3T3 cells. (B) Competitive binding of [^{125}I]-rIFI16 on HUVEC, HeLa, HaCaT, HDF, and 3T3 cells. (C) The binding affinity (Kd), total bound ligand (B_{max}) and the estimated number of binding sites per cell for different cell lines. The experiment was carried out in triplicates and data was analyzed using non-linear regression equations from GraphPad Prism with 95% confidence intervals. All the experiments have been repeated at least three times and one representative is reported.
doi:10.1371/journal.pone.0063045.g005

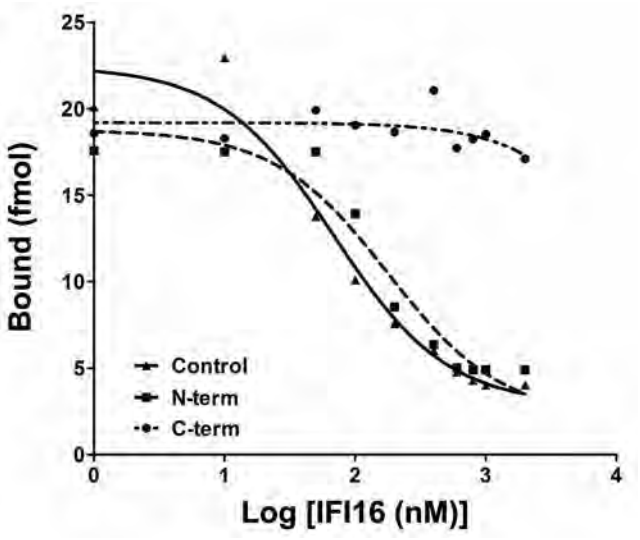

Figure 6. Binding inhibition of [^{125}I]-rIFI16 using anti-IFI16 polyclonal antibodies. Antibody inhibition curve of HUVEC using anti-rIFI16 N-terminal (1–205 aa) polyclonal antibodies (dashed) and C-term polyclonal antibodies (dot-dashed). Competitive binding of rIFI16 and [^{125}I]-rIFI16 to HUVEC (plain) was used as the control condition. The experiment was carried out in triplicates and data was analyzed using non-linear regression equations from GraphPad Prism with 95% confidence intervals. All the experiments have been repeated at least three times and one representative is reported.
doi:10.1371/journal.pone.0063045.g006

istics were shown by different epithelial cell lines while a completely un-related cell line like fibroblasts demonstrated non-specific binding. This explains the specificity of IFI16 binding which is mostly restricted towards endothelium and epithelium. Neutralization experiments employing antibodies directed against different regions of the protein allowed us to demonstrate that the N-terminus, containing the PYD domain, is responsible for binding interaction. Consistent with this observation, the same antibodies were able to neutralize the biological activity of extracellular IFI16, as described earlier.

In summary, our results provide evidence for a novel alarmin function of IFI16 protein which is overexpressed upon inflammatory stimuli and then released in the extracellular environment. Once released, IFI16 binds to neighboring cells propagating the stress signal causing damage. The presence of anti-IFI16 autoantibodies have been detected in many autoimmune diseases [25–28], thus the release of IFI16 in the extracellular milieu marks the first step in the development of autoimmunity.

Acknowledgments

We gratefully acknowledge the help of Andrea Graziani and Gianluca Baldanzi, Medical School of Novara for their guidance regarding the receptor binding studies. We also thank Donato Colangelo, Medical School of Novara, for helpful suggestions on evaluating binding kinetics data. Finally, we thanks FIRMA group and Piero Stratta, Medical School of Novara for giving us the patients' sera.

Author Contributions

Conceived and designed the experiments: SL MG. Performed the experiments: FG MB MDA VDO VC. Analyzed the data: FG MB MDA VDO VC. Contributed reagents/materials/analysis tools: AT. Wrote the paper: SL MG.

References

1. Elkon KB, Wiedeman A (2012) Type I IFN system in the development and manifestations of SLE. Curr Opin Rheumatol 24: 499–505.
2. Pollard KM, Hultman P, Toomey CB, Cauvi DM, Hoffman HM, et al. (2012) Definition of IFN-gamma-related pathways critical for chemically-induced systemic autoimmunity. J Autoimmun 39: 323–331.
3. Choubey D, Moudgil KD (2011) Interferons in autoimmune and inflammatory diseases: regulation and roles. J Interferon Cytokine Res 31: 857–865.
4. Crow MK (2010) Type I interferon in organ-targeted autoimmune and inflammatory diseases. Arthritis Res Ther 12 Suppl 1: S5.
5. Ronnblom L (2010) Potential role of IFNalpha in adult lupus. Arthritis Res Ther 12 Suppl 1: S3.
6. Higgs BW, Liu Z, White B, Zhu W, White WI, et al. (2011) Patients with systemic lupus erythematosus, myositis, rheumatoid arthritis and scleroderma share activation of a common type I interferon pathway. Ann Rheum Dis 70: 2029–2036.
7. Mavragani CP, Crow MK (2010) Activation of the type I interferon pathway in primary Sjogren's syndrome. J Autoimmun 35: 225–231.
8. Kong JS, Teuber SS, Gershwin ME (2006) Potential adverse events with biologic response modifiers. Autoimmun Rev 5: 471–485.
9. Sozzani S, Bosisio D, Scarsi M, Tincani A (2010) Type I interferons in systemic autoimmunity. Autoimmunity 43: 196–203.
10. Higgs BW, Zhu W, Richman L, Fiorentino DF, Greenberg SA, et al. (2012) Identification of activated cytokine pathways in the blood of systemic lupus erythematosus, myositis, rheumatoid arthritis, and scleroderma patients. Int J Rheum Dis 15: 25–35.
11. Selmi C, Lleo A, Zuin M, Podda M, Rossaro L, et al. (2006) Interferon alpha and its contribution to autoimmunity. Curr Opin Investig Drugs 7: 451–456.
12. Bach JF (2005) Infections and autoimmune diseases. J Autoimmun 25 Suppl: 74–80.
13. Cridland JA, Curley EZ, Wykes MN, Schroder K, Sweet MJ, et al. (2012) The mammalian PYHIN gene family: phylogeny, evolution and expression. BMC Evol Biol 12: 140.
14. Gariglio M, Mondini M, De Andrea M, Landolfo S (2011) The multifaceted interferon-inducible p200 family proteins: from cell biology to human pathology. J Interferon Cytokine Res 31: 159–172.
15. Gariglio M, Azzimonti B, Pagano M, Palestro G, De Andrea M, et al. (2002) Immunohistochemical expression analysis of the human interferon-inducible gene IFI16, a member of the HIN200 family, not restricted to hematopoietic cells. J Interferon Cytokine Res 22: 815–821.
16. Cristea IM, Moorman NJ, Terhune SS, Cuevas CD, O'Keefe ES, et al. (2010) Human cytomegalovirus pUL83 stimulates activity of the viral immediate-early promoter through its interaction with the cellular IFI16 protein. J Virol 84: 7803–7814.
17. Li T, Diner BA, Chen J, Cristea IM (2012) Acetylation modulates cellular distribution and DNA sensing ability of interferon-inducible protein IFI16. Proc Natl Acad Sci U S A 109: 10558–10563.
18. Gariano GR, Dell'Oste V, Bronzini M, Gatti D, Luganini A, et al. (2012) The intracellular DNA sensor IFI16 gene acts as restriction factor for human cytomegalovirus replication. PLoS Pathog 8: e1002498.
19. Unterholzner L, Bowie AG (2011) Innate DNA sensing moves to the nucleus. Cell Host Microbe 9: 351–353.
20. Sponza S, De Andrea M, Mondini M, Gugliesi F, Gariglio M, et al. (2009) Role of the interferon-inducible IFI16 gene in the induction of ICAM-1 by TNF-alpha. Cell Immunol 257: 55–60.
21. Gugliesi F, Mondini M, Ravera R, Robotti A, de Andrea M, et al. (2005) Up-regulation of the interferon-inducible IFI16 gene by oxidative stress triggers p53 transcriptional activity in endothelial cells. J Leukoc Biol 77: 820–829.
22. Mondini M, Costa S, Sponza S, Gugliesi F, Gariglio M, et al. (2010) The interferon-inducible HIN-200 gene family in apoptosis and inflammation: implication for autoimmunity. Autoimmunity 43: 226–231.
23. Gugliesi F, De Andrea M, Mondini M, Cappello P, Giovarelli M, et al. (2010) The proapoptotic activity of the Interferon-inducible gene IFI16 provides new insights into its etiopathogenetic role in autoimmunity. J Autoimmun 35: 114–123.
24. Caposio P, Gugliesi F, Zannetti C, Sponza S, Mondini M, et al. (2007) A novel role of the interferon-inducible protein IFI16 as inducer of proinflammatory molecules in endothelial cells. J Biol Chem 282: 33515–33529.
25. Rekvig OP, Putterman C, Casu C, Gao HX, Ghirardello A, et al. (2012) Autoantibodies in lupus: culprits or passive bystanders? Autoimmun Rev 11: 596–603.
26. Mondini M, Vidali M, Airo P, De Andrea M, Riboldi P, et al. (2007) Role of the interferon-inducible gene IFI16 in the etiopathogenesis of systemic autoimmune disorders. Ann N Y Acad Sci 1110: 47–56.
27. Mondini M, Vidali M, De Andrea M, Azzimonti B, Airo P, et al. (2006) A novel autoantigen to differentiate limited cutaneous systemic sclerosis from diffuse cutaneous systemic sclerosis: the interferon-inducible gene IFI16. Arthritis Rheum 54: 3939–3944.

28. Costa S, Mondini M, Caneparo V, Afeltra A, Airo P, et al. (2011) Detection of anti-IFI16 antibodies by ELISA: clinical and serological associations in systemic sclerosis. Rheumatology (Oxford) 50: 674–681.
29. Costa S, Borgogna C, Mondini M, De Andrea M, Meroni PL, et al. (2011) Redistribution of the nuclear protein IFI16 into the cytoplasm of ultraviolet B-exposed keratinocytes as a mechanism of autoantigen processing. Br J Dermatol 164: 282–290.
30. Schattgen SA, Fitzgerald KA (2011) The PYHIN protein family as mediators of host defenses. Immunol Rev 243: 109–118.
31. Baggetta R, De Andrea M, Gariano GR, Mondini M, Ritta M, et al. (2010) The interferon-inducible gene IFI16 secretome of endothelial cells drives the early steps of the inflammatory response. Eur J Immunol 40: 2182–2189.
32. Pauwels R, Balzarini J, Baba M, Snoeck R, Schols D, et al. (1988) Rapid and automated tetrazolium-based colorimetric assay for the detection of anti-HIV compounds. J Virol Methods 20: 309–321.
33. Gugliesi F, Dell'oste V, De Andrea M, Baggetta R, Mondini M, et al. (2011) Tumor-derived endothelial cells evade apoptotic activity of the interferon-inducible IFI16 gene. J Interferon Cytokine Res 31: 609–618.
34. Koristka S, Cartellieri M, Arndt C, Bippes CC, Feldmann A, et al. (2013) Retargeting of regulatory T cells to surface-inducible autoantigen La/SS-B. J Autoimmun In press.
35. Imai Y, Leung CK, Friesen HG, Shiu RP (1982) Epidermal growth factor receptors and effect of epidermal growth factor on growth of human breast cancer cells in long-term tissue culture. Cancer Res 42: 4394–4398.
36. Coleman JW, Godfrey RC (1981) The number and affinity of IgE receptors on dispersed human lung mast cells. Immunology 44: 859–863.
37. Guiducci S, Distler O, Distler JH, Matucci-Cerinic M (2008) Mechanisms of vascular damage in SSc–implications for vascular treatment strategies. Rheumatology (Oxford) 47 Suppl 5: v18–20.
38. Bianchi ME (2007) DAMPs, PAMPs and alarmins: all we need to know about danger. J Leukoc Biol 81: 1–5.
39. Harris HE, Andersson U, Pisetsky DS (2012) HMGB1: a multifunctional alarmin driving autoimmune and inflammatory disease. Nat Rev Rheumatol 8: 195–202.
40. Keating SE, Baran M, Bowie AG (2011) Cytosolic DNA sensors regulating type I interferon induction. Trends Immunol 32: 574–581.
41. Kaplan MJ (2009) Endothelial damage and autoimmune diseases. Autoimmunity 42: 561–562.
42. Rashtak S, Pittelkow MR (2008) Skin involvement in systemic autoimmune diseases. Curr Dir Autoimmun 10: 344–358.
43. Bachmann M, Zaubitzer T, Muller WE (1992) The autoantigen La/SSB: detection on and uptake by mitotic cells. Exp Cell Res 201: 387–398.

This is a resubmission.

Manuscript #	JVI00384-14
Current Revision #	0
Submission Date	2014-02-12 04:18:50
Current Stage	Under Review
Title	Early stage IFI16 cytoplasmic translocation and late stage entrapment into egressing virions during HCMV infection
Running Title	Nuclear IFI16 mislocalization during HCMV infection
Manuscript Type	Full-Length Text
Journal Section	Virus-Cell Interactions
Corresponding Author	Prof. Santo Landolfo (University of Turin)
Contributing Authors	Valentina Dell'Oste , Dr. Deborah Gatti , Dr. Francesca Gugliesi , Dr. Marco De Andrea , **Mandar Bawadekar** , Dr. Irene Lo Cigno , Dr. Matteo Biolatti , Dr. Marta Vallino , Prof. Manfred Marschall , Prof. Marisa Gariglio
Abstract	Intrinsic immune mechanisms mediated by constitutively expressed proteins termed "restriction factors" provide frontline antiviral defense. We recently demonstrated that the DNA sensor IFI16 restricts HCMV replication by down-regulating viral early and late but not immediate-early mRNAs and their protein expression. Here, we show that at an early time point during the in vitro infection of low-passage human embryonic lung fibroblasts (HELF), IFI16 binds to HCMV DNA. However, during a later phase following infection, IFI16 is mislocalized to the cytoplasmic virus assembly complex (AC), where it colocalizes with viral structural proteins. Indeed, upon its binding to pUL97, IFI16 undergoes phosphorylation and relocalizes to the cytoplasm of HCMV-infected cells. ESCRT (Endosomal Sorting Complex Required for Transport) machinery regulates the translocation of IFI16 into the virus AC by sorting and trafficking IFI16 into multivesicular bodies (MVB), as demonstrated by the interaction of IFI16 with two MVB markers: Vps4 and TGN46. Finally, IFI16 becomes incorporated into the newly assembled virions as demonstrated by Western blot analysis of purified virions and electron microscopy. Together, these results suggest that HCMV has evolved mechanisms to mislocalize and hijack IFI16, trapping it within mature virions. However, the significance of this IFI16 trapping following nuclear mislocalization remains to be established.
Importance	Intracellular viral DNA sensors and restriction factors are critical components of host defence, which alarm and sensitize immune system against intruding pathogens. We have recently demonstrated that the DNA sensor IFI16 restricts HCMV replication by down-regulating viral early and late but not immediate-early mRNAs and their protein expression. However, viruses are known to evolve numerous strategies to cope and counteract such restriction factors and neutralize the first line of host defence mechanisms. Our findings describe that during early stages of infection, IFI16 successfully recognizes HCMV DNA. However, in late stages HCMV mislocalizes IFI16 into the cytoplasmic viral assembly complex (AC) and finally entraps the protein into mature virions. This work clarifies the mechanisms HCMV relies to overcome intracellular viral restriction, which provides new insights about the relevance of DNA sensors during HCMV infection.
Editor	Dr. Klaus Frueh
Suggested Reviewers to Include	David Johnson (Oregon Health Sciences University), John Sinclair (Department of Medicine, Level 5), Wolfram Brune (Heinrich Pette Institute), Ganes Sen (Cleveland Clinic Foundation)
Suggested Reviewers to Exclude	Ileana Cristea (Princeton University), David Knipe (Harvard Medical School), Andrew Bowie (Trinity College)
Keywords	Human Cytomegalovirus, Interferon-inducible genes, IFI16, Restriction factors, pUL97, Nuclear mislocalization, Multivesicular bodies, Virus entrapment
Research Areas	Virology, Host-Microbial Interactions, Pathogenesis and Host Response
Conflict of Interest	No conflict of interest.
Funding Sources	Research Funding from Italian Ministry of University and Reasearch (MIUR): PRIN 2012: 2012SNMJRL; Research Funding from Italian Ministry of University and Research (MIUR): PRIN 2012: 20127MFYBR; Research Funding from the University of Turin (Italy); European Society of Clinical Microbiology and Infectious Diseases (ESCMID): ESCMID Research Grant 2013; Deutsche Forschungsgemeinschaft: SFB 796/C3; Bayerische Forschungstiftung: MM/4SC; Wihelm Sander-Stiftung: 2011.085.1; Research Funding from Italian Ministry of University and Research (MIUR): FIRB 2010: RBFR08UUTP
	Yes, I agree to pay the color charges.

Early stage IFI16 cytoplasmic translocation and late stage entrapment into egressing virions during HCMV infection.

Valentina Dell'Oste[a*], Deborah Gatti[a*], Francesca Gugliesi[a], Marco De Andrea[a,b], Mandar Bawadekar[b], Irene Lo Cigno[b], Matteo Biolatti[a], Marta Vallino[c], Manfred Marschall[d], Marisa Gariglio[b] and Santo Landolfo[a#].

Department of Public Health and Pediatric Sciences, University of Turin, Turin, Italy[a]; Department of Translational Medicine, University of Piemonte Orientale "A. Avogadro", Novara, Italy[b]; Institute of Plant Virology, National Research Council, Turin, Italy[c]; Institute for Clinical and Molecular Virology, Division of Biotechnology, University of Erlangen-Nuremberg, Erlangen, Germany[d]

Running Head: Nuclear IFI16 mislocalization during HCMV infection

[#] Address correspondence to Santo Landolfo, santo.landolfo@unito.it

[*]V.D.O. and D.G. contributed equally to this work and share the first authorship

Word count (abstract): 201

Word count (text): 6590

ABSTRACT

Intrinsic immune mechanisms mediated by constitutively expressed proteins termed "restriction factors" provide frontline antiviral defense. We recently demonstrated that the DNA sensor IFI16 restricts HCMV replication by down-regulating viral early and late but not immediate-early mRNAs and their protein expression. Here, we show that at an early time point during the *in vitro* infection of low-passage human embryonic lung fibroblasts (HELF), IFI16 binds to HCMV DNA. However, during a later phase following infection, IFI16 is mislocalized to the cytoplasmic virus assembly complex (AC), where it colocalizes with viral structural proteins. Indeed, upon its binding to pUL97, IFI16 undergoes phosphorylation and relocalizes to the cytoplasm of HCMV-infected cells. ESCRT (Endosomal Sorting Complex Required for Transport) machinery regulates the translocation of IFI16 into the virus AC by sorting and trafficking IFI16 into multivesicular bodies (MVB), as demonstrated by the interaction of IFI16 with two MVB markers: Vps4 and TGN46. Finally, IFI16 becomes incorporated into the newly assembled virions as demonstrated by Western blot analysis of purified virions and electron microscopy. Together, these results suggest that HCMV has evolved mechanisms to mislocalize and hijack IFI16, trapping it within mature virions. However, the significance of this IFI16 trapping following nuclear mislocalization remains to be established.

IMPORTANCE

Intracellular viral DNA sensors and restriction factors are critical components of host defence, which alarm and sensitize immune system against intruding pathogens. We have recently demonstrated that the DNA sensor IFI16 restricts HCMV replication by down-regulating viral early and late but not immediate-early mRNAs and their protein expression. However, viruses are known to evolve numerous strategies to cope and counteract such restriction factors and neutralize the first line of host defence mechanisms. Our findings describe that during early stages of infection, IFI16 successfully recognizes HCMV DNA. However, in late stages HCMV mislocalizes IFI16 into the cytoplasmic viral assembly complex (AC) and finally entraps the protein into mature virions. This work clarifies the mechanisms HCMV relies to overcome intracellular viral restriction, which provides new insights about the relevance of DNA sensors during HCMV infection.

INTRODUCTION

Intrinsic immunity constitutes a frontline antiviral defense system mediated by constitutively expressed proteins, termed restriction factors (RF), that are already present and active before a virus enters a cell (1, 2). The term "restriction factor" was originally adopted by investigators studying retroviruses. In the case of primate lentiviruses, the proteins TRIM5a and tetherin (CD317, BST/HMI), as well as members of the APOBEC family of cytidine deaminases, are prominent examples of host cell factors that can restrict the replication of human immunodeficiency virus type 1 (HIV-1) at distinct steps of the viral life cycle. However, HIV-1 has evolved evasion strategies to counter all of these factors. One evasion strategy that viruses may use is to exploit the effects of a RF for its own purposes, or to generate an interfering protein that neutralizes the effect of a RF. Another strategy involves the virus hijacking a RF during its phase of maturation to guarantee protection (reviewed in 3, 4). While the interference of retroviral replication by cellular RFs and retroviral evasion strategies have been studied in great detail, research into the ways through which RFs restrict other viral infections, such as rhabdoviruses, filoviruses, influenza viruses, hepatitis C virus, and herpesviruses, is still in its infancy (reviewed in 5). In particular, in the case of the human cytomegalovirus (HCMV), a β-herpesvirus, the cellular components of nuclear domains 10 (ND10s) (i.e. promyelocytic leukemia protein (PML), hDaxx, and Sp100) have been identified as restriction factors that are involved in mediating intrinsic immunity against this virus (6-8).

The IFI16 protein, a member of the p200 family of proteins, now designated the PYHIN family, contains an N-terminal PYRIN domain (PYD) and two partially conserved 200 amino acid-long domains (HIN domains). IFI16 displays multifaceted activity due to its ability to bind to various target proteins (i.e. transcription factors, signaling proteins, and tumor suppressor proteins) and to modulate various cell functions (9). In addition, IFI16 has been shown to bind to and function as a pattern recognition receptor (PRR) of virus-derived intracellular DNA, and trigger the expression of antiviral

cytokines via the STING-TBK1-IRF3 signaling pathway (10-20). Although many different functions have been ascribed to IFI16 (and to other proteins of the PYHIN family), its role as an antiviral restriction factor has not yet been fully described. Recent studies from our laboratory implicate the involvement of IFI16 in host defense against HCMV (21). The evidence supporting such a role of IFI16 is as follows: (i) small interfering RNA (siRNA)-mediated depletion of IFI16 in primary human embryonic lung fibroblasts (HELF) significantly increases HCMV replication efficiency as a result of augmented viral DNA synthesis; (ii) similarly, viral plaque formation is enhanced in the presence of an exogenous dominant-negative IFI16 mutant that competes with the endogenous IFI16; (iii) overexpression of functional IFI16 in HCMV-infected HELFs decreases both virus yield and viral DNA copy number; and (iv) early and late, but not immediate-early viral mRNAs and proteins are strongly down-regulated under these same conditions, suggesting that IFI16 exerts its main antiviral effect at the level of viral genome synthesis. This unique defense mechanism distinguishes the activity of IFI16 from that described for ND10.

In more general terms, human viruses have to face powerful RF responses and thus have evolved a number of strategies to overcome RF attack. Viral antagonists can act through highly specialized mechanisms, such as coupling RFs to protein degradation pathways, causing their relocalization and thus down-regulating their functionality, or even by mimicking RF substrates (5). In the case of HCMV, viral regulatory proteins (such as IE1p72, pp71, and others) mediate an efficient evasion from the antiviral state instituted by ND10, either by means of proteasomal degradation or by disrupting the host's subnuclear structure (6, 22).

In this study, we investigated the mechanisms used by HCMV to evade IFI16 restriction activity. We observed that starting from 72-96 hours post-infection (hpi), nuclear levels of IFI16 protein started to decrease in the nucleus and gradually increased in the cytoplasm of infected cells where it relocalized to the virus assembly complex (AC), as shown by its colocalization with the viral structural

proteins gB and pp65. Finally, through the use of immunogold electron microscopy and coprecipitation experiments, we provide evidence indicating that IFI16 eventually transits into the maturing virions embedded in the outer tegument layer. In conclusion, these data suggest that in order to overcome the restriction activity of IFI16, HCMV may stimulate its subcellular relocalization from the nucleus to the viral AC, followed by its inclusion into mature virions.

MATERIALS AND METHODS

Cells, viruses, and DNA constructs. Low-passage human embryonic lung fibroblasts (HELF) and human embryo kidney 293 cells (HEK 293) (Microbix Biosystems Inc.) were cultured in Eagle's minimal essential medium (Life Technologies Italia) supplemented with 10% fetal calf serum (FCS, Sigma-Aldrich). Low passage human umbilical vein endothelial cells (HUVECs) were grown in Endothelial cell growth medium-2 (EGM-2) (Lonza) supplemented with 2% Fetal Bovine Serum and 1% Penicillin-Streptomycin solution (Sigma-Aldrich) as previously described (23). The HCMV laboratory strain AD169 (ATCC-VR538) and the HCMV clinical isolate derivative VR1814 were propagated and titrated as previously described (21, 24). UV-inactivated AD169 was prepared using a double pulse of UV-B light (1.2 J/cm^2). The mutant HCMV (AD169) BAC213 (ΔUL97/GFP$^+$) was produced as previously described (25, 26). siRNA UL97 and siRNA CTRL were purchased from SIGMA and electroporated at a final concentration of 300 nM. Plasmids expressing WT and DN forms of Vps4A (pBJ-Vps4A$_{WT}$ and pBJ-Vps4A$_{E228Q}$, respectively) were obtained as previously described (27, 28).

Antibodies and reagents. Primary antibodies were obtained from various sources, as shown in Supplementary Table S1. Conjugated antibodies were as follow: fluorescein-isothiocyanate (FITC)-anti-rabbit (Sigma-Aldrich), Texas Red-anti-mouse and anti-rabbit (Invitrogen S.A.); horseradish peroxidase (HRP)-anti-mouse, HRP-anti-rabbit (GE Healthcare). The chemicals used in this study

were: Gö6976 (inhibitor of serine/threonine protein kinases, particularly pUL97 and PKC; Calbiochem) (29); phosphonoformic acid (PFA, Foscarnet) and Ganciclovir (HCMV inhibitors, Sigma-Aldrich).

Cell Viability Assay. Cells were seeded at a density of $1x10^4$/well in a 96-well culture plate. After 24 hours, cells were treated with different doses (from 0.5 to 5 μM) of Gö6976. 72 hours after treatment, cell viability was determined using the 3-(4,5-dimethylthiazol-2-yl)-2,5-diphenyltetrazolium bromide (MTT) (Sigma-Aldrich) method.

Quantitative Real-Time RT-PCR. Real-time quantitative reverse transcription-PCR (RT-PCR) analysis was performed on an Mx 3000 P apparatus (Stratagene). Total RNA was extracted with the NucleoSpin RNA kit (Macherey-Nagel) and 1 μg was retrotranscribed using the Revert-Aid H-Minus FirstStrand cDNA Synthesis Kit (Fermentas). Reverse-transcribed cDNAs were amplified in duplicate using Brilliant Sybr green QPCR master mix (Fermentas) for IFI16; the housekeeping gene Glyceraldehyde-3-phosphate dehydrogenase (GADPH) was used to normalize for variations in cDNA levels (Primer sequences: IFI16 forward: ACTGAGTACAACAAAGCCATTTGA; IFI16 reverse: TTGTGACATTGTCCTGTCCCCAC; GADPH forward: TCGGAGTCAACGGATTTGGTC; GADPH reverse: CGTTCTCAGCCTTGACGGTG).

ChIP assay. Similar to the method published by Cristea et al. (11) and Li et al. (18). HELFs were infected with HCMV at an MOI of 5. At 6 hpi, cells were cross-linked with 1% paraformaldehyde for 15 min and then processed for ChIP assay, using the EpiTect ChIP OneDay Kit (Qiagen) according to the manufacturer's instruction. Anti-IFI16 antibody (5 μg) was used to pull down the protein-chromatin complexes. Rabbit IgG was used as a negative control. The immunoprecipitated DNA was recovered by column purification and analyzed by PCR using HCMV or human specific primers (primer sequences are available on request).

Immunofluorescence microscopy. Immunofluorescence analysis was performed as previously described (30) using the appropriate dilution of primary antibodies (Table S1) for 1h at room

temperature (RT), followed by 1h with secondary antibodies in the dark at RT. Nuclei were counterstained with DAPI where indicated. Finally, coverslips were mounted with Vectashield mounting medium (Vector Laboratories Ltd,) and cells visualized with a Leica TCS SP2 confocal microscope, equipped with a UV laser (351–364 nm) and argon–krypton laser (457–675 nm) (Leica Microsystems S.r.l.), using a 63X oil immersion objective NA 1.4. Fluorescence *in-situ* hybridization was combined with immunofluorescence by performing the hybridization first as described below and then incubating the coverslips with primary and secondary antibodies.

Fluorescence *in-situ* hybridization (FISH). HCMV-infected HELFs were grown on glass slides, fixed as described above, and permeabilized with 0.5% Triton-X100 for 20 min at 4°C. The probe used for FISH was a BAC DNA containing the entire HCMV genome (a gift from Jay Nelson, Oregon Health and Science University), labeled using the biotin-nick translation system (Roche Diagnostics GmbH) according to the manufacturer's protocol. The probe was added to the hybridization buffer (0.2 ng/µl yeast t-RNA, 50% formamide, 15% SSC, 0.1% Tween-20) at a concentration of 2 ng/µl, then incubated at 72°C for 5 min in order to denature the probe and the sample. Hybridization was continued overnight at 37°C in a humidified chamber. After stringent washing, cells were blocked with 10% normal goat serum. HCMV probes were then detected using the tyramide signal amplification procedure, according to manufacturer's instructions (PerkinElmer Life and Analytical Sciences Inc.). Images were analyzed using a confocal laser scanning microscope.

Immunoprecipitation assay. Uninfected cells or cells infected with HCMV (MOI of 1) for different times were washed and lysed in RIPA buffer. 200 µg of protein were incubated with 2 µg immunoprecipitating or control antibody for 1h at room temperature with rotation and the immune complexes were collected using protein G–Sepharose (Sigma-Aldrich). The Sepharose beads were pelleted and washed three times with RIPA buffer, boiled with sample buffer, and resolved on an 8% SDS-PAGE gel to assess the protein binding by Western blot.

Western blot analysis. Nuclear and cytoplasmic extracts were collected using the Nuclear Extract Kit (Active Motif), according to the manufacturer's instructions, and subjected to immunoblot analysis as previously described (31). Briefly, an equal amount of cell extracts were fractionated by electrophoresis on sodium dodecyl sulfate polyacrylamide gels and transferred to Immobilon-P membranes (Millipore). After blocking, membranes were incubated overnight at 4°C with the appropriate primary antibodies. Membranes were then washed and incubated for 1h at RT with secondary antibodies. Proteins were detected using an enhanced chemiluminescence detection kit (Thermo SCIENTIFIC).

Scanning densitometry of the bands was performed using Quantity One software, version 4.6.9 (Bio-Rad Laboratories S.r.l.). Background values were subtracted from each calculated value.

Virion purification and viral protein extraction. Virus containing media was collected at 192h post-infection (MOI of 1), centrifuged at 3000 rpm for 10 min to remove large cellular debris, and then filtered using a Filtropur 0.45 (Sarstedt). To pellet viral particles, the media was then centrifuged at 13000 g for 2h at 4°C in a Beckman SW32 Ti rotor. The viral pellet was resuspended in PBS1X and centrifuged in a 20-41-70% discontinuous sucrose gradient composed of the following steps: 0.5 ml 60% (w/w) sucrose, 1.5 ml 41% sucrose, and 1 ml 20% sucrose. Sucrose solutions were made in PBS1X. Following centrifugation overnight at 130000 g at 4°C, using a Beckman SW40 Ti rotor, the virus containing band was removed from the gradient and lysed with 50 mM Tris HCl pH 6.8, 2% SDS, for 30 min at 4°C. After heating for 10 min at 95°C and clarification, the viral protein extract was collected.

***In vitro* kinase assay.** The kinase activity of FLAG-tagged pUL97 was determined *in vitro* after immunoprecipitation of the kinase from whole-cell lysates of HEK 293 cells, previously electroporated using a MicroPorator MP-100 (Digital BioTechnology), according to the manufacturer's instructions (a single 1200 V pulse, 30 ms pulse width). The following UL97 expression constructs were employed:

pcDNA-UL97-M2, pcDNA-UL97(181-707)-M2, and pcDNA-UL97(1-595)-M2 (25). Immunoprecipitates were subsequently pelleted, washed, and subjected to *in vitro* kinase assay reaction [2.5 μCi of γ-^{32}P ATP (Amersham Biosciences)] at 30°C for 30 min, as previously described (26), in the presence of the recombinant full-length IFI16 as substrate (5 μg). Following incubation, samples were separated by SDS-PAGE, transferred to Immobilon-P membranes (Millipore), and processed for autoradiography and immunoblotting.

Immunogold labeling of isolated viral particles. For transmission electron microscopic analysis, samples were allowed to adsorb onto carbon and formvar-coated grids and fixed in 4% paraformaldehyde. Grids were then washed with PBS and water and, when appropriate, samples were permeabilized using 0.2% Triton. The grids were stained with primary antibodies followed by gold-labeled secondary antibodies in the presence of 10% human serum (32). Grids were then negatively stained using 0.5% uranyl acetate for 1 min. Images were captured using a CM 10 electron microscope (Philips).

RESULTS

IFI16 colocalizes with HCMV genome early during infection. IFI16 has previously been shown to interact with HSV-1 as well as HCMV DNA early during infection (13, 15, 17, 18, 33, 34). To confirm that endogenous IFI16 interacts with viral DNA during natural HCMV infection, HELFs were mock infected or infected with HCMV for 12h. Combined immunofluorescence and FISH analysis was performed using IFI16 antibodies and a probe for the HCMV genome. In mock infected cells, IFI16 was distributed into defined spots, which appear to reorganize following HCMV infection and colocalize with the HCMV-DNA (Fig. 1A). The colocalization of IFI16 with the viral genome is reinforced by Z stack images, generated by 3D reconstruction of confocal images to improve colocalization analysis (Fig. 1A, far right pictures). Consistent with FISH analysis and in accord with

the results reported by Li et al. (18), ChIP assays at 6 hpi demonstrated that endogenous IFI16 specifically recognizes virus DNA loci, but not host chromosomal DNA (Fig. 1B). Altogether, these results are compatible with the proposed role of IFI16 as a nuclear sensor for HCMV DNA.

HCMV relocalizes IFI16 nuclear protein into the cytoplasm. IFI16 is typically located within the nucleus (11, 15, 35, 36), but it translocates to the cytoplasm following infection with HSV-1 (12, 13, 15, 17, 34), KSHV (14, 16), or EBV (10). To determine the subcellular localization of IFI16 during early and late infection with HCMV, two different approaches were adopted: Western blot analysis and immunofluorescence (IF). In the first case, HELFs, synchronized by serum starvation to increase infection efficiency (37, 38), were mock infected or infected with HCMV at an MOI of 1; they were then fractionated into nuclear and cytoplasmic components. The purity of the nuclear and cytoplasmic fractions was monitored by Western blot for the presence of TATA binding protein (TBP) and tubulin, respectively (Fig. 1C). IEA protein labeling was used to assess HCMV infection by Western blot (Fig. S1, panel A). In mock infected cells, IFI16 was exclusively nuclear (Fig. 1C, lane 1). Notably, at 24 hpi, HCMV-infected cells showed an increase in nuclear IFI16 that peaked at 48h then decreased at 96 hpi and almost disappeared at 144 hpi (Fig. 1C, lane 2-6). However, at 48 hpi IFI16 was also detected at appreciable levels in the cytoplasm of HCMV-infected cells and gradually increased at later time points (Fig. 1C, lane 10). Consistent with the Western blot results, RT-PCR analysis confirmed that HCMV infection upregulates IFI16 also at the mRNA level (~2 fold between 12 and 24 hours of HCMV *vs*. mock infected cells) (Fig. S1, panel B).

These results demonstrate that HCMV induces the cytoplasmic translocation of IFI16 early on during infection. In apparent contrast to our results, Li et al. (18) and Cristea et al. (11) found that endogenous IFI16 remained nuclear during early HCMV infection. In our study, nuclear delocalization started from 96 hpi, a time point not examined by Cristea et al. (11) and Li et al. (18). Moreover, IFI16 nuclear egress into the cytoplasm was only observed when synchronized cell cultures were used. This condition

was created to increase virus infection efficiency. Thus, considering the different post infection time points analyzed and the virus MOI employed, the discrepancies between our results the results reported by the other investigators can be easily explained.

To gain deeper insight into the nuclear disappearance of IFI16, a detailed analysis using confocal microscopy at time points ranging from 12 hpi to 144 hpi was performed. As shown in Fig. 1, panel D, and Fig. S1, panel C, all infected cells positive for IEA staining showed the nuclear presence of IFI16 during the first 12 hpi. In contrast, between 72 and 96 hpi, IFI16 became undetectable in the nucleus of the majority of the cells, accompanied by its appearance in the cytoplasm. Consistent with the Western blot outcome, the IFI16 nuclear decline in infected cells was accompanied by the appearance of IFI16 in the cytoplasm, specifically in the compartment that overlapped with the virus AC, as shown by its colocalization with the viral glycoprotein gB. To verify that the signal observed in the AC was specific for IFI16 and not due to rabbit IgG binding to HCMV-encoded Fc receptor-like proteins (39, 40), the staining was performed after blocking the Fc receptors using 10% HCMV negative human serum prior to the addition of the specific rabbit IgG, as described in Buchkovich et al. (41). Similar results were obtained using monoclonal anti-IFI16 antibodies (Santa Cruz) (data not shown), which have also been used in other studies to demonstrate the nuclear export of IFI16 (14, 15).

Finally, to exclude the possibility that IFI16 nuclear egression was limited to HELF cells infected by the AD169 strain, IF analysis was performed on human umbilical vein endothelial cells (HUVEC) infected with the endotheliotropic VR1814 strain. A similar pattern of IFI16 relocalization from the nucleus accompanied by its appearance in the AC compartment was observed, demonstrating that IFI16 nuclear delocalization is related to HCMV infection (Fig. S1 panel D).

HCMV early/late proteins induce the nucleo-cytoplasmic relocalization of IFI16. The observation that the relocalization of IFI16 protein into the cytoplasm sharply increases from 48 hpi, accompanied by its gradual nuclear disappearance, suggests that an early or late viral protein(s) is(are) responsible

for driving IFI16 into the cytoplasm. To test this possibility, HELFs were infected with UVB-inactivated HCMV, or with wild-type HCMV in the presence of 100 μM phosphonoformic acid (PFA) or 100 μM ganciclovir (GCV). To confirm that the infection was successfully established, FISH staining was performed (Fig. S2). As shown in Fig. 2, all treatments blocked IFI16 nucleo-cytoplasmic translocation. Since treatment with PFA or GCV inhibits viral DNA synthesis and the accumulation of early-late and late viral proteins to different extents, an early-late or late HCMV gene product is likely to be responsible for IFI16 subcellular relocalization.

HCMV pUL97 contributes to the nucleo-cytoplasmic translocation of IFI16. To gain insight into the mechanism responsible for the HCMV-induced nuclear reduction and relocalization of IFI16 into the cytoplasm, we focused on the recently described HCMV nuclear egress complex (NEC) composed of viral and cellular proteins (25, 26, 42). In this context, the viral protein kinase pUL97 is known to play an important role by phosphorylating and reorganizing nuclear lamins A/C, a step required for the nuclear egress of viral capsids (26, 43). We therefore hypothesized that pUL97 might also be involved in the regulation of IFI16 nucleo-cytoplasmic relocalization. To test this, HELFs were infected with a GFP-tagged recombinant UL97 deletion mutant BAC (BAC ΔUL97), or AD169 (AD169 UL97^{+}) as control (25, 43), and used for immunostaining at 32 days post infection (dpi) or 96 hpi, respectively. The lack of production of pUL97 by BAC ΔUL97 was confirmed by immunofluorescence staining (data not shown). The choice to perform the experiments at different time points was due to the delayed replication kinetics of viruses lacking a functional pUL97 kinase compared to the wild-type strain, as previously reported (25, 44, 45). As shown in Fig. 3A, many AD169 UL97^{+}-infected cells showed IFI16 relocalization into the cytoplasm. In contrast, cells infected with a UL97 deletion mutant BAC (BAC ΔUL97) displayed IFI16 nuclear accumulation (Fig. 3A, panel 1). To gain further supporting evidence of the specific involvement of pUL97 in the cytoplasmic relocalization of IFI16, HELFs were electroporated with a mixture of three different small interfering RNAs targeting the UL97 gene

299 (siRNA UL97) or with scrambled control siRNA (siRNA CTRL). Twenty-four hours later, cells were
300 infected with HCMV for a duration of 72h. The siRNA-mediated knock-down reduced the expression
301 of pUL97 protein by approximately 90-95%, as indicated by Western blot analysis (Fig. S3, panel A).
302 As shown in Fig. 3A (panel 2), and consistent with the results of the BAC mutant experiments,
303 inhibition of pUL97 expression prevented IFI16 nuclear egress compared to infected cells pre-treated
304 with control siRNA. Moreover, treating infected cells with the pUL97 inhibitor Gö6976 (2 μM, (26))
305 strongly suppressed IFI16 relocalization (Fig. 3A, panel 3), in agreement with the results of previous
306 studies (26, 29). No such effect was observed when cells were treated with vehicle control (DMSO). To
307 exclude the possibility that the Gö6976 inhibitor might influence the observed effect independent of
308 viral infection, the MTT assay was used to examine and quantify its effect on HELF survival (Fig. S3,
309 panel B). Finally, to investigate whether pUL97 alone is sufficient to induce IFI16 nuclear egress in the
310 absence of other viral gene products, the protein was transfected into HELFs. In contrast to what we
311 observed following virus infection, IFI16 retained its nuclear localization 72h after protein
312 electroporation, indicating that pUL97 alone, in the absence of viable and functional virus, is not
313 sufficient to trigger the relocalization of IFI16 into the cytoplasm (Fig. S3, panel C).

314 To investigate the interplay between IFI16 and pUL97, total protein extracts from HELFs
315 infected with HCMV for 96h were used for coimmunoprecipitation with anti-IFI16 or the appropriate
316 control antibodies. Precipitates were then immunostained with a monoclonal anti-pUL97 antibody. As
317 shown in Fig. 3B (left panel), virus pUL97 indeed binds to IFI16. This interaction is specific as no
318 migrating bands were present when coprecipitation was performed using control antibodies. The
319 presence of pUL97 in all protein extracts was monitored by the staining of INPUT (non-
320 immunoprecipitated whole cell extract) control samples (Fig. 3B). To confirm further the specificity of
321 the interaction, coimmunoprecipitation and immunoblotting experiments were performed in reverse
322 order, i.e., anti-UL97 was used for immunoprecipitation and anti-IFI16 for immunoblotting (Fig. 3B,

right panel). In line with previous results, a band corresponding to IFI16 was detectable when protein extracts were immunoprecipitated with an antibody against virus pUL97.

The interaction between IFI16 and pUL97 suggested that IFI16 might be directly phosphorylated by pUL97 kinase. To address this hypothesis, we performed an *in vitro* kinase assay (26) using wild-type and mutant pUL97, immunoprecipitated from lysates of transiently transfected HEK 293 cells, and incubated with highly purified recombinant IFI16 protein as substrate. IFI16 phosphorylation was exclusively detectable for wild-type pUL97 and catalytically active pUL97 [N-terminally truncated pUL97-(181-707)] (Fig. 3C, lanes 1 and 2, respectively), whereas an inactive C-terminally truncated version (pUL97-1-595) (lane 3) did not produce a phosphorylation signal.

IFI16 co-localizes with the viral AC following nuclear egress. It has been proposed that HCMV acquires its final envelope from the trans-Golgi network (TGN) or from TGN-derived particles (28, 42). In addition, many cellular markers, like those of early, recycling, and late endosomes, as well as the Endosomal Sorting Complex Required for Transport (ESCRT) and several viral tegument and envelope proteins, including gB, all localize to the AC (28). Since IFI16 staining appears to overlap with the AC, as shown by confocal analysis, we wanted to gain insights into the fate of IFI16 following nuclear egression. We performed an immunofluorescence assay at 96 hpi using anti-IFI16 antibodies together with antibodies recognizing the virion envelope protein gB, vacuolar protein sorting-4A (Vps4A, a component of the ESCRT machinery), or TGN46 (a marker of the trans-Golgi network) (Fig. 4A). As shown in Fig. 1D and 4A (confocal Z stack images), a high level of IFI16 colocalization could be detected with viral gB, Vps4A, and TGN46. These results strongly suggest that IFI16 mislocalizes out of the nucleus and associates with AC-containing virion particles.

To define better the relationship between IFI16 and ESCRT components, total protein extracts from HELFs infected with HCMV for 96h were immunoprecipitated with anti-Vps4A or control antibodies, and immunoblotted with polyclonal anti-IFI16 antibodies. As shown in Fig. 4B (upper

panel), no interaction between Vps4A and IFI16 was observed in mock-infected cells. In contrast, HCMV infection induced a strong interaction between Vps4A and IFI16 as shown by the co-IP reactions. The same results were obtained in reverse order (Fig. 4B, lower panel). Vps4A induction by HCMV was also evident in the very same total protein extracts. Finally, no bands were detected when cell extracts were immunoprecipitated with control antibodies. Overall, these results indicate that there might be a connection between the egress of viral proteins from the nucleus and the mislocalization of IFI16 protein into the AC.

Functional significance of the IFI16-Vps4 interaction. To evaluate the impact of dysfunctional MVBs on IFI16 localization, we used a previously described construct expressing a dominant negative Vps4A (27, 28). HELF cells were transfected with FLAG-tagged pBJ5-Vps4A$_{E228Q}$ or the corresponding wild-type form pBJ5-Vps4A$_{WT}$ and 24 hours later infected with HCMV. The transfection efficiency of HELFs is low (~20%), such that only the FLAG-expressing subpopulation of cells was studied. Confocal microscopy at 72 hpi (96% HCMV-positive cells, data not shown) demonstrated that in the pBJ5-Vps4$_{E228Q}$-transfected cells IFI16 remains strictly nuclear (Fig. 4C, lower panel) in all of the infected cells. In contrast, in cells transfected with the wild-type vector, we observed that IFI16 mislocalizes to the cytoplasm (upper panels), confirming the dependence of IFI16 mislocalization on functional MVB biogenesis, which serves as a platform for HCMV envelopment/egress.

Immunogold labeling of IFI16 in purified HCMV particles. The colocalization of IFI16 and viral gB in the AC opened up the possibility that IFI16 may be incorporated into viral particles during maturation. To investigate this possibility, HCMV virions were fractionated by sucrose gradient from supernatants of HELFs infected at an MOI of 1 for 192 hours, and analyzed by Western blot for the viral proteins IEA, UL44, and pp65, and cellular proteins IFI16 and p53 (the latter is translocated into the cytoplasm during HCMV infection) (46). As shown in Fig. 5A, pp65 and IFI16 were detected in

371 highly purified virions, indicating their incorporation. The specificity of IFI16 incorporation into viral
372 particles was supported by the finding that neither of the nonstructural viral proteins, such as IEA,
373 UL44 nor cellular p53, were identified by Western blot analysis. Importantly, total cell extracts from
374 mock- or HCMV-infected HELFs were included in order to estimate the levels of IFI16 induction by
375 HCMV infection. The presence of IFI16 in purified virions was confirmed by coimmunoprecipitation
376 experiments using anti-pp65 antibodies. As shown in Fig. 5B, IFI16 indeed interacted with the HCMV
377 tegument protein pp65. Consistent with our results, Li et al. (18) have recently demonstrated that early
378 during infection, pp65 associates with IFI16 by interacting with its pyrin domain, inhibiting its
379 subsequent immune signaling (11, 18).

380 To investigate further the incorporation of IFI16 into mature virions, we labeled purified virus
381 particles with IFI16-specific antibodies followed by gold-conjugated secondary antibodies and
382 analyzed them by means of electron microscopy. The integrity of the purified virions was further
383 verified by negative staining that showed two classes of spherical enveloped particles: 200 nm diameter
384 HCMV virions and larger structures corresponding to dense bodies (DBs). The ratio of virions to DBs
385 was about 1:2. The specificity of the immunogold labeling was assessed by omitting the primary
386 antibody. The virus preparation was permeabilized or left unmasked, so that antibodies could recognize
387 within the inner layers of the viral particles or on their surface, respectively. As shown in Fig. 5C, gB,
388 used as a control, was observed in the outer envelope of the purified virions, while pp65 was present
389 inside the viral particles. Altogether, these results demonstrate that a percentage of IFI16 protein
390 becomes trapped within mature virions.

391

392 ## DISCUSSION

393 The importance of the role played by restriction factors in controlling viral infection is substantiated by
394 the diverse mechanisms the viruses have evolved to antagonize it (47-49). We recently demonstrated

395 that the IFN-inducible protein IFI16 may act as a restriction factor for HCMV replication by down-
396 regulating viral early and late mRNA and protein expression (21). In this study, we examined how
397 HCMV can overcome the antiviral activity of the nuclear restriction factor IFI16. Consistent with its
398 property as a pathogenic DNA sensor, (10-14, 17-20, 33, 50), detailed kinetics studies exploiting
399 immunofluorescence show that in the early phases of infection, IFI16 binds to viral DNA, also
400 confirmed by FISH combined with Western blot analysis. These results are in line with previous
401 studies showing that following HCMV infection IFI16 binds viral DNA and triggers the expression of
402 antiviral cytokines via the STING-TBK1-IRF3 signaling pathway (18).

403 During a late phase post infection, however, IFI16 levels decreases inside the nucleus and this is
404 accompanied by a parallel increase in its presence in the cytoplasmic AC, as shown by Western blot
405 and confocal microscopy analysis. This nucleo-cytoplasmic egress of IFI16 in HCMV-infected cells is
406 driven, at least in part, by the viral protein kinase pUL97, which binds and phosphorylates nuclear
407 IFI16. Subsequently, the IFI16-AC complex mediates its incorporation into newly assembled virions.
408 IFI16 mislocalization and assembly into mature virions appears to be regulated by the ESCRT
409 machinery through its sorting and trafficking into multivesicular bodies.

410 Other studies have examined the effects of herpesvirus infection on IFI16 degradation. Orzalli
411 et al. (15, 51) demonstrated that during HSV-1 infection, the viral nuclear ICP0 protein leads to IFI16
412 degradation. Similarly, Johnson et al. (13) showed that HSV-1 specifically targets IFI16 for rapid
413 proteasomal degradation later on post-infection. Interestingly, another herpesvirus, namely KSHV,
414 which undergoes latency in endothelial cells, was not found to cause IFI16 degradation early on during
415 infection, suggesting a relationship between virus replication/latency and IFI16 fate (13, 14).

416 Although the egression of IFI16 from the nucleus into the cytoplasm following pathogenic or
417 damaged DNA sensing has now been widely demonstrated, the mechanisms it relies on have not been
418 clarified. Therefore, in the present study we sought to exploit the HCMV model in order to gain some

419 insight into the mechanisms underlying IFI16 mislocalization. The finding that IFI16 egress from the
420 nucleus was first detected at 48 hpi and the fact that it could be blocked by pre-treating cells with
421 inhibitors of viral L gene expression suggest that HCMV L genes may be responsible for IFI16
422 mislocalization. During HCMV replication, DNA-filled capsids bud through the inner nuclear
423 membrane (INM) and transit from the nucleus direct to the AC located in the cytoplasm close to the
424 nuclear membrane (42). The HCMV-specific nuclear egress complex (NEC) is composed of both viral
425 and cellular proteins, in particular protein kinases with the capacity to induce the destabilization of the
426 nuclear lamina (43). The viral protein kinase pUL97, along with cellular protein kinase C (PKC), plays
427 an important role by phosphorylating several types of nuclear lamins, events that lead to the
428 reorganization of the proteinaceous network underlying the inner nuclear membrane and the egression
429 of the DNA-filled capsids (26, 43, 52). By combining molecular-virological analyses with biochemical
430 and pharmacological approaches we demonstrate that pUL97 binds and phosphorylates IFI16 *in vitro*,
431 triggering its relocalization from the nucleus into the cytoplasm of HCMV-infected cells. This assertion
432 is based on the finding that the lack of viral pUL97 expression (BAC ΔUL97) and/or the inhibition of
433 its kinase activity substantially reduce IFI16 relocalization. Together with the observation that IFI16 is
434 phosphorylated both *in vitro* and in HCMV infected cells by pUL97 kinase, our results demonstrate
435 that one of the viral candidates responsible for IFI16 subcellular relocalization and the inhibition of its
436 restriction activity could be pUL97. In HCMV infection, the transmembrane protein pUL50 anchors
437 the NEC within the inner nuclear membrane and associates with core NEC components, such as pUL53.
438 As a consequence, the NEC is able to recruit regulatory kinases, like pUL97, to disassemble the nuclear
439 lamina and to facilitate nuclear capsid egression. As IFI16 has been shown to interact with pUL97, we
440 can speculate that IFI16 might interact with further components of the NEC.

441 Post-translational modification provides a possible means of regulating IFI16 subcellular
442 localization. The acetylation and phosphorylation of different IFI16 motifs have been demonstrated to

443 regulate its subcellular localization in lymphocytes and macrophages (11, 34). In particular, acetylation
444 of the nuclear localization sequence promotes the cytoplasmic accumulation of IFII6 by inhibiting its
445 nuclear import (34). In HCMV-infected cells, IFI16 interacts with viral pUL97 and undergoes *in vitro*
446 phosphorylation. Moreover, the nuclear accumulation of IFI16 can be observed upon treatment with
447 Gö6976, an inhibitor of pUL97 phosphorylation (26, 29). Together, these results suggest that
448 phosphorylation by pUL97 may regulate the relocalization of IFI16 from the nucleus to the cytoplasm.
449 Although the replication of all herpesviruses includes nuclear and cytoplasmic maturation
450 events, the AC is a unique feature of beta-herpesvirus-infected cells (53). Virus particles congregate in
451 the AC during the late phases of infection (42), consistent with its important role in controlling final
452 tegumentation, envelopment, and egress from the cell. Immunofluorescence analysis starting at 24 hpi
453 demonstrates that IFI16 co-localizes outside the nucleus of infected cells in a structure that seems to be
454 the AC. The AC was recognized based on the hallmark morphology of CMV-infected cells which
455 consist of an enlargement of the nucleus that transforms into a kidney-shaped form, with the AC
456 pressing against the newly formed depression in the nucleus (54). To confirm definitively the nature of
457 the AC, confocal laser microscopy was performed using antibodies against host proteins of the MVBs
458 included in the AC, such as the ATPase Vps4A involved in the ESCRT pathway, the trans-Golgi
459 network marker TGN46, and the viral protein gB, known to colocalize to the AC during the late phase
460 of HCMV infection. Moreover, using coimmunoprecipitation experiments we found that IFI16
461 interacts with Vps4A upon HCMV infection. Overall, these results demonstrate that HCMV induces
462 IFI16 to mislocalize to MVBs, where the virus undergoes final maturation.
463 To provide a functional significance of the colocalization experiments, we evaluated the impact
464 of inhibiting the final component of the ESCRT machinery, Vps4A, using a dominant negative mutant
465 ($Vps4A_{E228Q}$) known to impair MVB biogenesis and HCMV plaque formation (28). The nuclear
466 retention of IFI16 in cells where MVB biogenesis was inhibited suggests a strict dependence of IFI16

467 subcellular localization on HCMV replication and designates Vps4A as a key player in the evasion
468 mechanism employed by HCMV to escape IFI16.

469 The presence of IFI16 in the AC and the lack of protein degradation in the late stages of
470 infection could suggest that IFI16 is incorporated into the maturing virion particles. To investigate this
471 possibility, we purified HCMV virions and applied Western blot and electron microscopy analysis to
472 ascertain whether HCMV virions may actually contain the mislocalized IFI16. Intriguingly, Western
473 blot analysis demonstrates the presence of IFI16, but not p53, in the viral protein extract. Moreover, the
474 immunolocalization results confirmed the incorporation of IFI16 into purified virions, and in particular
475 in the outer layer of the tegument in the proximity of pp65, as shown by co-precipitation experiments.
476 This finding leans toward excluding the possibility that IFI16 non-specifically aggregates to virions
477 during their maturation. Consistent with our results, previous studies based on mass spectrometry
478 approaches have demonstrated the presence of at least 70 host cellular and 71 HCMV proteins in
479 mature virions (55, 56). More recently, it has been demonstrated that HCMV may include both trans-
480 Golgi network and endosomal markers when undergoing final envelopment (32). Altogether, these
481 findings raise some important questions. The first one asks how specific the inclusion of host proteins
482 in HCMV virions is, since only a percentage of virus particles contain IFI16. The observation that
483 IFI16, but not p53, another protein egressing from the nucleus during HCMV infection, is included in
484 the virion, suggests that some mechanisms of selecting host proteins must exist. The second important
485 question that needs addressing is whether HCMV includes IFI16 in the virion in order to evade its
486 restriction activity. At the moment, no evidence exists suggesting a functional consequence of IFI16
487 embedded within the viral particles, thus only speculations can be put forward. However, some
488 observations may help to explain why the virus hijacks IFI16 and embeds it into the outer layer of the
489 tegument. First, IFI16 triggers the activity of transcription factor NFκB that is needed in the first steps
490 of HCMV infection (57, 58). Second, it has been demonstrated that pp65 (pUL83) triggers the

491 expression of the viral immediate-early promoter through its interaction with IFI16 protein (11, 18).
492 Finally, overexpression of IFI16 up-regulates immediate-early protein expression during the first hours
493 of infection (21). Altogether, these observations suggest that HCMV may hijack IFI16 in order to
494 exploit its capacity to enhance the transcription of IE genes during the early steps of infection, followed
495 by the relocalization of IFI16 into the cytoplasmic AC with the scope of concealing its restriction
496 activity during the late steps of infection.
497

498 **ACKNOWLEDGEMENTS**

499 We thank Edward S. Mocarski for his critical review of the manuscript, and Thomas Mertens
500 for providing us the anti-UL97 antibodies. This study was supported by: MIUR PRIN 2012 to SL
501 (2012SNMJRL) and VDO (20127MFYBR); MIUR FIRB 2010 to MDA (RBFR08UUTP); research
502 funding from the University of Turin 2013 to SL, MDA, and VDO; ESCMID Research Grant 2013 to
503 VDO. MM was supported by the Deutsche Forschungsgemeinschaft (SFB 796/C3), Bayerische
504 Forschungsstiftung (grant MM/4SC) and Wilhelm Sander-Stiftung (grant 2011.085.1).
505

506 **REFERENCES**

507 1. **Bieniasz PD.** 2004. Intrinsic immunity: a front-line defense against viral attack. Nat. Immunol.
508 **5:**1109-1115.
509 2. **Roy CR, Mocarski ES.** 2007. Pathogen subversion of cell-intrinsic innate immunity. Nat
510 Immunol. **8:**1179-1187.
511 3. **Douglas JL, Gustin JK, Viswanathan K, Mansouri M, Moses AV, Fruh K.** 2010. The great
512 escape: viral strategies to counter BST-2/tetherin. PLoS Pathog. **6:**e1000913.
513 4. **Takeuchi H, Matano T.** 2008. Host factors involved in resistance to retroviral infection.
514 Microbiol. Immunol. **52:**318-325.

5. **Duggal NK, Emerman M.** 2012. Evolutionary conflicts between viruses and restriction factors shape immunity. Nat. Rev. Immunol. **12:**687-695.

6. **Tavalai N, Stamminger T.** 2011. Intrinsic cellular defense mechanisms targeting human cytomegalovirus. Virus Res. **157:**128-133.

7. **Ahn JH, Hayward GS.** 2000. Disruption of PML-associated nuclear bodies by IE1 correlates with efficient early stages of viral gene expression and DNA replication in human cytomegalovirus infection. Virology. **274:**39-55.

8. **Tavalai N, Stamminger T.** 2009. Interplay between Herpesvirus Infection and Host Defense by PML Nuclear Bodies. Viruses. **1:**1240-1264.

9. **Gariglio M, Mondini M, De Andrea M, Landolfo S.** 2011. The multifaceted interferon-inducible p200 family proteins: from cell biology to human pathology. J. Interferon Cytokine Res. **31:**159-172.

10. **Ansari MA, Singh VV, Dutta S, Veettil MV, Dutta D, Chikoti L, Lu J, Everly D, Chandran B.** 2013. Constitutive interferon-inducible protein 16-inflammasome activation during Epstein-Barr virus latency I, II, and III in B and epithelial cells. J. Virol. **87:**8606-8623.

11. **Cristea IM, Moorman NJ, Terhune SS, Cuevas CD, O'Keefe ES, Rout MP, Chait BT, Shenk T.** 2010. Human cytomegalovirus pUL83 stimulates activity of the viral immediate-early promoter through its interaction with the cellular IFI16 protein. J. Virol. **84:**7803-7814.

12. **Horan KA, Hansen K, Jakobsen MR, Holm CK, Soby S, Unterholzner L, Thompson M, West JA, Iversen MB, Rasmussen SB, Ellermann-Eriksen S, Kurt-Jones E, Landolfo S, Damania B, Melchjorsen J, Bowie AG, Fitzgerald KA, Paludan SR.** 2013. Proteasomal degradation of herpes simplex virus capsids in macrophages releases DNA to the cytosol for recognition by DNA sensors. J. Immunol. **190:**2311-2319.

13. **Johnson KE, Chikoti L, Chandran B.** 2013. Herpes Simplex Virus 1 Infection Induces Activation and Subsequent Inhibition of the IFI16 and NLRP3 Inflammasomes. J. Virol. **87:**5005-5018.

14. **Kerur N, Veettil MV, Sharma-Walia N, Bottero V, Sadagopan S, Otageri P, Chandran B.** 2011. IFI16 Acts as a Nuclear Pathogen Sensor to Induce the Inflammasome in Response to Kaposi Sarcoma-Associated Herpesvirus Infection. Cell Host Microbe. **9:**363-375.

15. **Orzalli MH, DeLuca NA, Knipe DM.** 2012. Nuclear IFI16 induction of IRF-3 signaling during herpesviral infection and degradation of IFI16 by the viral ICP0 protein. Proc. Natl. Acad. Sci. U. S. A. **109:**E3008-3017.

16. **Singh VV, Kerur N, Bottero V, Dutta S, Chakraborty S, Ansari MA, Paudel N, Chikoti L, Chandran B.** 2013. Kaposi's Sarcoma-Associated Herpesvirus Latency in Endothelial and B Cells Activates Gamma Interferon-Inducible Protein 16-Mediated Inflammasomes. J. Virol. **87:**4417-4431.

17. **Unterholzner L, Keating SE, Baran M, Horan KA, Jensen SB, Sharma S, Sirois CM, Jin T, Latz E, Xiao TS, Fitzgerald KA, Paludan SR, Bowie AG.** 2010. IFI16 is an innate immune sensor for intracellular DNA. Nat. Immunol. **11:**997-1004.

18. **Li T, Chen J, Cristea IM.** 2013. Human Cytomegalovirus Tegument Protein pUL83 Inhibits IFI16-Mediated DNA Sensing for Immune Evasion. Cell Host Microbe. **14:**591-599.

19. **Berg RK, Rahbek SH, Kofod-Olsen E, Holm CK, Melchjorsen J, Jensen DG, Hansen AL, Jorgensen LB, Ostergaard L, Tolstrup M, Larsen CS, Paludan SR, Jakobsen MR, Mogensen TH.** 2013. T Cells Detect Intracellular DNA but Fail to Induce Type I IFN Responses: Implications for Restriction of HIV Replication. PLoS One. **9:**e84513.

20. **Monroe KM, Yang Z, Johnson JR, Geng X, Doitsh G, Krogan NJ, Greene WC.** 2014. IFI16 DNA Sensor Is Required for Death of Lymphoid CD4 T Cells Abortively Infected with HIV. Science. **24:**428-32.

21. **Gariano GR, Dell'Oste V, Bronzini M, Gatti D, Luganini A, De Andrea M, Gribaudo G, Gariglio M, Landolfo S.** 2012. The intracellular DNA sensor IFI16 gene acts as restriction factor for human cytomegalovirus replication. PLoS Pathog. **8:**e1002498.

22. **Saffert RT, Kalejta RF.** 2006. Inactivating a cellular intrinsic immune defense mediated by Daxx is the mechanism through which the human cytomegalovirus pp71 protein stimulates viral immediate-early gene expression. J. Virol. **80:**3863-3871.

23. **Baggetta R, De Andrea M, Gariano GR, Mondini M, Ritta M, Caposio P, Cappello P, Giovarelli M, Gariglio M, Landolfo S.** 2010. The interferon-inducible gene IFI16 secretome of endothelial cells drives the early steps of the inflammatory response. Eur. J. Immunol. **40:**2182-2189.

24. **Revello MG, Lilleri D, Zavattoni M, Stronati M, Bollani L, Middeldorp JM, Gerna G.** 2001. Human cytomegalovirus immediate-early messenger RNA in blood of pregnant women with primary infection and of congenitally infected newborns. J. Infect. Dis. **184:**1078-1081.

25. **Marschall M, Marzi A, aus dem Siepen P, Jochmann R, Kalmer M, Auerochs S, Lischka P, Leis M, Stamminger T.** 2005. Cellular p32 recruits cytomegalovirus kinase pUL97 to redistribute the nuclear lamina. J. Biol. Chem. **280:**33357-33367.

26. **Milbradt J, Webel R, Auerochs S, Sticht H, Marschall M.** 2010. Novel mode of phosphorylation-triggered reorganization of the nuclear lamina during nuclear egress of human cytomegalovirus. J. Biol. Chem. **285:**13979-13989.

27. **Strack B, Calistri A, Craig S, Popova E, Gottlinger HG.** 2003. AIP1/ALIX is a binding partner for HIV-1 p6 and EIAV p9 functioning in virus budding. Cell. **114:**689-699.

584 28. **Tandon R, AuCoin DP, Mocarski ES.** 2009. Human cytomegalovirus exploits ESCRT
585 machinery in the process of virion maturation. J. Virol. **83:**10797-10807.
586 29. **Marschall M, Stein-Gerlach M, Freitag M, Kupfer R, van Den Bogaard M, Stamminger T.**
587 2001. Inhibitors of human cytomegalovirus replication drastically reduce the activity of the
588 viral protein kinase pUL97. J. Gen. Virol. **82:**1439-1450.
589 30. **Costa S, Borgogna C, Mondini M, De Andrea M, Meroni PL, Berti E, Gariglio M,**
590 **Landolfo S.** 2011. Redistribution of the nuclear protein IFI16 into the cytoplasm of ultraviolet
591 B-exposed keratinocytes as a mechanism of autoantigen processing. Br. J. Dermatol. **164:**282-
592 290.
593 31. **Gugliesi F, Mondini M, Ravera R, Robotti A, de Andrea M, Gribaudo G, Gariglio M,**
594 **Landolfo S.** 2005. Up-regulation of the interferon-inducible IFI16 gene by oxidative stress
595 triggers p53 transcriptional activity in endothelial cells. J. Leukoc. Biol. **77:**820-829.
596 32. **Cepeda V, Esteban M, Fraile-Ramos A.** 2010. Human cytomegalovirus final envelopment on
597 membranes containing both trans-Golgi network and endosomal markers. Cell. Microbiol.
598 **12:**386-404.
599 33. **Cuchet-Lourenco D, Anderson G, Sloan E, Orr A, Everett RD.** 2013. The Viral Ubiquitin
600 Ligase ICP0 Is neither Sufficient nor Necessary for Degradation of the Cellular DNA Sensor
601 IFI16 during Herpes Simplex Virus 1 Infection. J. Virol. **87:**13422-13432.
602 34. **Li T, Diner BA, Chen J, Cristea IM.** 2012. Acetylation modulates cellular distribution and
603 DNA sensing ability of interferon-inducible protein IFI16. Proc. Natl. Acad. Sci. U. S. A.
604 **109:**10558-10563.
605 35. **Gariglio M, Azzimonti B, Pagano M, Palestro G, De Andrea M, Valente G, Voglino G,**
606 **Navino L, Landolfo S.** 2002. Immunohistochemical expression analysis of the human

607 interferon-inducible gene IFI16, a member of the HIN200 family, not restricted to
608 hematopoietic cells. J. Interferon Cytokine Res. **22:**815-821.
609 36. **Veeranki S, Choubey D.** 2012. Interferon-inducible p200-family protein IFI16, an innate
610 immune sensor for cytosolic and nuclear double-stranded DNA: regulation of subcellular
611 localization. Mol. Immunol. **49:**567-571.
612 37. **Murphy EA, Streblow DN, Nelson JA, Stinski MF.** 2000. The human cytomegalovirus IE86
613 protein can block cell cycle progression after inducing transition into the S phase of permissive
614 cells. J. Virol. **74:**7108-7118.
615 38. **Noris E, Zannetti C, Demurtas A, Sinclair J, De Andrea M, Gariglio M, Landolfo S.** 2002.
616 Cell cycle arrest by human cytomegalovirus 86-kDa IE2 protein resembles premature
617 senescence. J. Virol. **76:**12135-12148.
618 39. **Alwine JC.** 2012. The human cytomegalovirus assembly compartment: a masterpiece of viral
619 manipulation of cellular processes that facilitates assembly and egress. PLoS Pathog.
620 **8:**e1002878.
621 40. **Atalay R, Zimmermann A, Wagner M, Borst E, Benz C, Messerle M, Hengel H.** 2002.
622 Identification and expression of human cytomegalovirus transcription units coding for two
623 distinct Fcgamma receptor homologs. J. Virol. **76:**8596-8608.
624 41. **Buchkovich NJ, Maguire TG, Paton AW, Paton JC, Alwine JC.** 2009. The endoplasmic
625 reticulum chaperone BiP/GRP78 is important in the structure and function of the human
626 cytomegalovirus assembly compartment. J. Virol. **83:**11421-11428.
627 42. **Tandon R, Mocarski ES.** 2012. Viral and host control of cytomegalovirus maturation. Trends
628 Microbiol. **20:**392-401.
629 43. **Marschall M, Feichtinger S, Milbradt J.** 2011. Regulatory roles of protein kinases in
630 cytomegalovirus replication. Adv. Virus. Res. **80:**69-101.

44. **Prichard MN, Gao N, Jairath S, Mulamba G, Krosky P, Coen DM, Parker BO, Pari GS.** 1999. A recombinant human cytomegalovirus with a large deletion in UL97 has a severe replication deficiency. J. Virol. **73:**5663-5670.

45. **Prichard MN, Sztul E, Daily SL, Perry AL, Frederick SL, Gill RB, Hartline CB, Streblow DN, Varnum SM, Smith RD, Kern ER.** 2008. Human cytomegalovirus UL97 kinase activity is required for the hyperphosphorylation of retinoblastoma protein and inhibits the formation of nuclear aggresomes. J. Virol. **82:**5054-5067.

46. **Utama B, Shen YH, Mitchell BM, Makagiansar IT, Gan Y, Muthuswamy R, Duraisamy S, Martin D, Wang X, Zhang MX, Wang J, Wang J, Vercellotti GM, Gu W, Wang XL.** 2006. Mechanisms for human cytomegalovirus-induced cytoplasmic p53 sequestration in endothelial cells. J. Cell. Sci. **119:**2457-2467.

47. **Yan N, Chen ZJ.** 2012. Intrinsic antiviral immunity. Nat. Immunol. **13:**214-222.

48. **Liu SY, Sanchez DJ, Cheng G.** 2011. New developments in the induction and antiviral effectors of type I interferon. Curr. Opin. Immunol. **23:**57-64.

49. **Paludan SR, Bowie AG, Horan KA, Fitzgerald KA.** 2011. Recognition of herpesviruses by the innate immune system. Nat. Rev. Immunol. **11:**143-154.

50. **Jakobsen MR, Bak RO, Andersen A, Berg RK, Jensen SB, Jin T, Laustsen A, Hansen K, Ostergaard L, Fitzgerald KA, Xiao TS, Mikkelsen JG, Mogensen TH, Paludan SR.** 2013. From the Cover: IFI16 senses DNA forms of the lentiviral replication cycle and controls HIV-1 replication. Proc. Natl. Acad. Sci. U. S. A. **110:**E4571-4580.

51. **Orzalli MH, Conwell SE, Berrios C, Decaprio JA, Knipe DM.** 2013. Nuclear interferon-inducible protein 16 promotes silencing of herpesviral and transfected DNA. Proc. Natl. Acad. Sci. U. S. A. **110:**E4492-4501.

52. **Sharma M, Kamil JP, Coughlin M, Reim NI, Coen DM.** 2013. Human Cytomegalovirus UL50 and UL53 Recruit Viral Protein Kinase UL97, Not Protein Kinase C, for Disruption of Nuclear Lamina and Nuclear Egress in Infected Cells. J. Virol. **88:**249-262.

53. **Das S, Vasanji A, Pellett PE.** 2007. Three-dimensional structure of the human cytomegalovirus cytoplasmic virion assembly complex includes a reoriented secretory apparatus. J. Virol. **81:**11861-11869.

54. **Das S, Pellett PE.** 2011. Spatial relationships between markers for secretory and endosomal machinery in human cytomegalovirus-infected cells versus those in uninfected cells. J. Virol. **85:**5864-5879.

55. **Baldick CJ, Jr., Shenk T.** 1996. Proteins associated with purified human cytomegalovirus particles. J. Virol. **70:**6097-6105.

56. **Varnum SM, Streblow DN, Monroe ME, Smith P, Auberry KJ, Pasa-Tolic L, Wang D, Camp DG, 2nd, Rodland K, Wiley S, Britt W, Shenk T, Smith RD, Nelson JA.** 2004. Identification of proteins in human cytomegalovirus (HCMV) particles: the HCMV proteome. J. Virol. **78:**10960-10966.

57. **Caposio P, Gugliesi F, Zannetti C, Sponza S, Mondini M, Medico E, Hiscott J, Young HA, Gribaudo G, Gariglio M, Landolfo S.** 2007. A novel role of the interferon-inducible protein IFI16 as inducer of proinflammatory molecules in endothelial cells. J. Biol. Chem. **282:**33515-33529.

58. **McCormick AL, Mocarski Jr ES.** 2007. Viral modulation of the host response to infection. *In:* Arvin A, Campadelli-Fiume G, Mocarski E, Moore PS, Roizman B, Whitley R, Yamanishi K (ed), Human Herpesviruses: Biology, Therapy, and Immunoprophylaxis, Cambridge: Cambridge University Press, Chapter 21.

678 **FIGURE LEGENDS**

679 **FIG 1** Effect of HCMV infection on IFI16 localization. (A) The HCMV genome is recognized by
680 IFI16 at early time points following infection. HELF cells were mock-infected (MOCK) or infected
681 with HCMV (strain AD169, MOI of 2 PFU/cell), fixed in 1% paraformaldehyde at 12 hours post
682 infection (hpi), and subjected to combined fluorescent *in-situ* hybridization (FISH) with a BAC DNA
683 probe containing the entire HCMV genome (red) and immunofluorescence analysis (IFA) with anti-
684 IFI16 antibodies (green). Cell nuclei are visualized in blue. Images were taken by confocal microscopy,
685 and the far right hand picture shows 3D image reconstruction of stacks of confocal images. At least five
686 fields were digitally reconstructed to generate the 3D images for each condition; representative images
687 are shown. (B) HELFs were infected at an MOI of 5 and processed for ChIP assays 6 hours later to test
688 the association of endogenous IFI16 with HCMV and host DNA. (C) IFI16 accumulates in the
689 cytoplasm of HCMV infected cells at late time points post infection. HELF cells were infected with
690 HCMV at an MOI of 1 PFU/cell. Nuclear and cytoplasmic fractions were prepared at the indicated time
691 points and subjected to Western blotting and subsequent densitometry for IFI16. Results were
692 normalized to TBP and tubulin, respectively (*$p<0.05$, ** $p<0.01$, *** $p< 0.001$, one-way ANOVA
693 followed by Bonferroni's post test). (D) Kinetics of IFI16 sub-cellular localization upon HCMV
694 infection. HELF cells were infected with HCMV at an MOI of 1 PFU/cell for the indicated time points
695 and subjected to confocal microscopy analysis. IFI16 (green) and viral proteins (red) were visualized
696 using primary antibodies followed by secondary antibody staining, in the presence of 10% human
697 serum. Nuclei are visualized in blue. The far right hand picture of each panel shows a Z stack of
698 confocal images, generating a 3D reconstruction, obtained as described in (A).

699 **FIG 2** HCMV inhibition blocks the mislocalization of IFI16. HELFs were infected with wild-type or
700 UV-inactivated HCMV (1 PFU/cell; 1.2 J/cm^2 for 2 pulses) and treated with phosphonoformic acid

(PFA, 100 μM) or Ganciclovir (GCV, 100 μM) as indicated. Cells were fixed 72h later in 1% paraformaldehyde and processed by immunofluorescence analysis for IFI16 (green) and gB (red).

FIG 3 pUL97 mediates HCMV-induced IFI16 mislocalization. (A) pUL97 inhibition impairs IFI16 nuclear egress. HELFs were treated as described in detail below and in the results section, fixed at the time points indicated below, and double stained with the appropriated antibodies. HELFs infected with a UL97 deletion mutant BAC (BAC ΔUL97) or with AD169 $UL97^{+}$ as a control at an MOI of 1 PFU/ml, were fixed and immunostained at 32 days or 96 hours post infection, respectively (*panel 1)*; HELFs were electroporated with a mixture of three different small interfering RNAs targeting UL97 (siRNA UL97) or with scrambled control siRNA (siRNA CTRL) and 24h later infected with HCMV at an MOI of 1 PFU/cell for 72h (*panel 2)*; HCMV-infected HELFs were treated with the pUL97 inhibitor Gö6976 (2 μM) or with an equal volume of vehicle control (DMSO) and immunostained after 72h *(panel 3)*. (B) IFI16 interacts with pUL97. Total cell protein extracts from HELFs infected with HCMV at an MOI of 1 for 96h were immunoprecipitated with polyclonal antibodies against IFI16 *(left panel)* or monoclonal antibodies against UL97 *(right panel)*, and control antibody. Samples were then immunoblotted with antibodies for pUL97 and IFI16, respectively. Non-immunoprecipitated whole cell extract (INPUT) obtained from HCMV-infected cells was employed to normalize the proteins subjected to immunoprecipitation. (C) Phosphorylation of IFI16 by pUL97 *in vitro*. HEK 293 cells were transfected with wild-type pUL97 (lane 1), catalytically active pUL97 (N-terminally truncated pUL97-181-707) (lane 2), or inactive C-terminally truncated pUL97 (pUL97-1-595, lane 3). At 48h post-transfection, cells were lysed and subjected to immunoprecipitation (IP) with monoclonal antibodies for pUL97, followed by *in vitro* kinase reaction with recombinant IFI16 (rIFI16) as substrate. Labeled phosphorylation products were separated by SDS-PAGE and visualized by exposing the blots to autoradiography film (*upper panel*). Lysate control samples taken prior to immunoprecipitation were

724 used for Western blot analysis with the monoclonal antibodies for pUL97 to monitor the levels of
725 expressed proteins (*lower panel*).
726 **FIG 4** HCMV infection induces IFI16 sorting into multivesicular bodies (MVBs). (A) IFI16
727 colocalizes with components of MVBs and the ESCRT pathway in HCMV-infected cells. HELF cells
728 were infected with HCMV at an MOI of 1 PFU/cell; 96 hours later cells were fixed, permeabilized, and
729 co-stained with anti-IFI16, anti-TGN46, anti-Vps4A, and anti-HCMV glycoprotein gB antibodies.
730 Nuclei were visualized in blue. Images were taken by confocal microscopy, and the far right hand panel
731 shows a 3D image reconstruction of stacks of confocal images. At least five fields were digitally
732 reconstructed for each condition and a representative image is shown. (B) IFI16 interacts with Vps4A
733 in HCMV-infected cells. Total cell protein extracts obtained by HELFs treated as described above were
734 immunoprecipitated with antibodies against Vps4A *(upper panel)* or IFI16 *(lower panel)*, and the
735 appropriate control antibody (CTRL). Immunoprecipitated samples and whole cell extracts (INPUT)
736 were then immunoblotted using antibodies against Vps4A or IFI16. (C) Effect of blocking MVB
737 biogenesis on IFI16 localization. HELF cells co-transfected with a construct expressing Vps4A
738 ($Vps4_{WT}$) or the mutated form $Vps4A_{E228Q}$ were infected with HCMV (MOI of 1 PFU/cell) 24 hours
739 post transfection. Cells were fixed and photographed at 72 hpi. Vps4A was detected by anti-FLAG
740 primary antibody (red) and IFI16 by the polyclonal anti-IFI16 antibody (green). Representative images
741 were taken using 63X magnification.
742 **FIG 5** IFI16 is associated with purified HCMV particles. (A) HCMV particles (indicated as virions)
743 were purified by sucrose gradient from supernatants of infected HELFs (192 hpi, MOI of 1) and
744 analyzed by immunoblotting for the viral proteins IEA, UL44, and pp65, and the cellular proteins IFI16
745 or p53. Total cell extract from MOCK- or HCMV-infected cells were included as controls. (B) IFI16
746 interacts with pp65 in purified virions. HELFs were infected as described for panel A. Protein extracts
747 were obtained from purified virions and immunoprecipitated with anti-pp65 *(upper panel)* or anti-IFI16

748 *(lower panel)* and the appropriate control antibodies (CTRL), and then immunoblotted with anti-IFI16
749 or anti-pp65 antibodies, respectively. Non-immunoprecipitated whole cell extracts (INPUT) were
750 immunoblotted with anti-IFI16 or anti-pp65 antibodies and employed to normalize the proteins
751 subjected to immunoprecipitation. (C) Immunoelectron microscopy analysis of purified virions stained,
752 in the presence of 10% human serum, for IFI16 and HCMV gB and pp65, or left unstained (secAb). 15
753 nm gold conjugated secondary antibody was used to detect proteins. Scale bar, 100 nm.

754
755
756

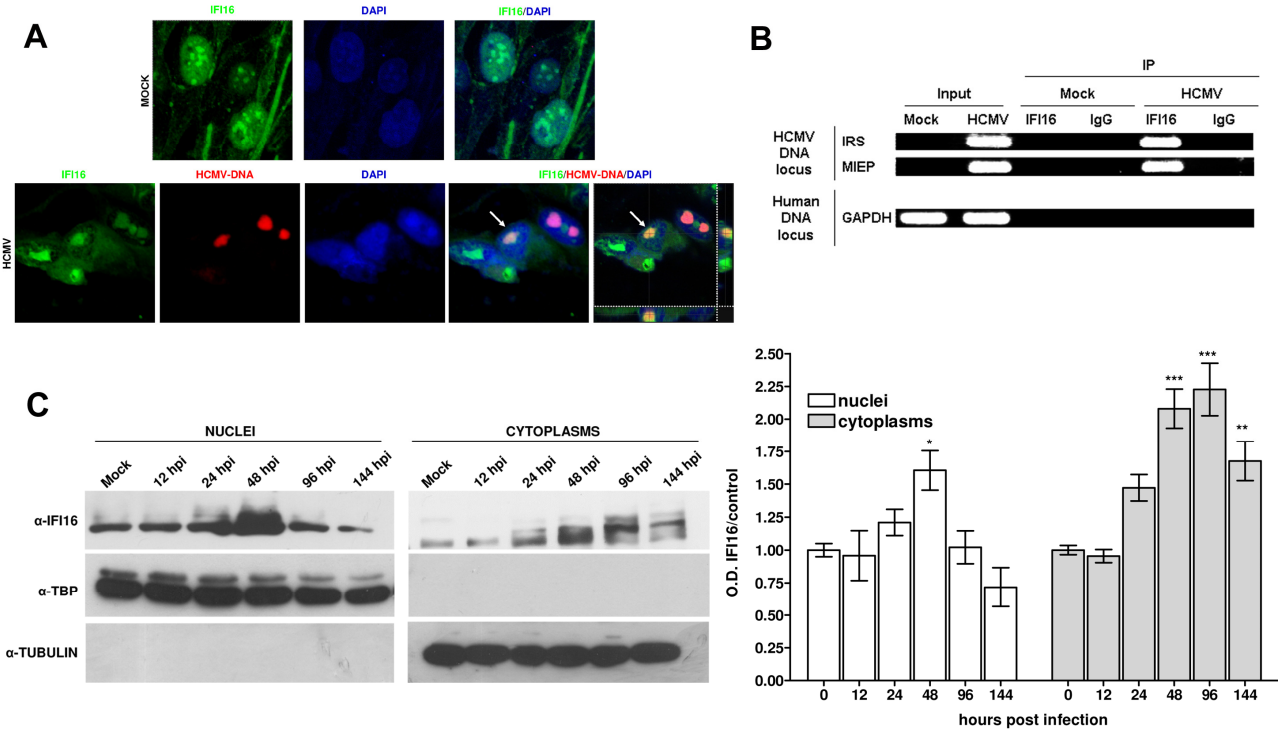
A
IFI16
DAPI
IFI16/DAPI
MOCK
IFI16
HCMV-DNA
DAPI
IFI16/HCMV-DNA/DAPI
HCMV
B
IP
Input
Mock
HCMV
Mock
HCMV
IFI16
IgG
IFI16
IgG
HCMV DNA locus
IRS
MIEP
Human DNA locus
GAPDH
C
NUCLEI
CYTOPLASMS
Mock
12 hpi
24 hpi
48 hpi
96 hpi
144 hpi
α-IFI16
α-TBP
α-TUBULIN
nuclei
cytoplasms
O.D. IFI16/control
hours post infection
D
IFI16
HCMV proteins
DAPI
IFI16/HCMV proteins/DAPI
12 hpi
IEA
24 hpi
IEA
48 hpi
UL44
72 hpi
gB
96 hpi
pp65
144 hpi
gB

FIG 1 Effect of HCMV infection on IFI16 localization. (A) The HCMV genome is recognized by IFI16 at early time points following infection. HELF cells were mock-infected (MOCK) or infected with HCMV (strain AD169, MOI of 2 PFU/cell), fixed in 1% paraformaldehyde at 12 hours post infection (hpi), and subjected to combined fluorescent *in-situ* hybridization (FISH) with a BAC DNA probe containing the entire HCMV genome (red) and immunofluorescence analysis (IFA) with anti-IFI16 antibodies (green). Cell nuclei are visualized in blue. Images were taken by confocal microscopy, and the far right hand picture shows 3D image reconstruction of stacks of confocal images. At least five fields were digitally reconstructed to generate the 3D images for each condition; representative images are shown. (B) HELFs were infected at an MOI of 5 and processed for ChIP assays 6 hours later to test the association of endogenous IFI16 with HCMV and host DNA. (C) IFI16 accumulates in the cytoplasm of HCMV infected cells at late time points post infection. HELF cells were infected with HCMV at an MOI of 1 PFU/cell. Nuclear and cytoplasmic fractions were prepared at the indicated time points and subjected to Western blotting and subsequent densitometry for IFI16. Results were normalized to TBP and tubulin, respectively (*$p<0.05$, ** $p<0.01$, *** $p< 0.001$, one-way ANOVA followed by Bonferroni's post test). (D) Kinetics of IFI16 sub-cellular localization upon HCMV infection. HELF cells were infected with HCMV at an MOI of 1 PFU/cell for the indicated time points and subjected to confocal microscopy analysis. IFI16 (green) and viral proteins (red) were visualized using primary antibodies followed by secondary antibody staining, in the presence of 10% human serum. Nuclei are visualized in blue. The far right hand picture of each panel shows a Z stack of confocal images, generating a 3D reconstruction, obtained as described in (A).

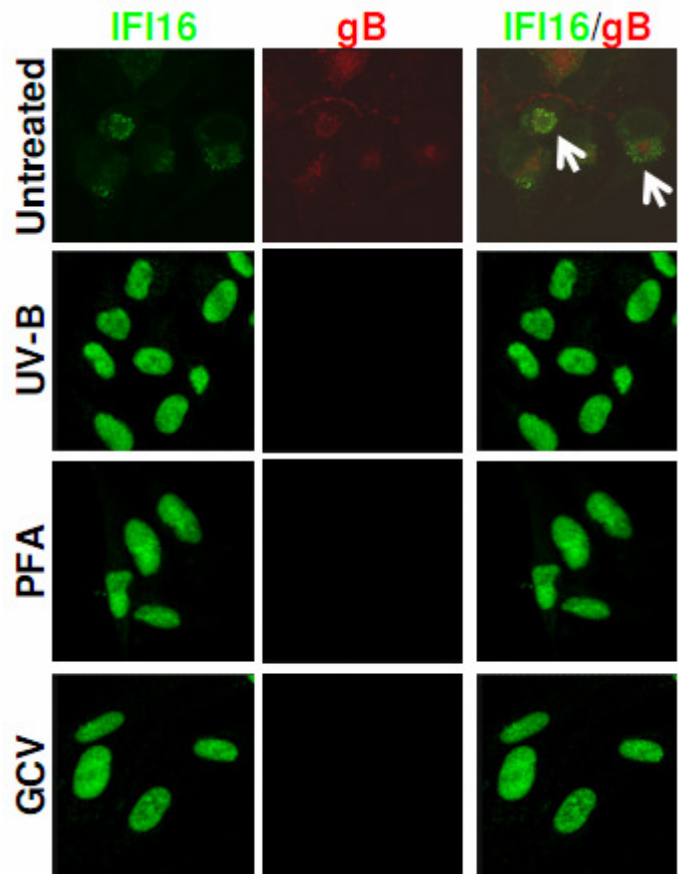

FIG 2 HCMV inhibition blocks the mislocalization of IFI16. HELFs were infected with wild-type or UV-inactivated HCMV (1 PFU/cell; 1.2 J/cm^2 for 2 pulses) and treated with phosphonoformic acid (PFA, 100 μM) or Ganciclovir (GCV, 100 μM) as indicated. Cells were fixed 72h later in 1% paraformaldehyde and processed by immunofluorescence analysis for IFI16 (green) and gB (red).

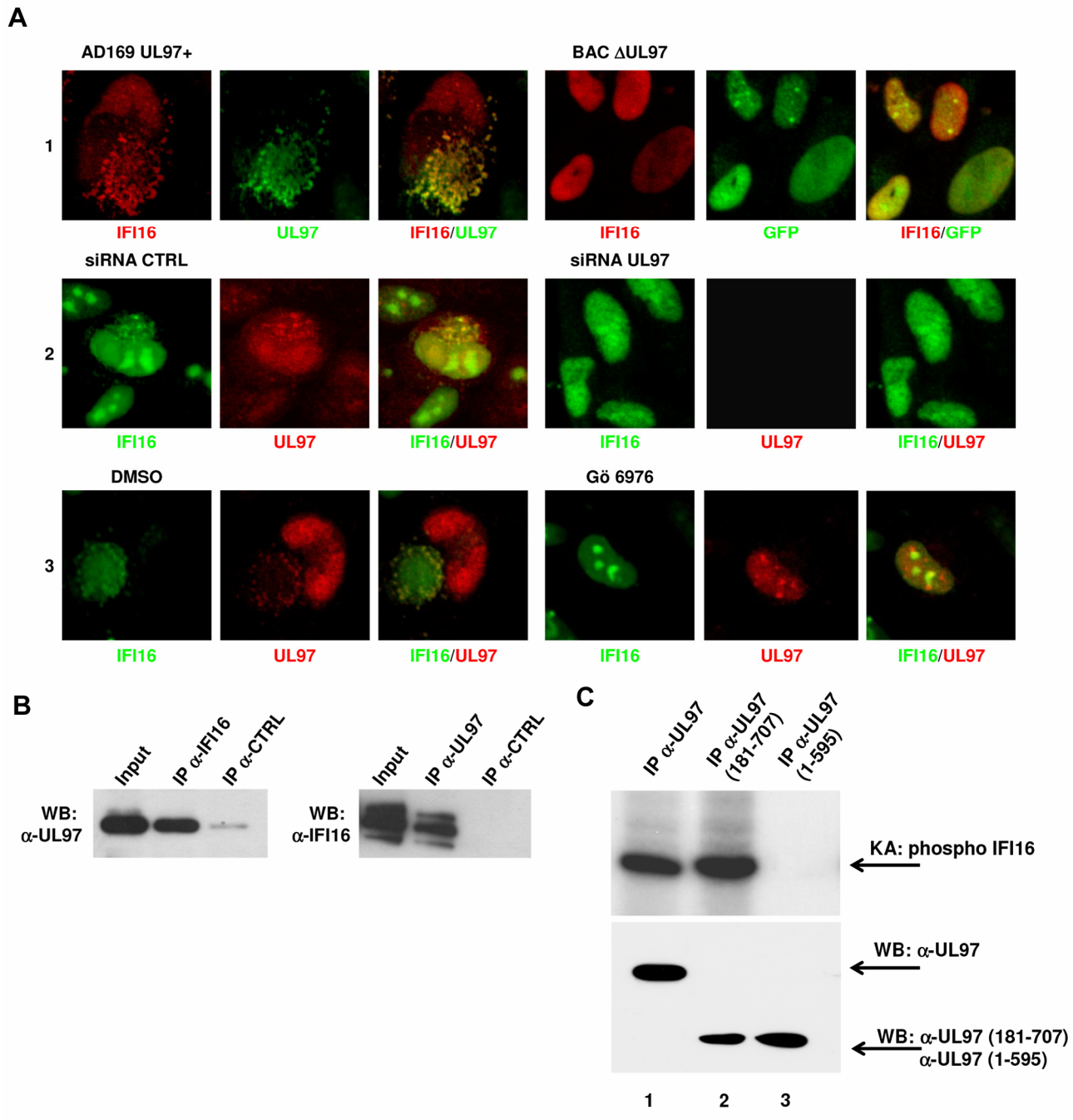

FIG 3 pUL97 mediates HCMV-induced IFI16 mislocalization. (A) pUL97 inhibition impairs IFI16 nuclear egress. HELFs were treated as described in detail below and in the results section, fixed at the time points indicated below, and double stained with the appropriated antibodies. HELFs infected with a UL97 deletion mutant BAC (BAC ΔUL97) or with AD169 UL97^{+} as a control at an MOI of 1 PFU/ml, were fixed and immunostained at 32 days or 96 hours post infection, respectively (*panel 1)*; HELFs were electroporated with a mixture of three different small interfering RNAs targeting UL97 (siRNA UL97) or with scrambled control siRNA (siRNA CTRL)

and 24h later infected with HCMV at an MOI of 1 PFU/cell for 72h (*panel 2)*; HCMV-infected HELFs were treated with the pUL97 inhibitor Gö6976 (2 μM) or with an equal volume of vehicle control (DMSO) and immunostained after 72h *(panel 3)*. (B) IFI16 interacts with pUL97. Total cell protein extracts from HELFs infected with HCMV at an MOI of 1 for 96h were immunoprecipitated with polyclonal antibodies against IFI16 *(left panel)* or monoclonal antibodies against UL97 *(right panel)*, and control antibody. Samples were then immunoblotted with antibodies for pUL97 and IFI16, respectively. Non-immunoprecipitated whole cell extract (INPUT) obtained from HCMV-infected cells was employed to normalize the proteins subjected to immunoprecipitation. (C) Phosphorylation of IFI16 by pUL97 *in vitro*. HEK 293 cells were transfected with wild-type pUL97 (lane 1), catalytically active pUL97 (N-terminally truncated pUL97-181-707) (lane 2), or inactive C-terminally truncated pUL97 (pUL97-1-595, lane 3). At 48h post-transfection, cells were lysed and subjected to immunoprecipitation (IP) with monoclonal antibodies for pUL97, followed by *in vitro* kinase reaction with recombinant IFI16 (rIFI16) as substrate. Labeled phosphorylation products were separated by SDS-PAGE and visualized by exposing the blots to autoradiography film (*upper panel*). Lysate control samples taken prior to immunoprecipitation were used for Western blot analysis with the monoclonal antibodies for pUL97 to monitor the levels of expressed proteins (*lower panel*).

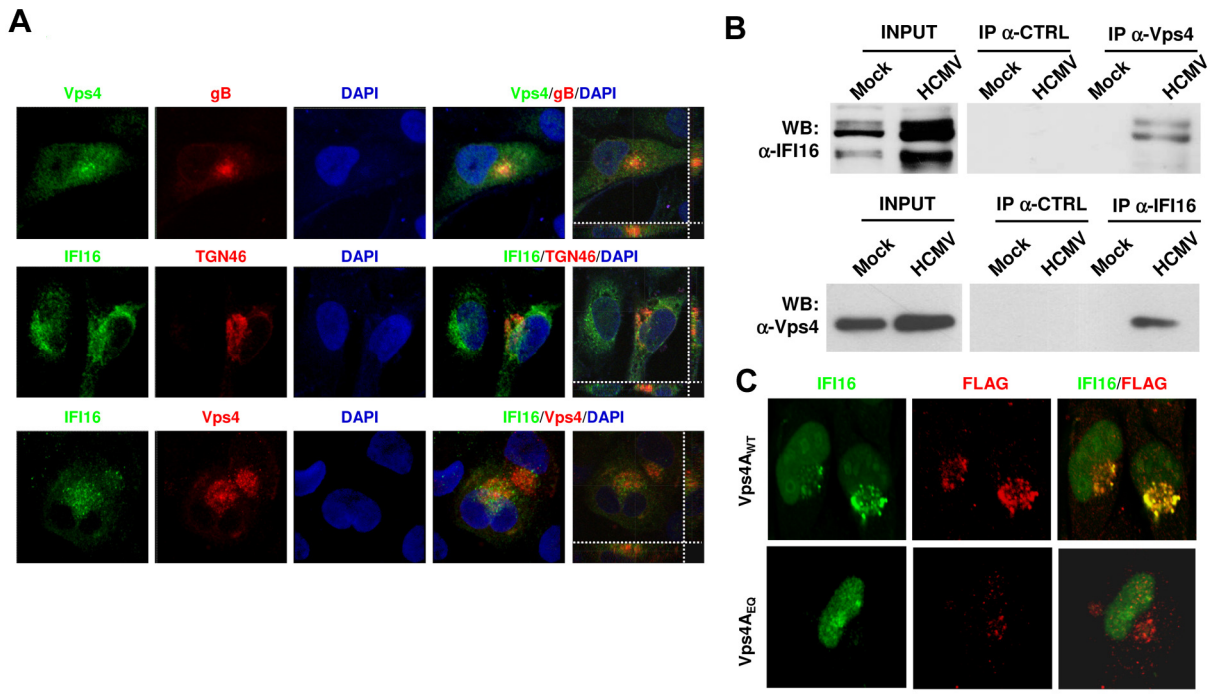

FIG 4 HCMV infection induces IFI16 sorting into multivesicular bodies (MVBs). (A) IFI16 colocalizes with components of MVBs and the ESCRT pathway in HCMV-infected cells. HELF cells were infected with HCMV at an MOI of 1 PFU/cell; 96 hours later cells were fixed, permeabilized, and co-stained with anti-IFI16, anti-TGN46, anti-Vps4A, and anti-HCMV glycoprotein gB antibodies. Nuclei were visualized in blue. Images were taken by confocal microscopy, and the far right hand panel shows a 3D image reconstruction of stacks of confocal images. At least five fields were digitally reconstructed for each condition and a representative image is shown. (B) IFI16 interacts with Vps4A in HCMV-infected cells. Total cell protein extracts obtained by HELFs treated as described above were immunoprecipitated with antibodies against Vps4A *(upper panel)* or IFI16 *(lower panel)*, and the appropriate control antibody (CTRL). Immunoprecipitated samples and whole cell extracts (INPUT) were then immunoblotted using antibodies against Vps4A or IFI16. (C) Effect of blocking MVB biogenesis on IFI16 localization. HELF cells co-transfected with a construct expressing Vps4A ($Vps4_{WT}$) or the mutated form $Vps4A_{E228Q}$ were infected with HCMV (MOI of 1 PFU/cell) 24 hours post transfection. Cells were fixed and photographed at 72 hpi. Vps4A was detected by anti-FLAG primary antibody (red) and

IFI16 by the polyclonal anti-IFI16 antibody (green). Representative images were taken using 63X magnification.

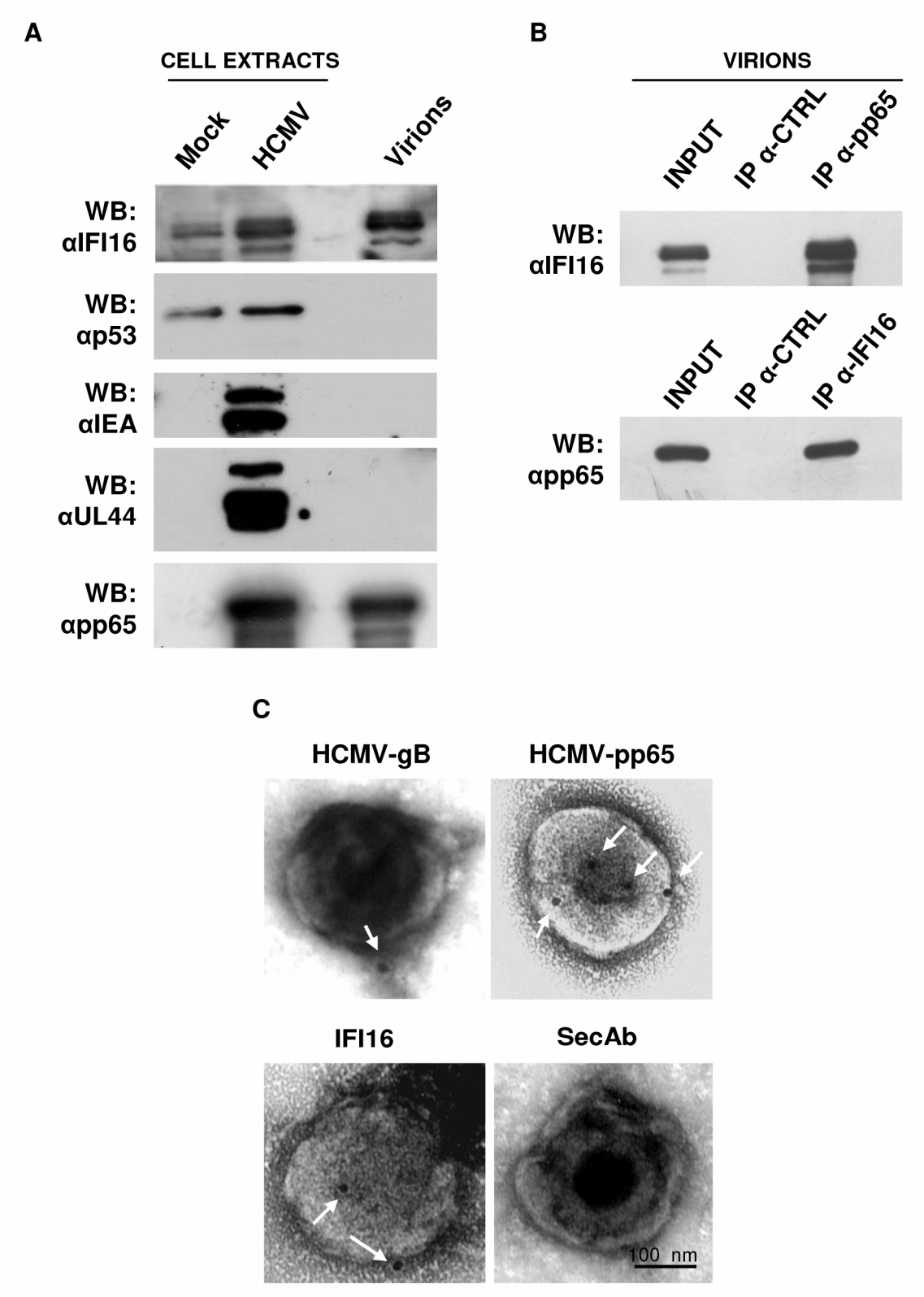

FIG 5 IFI16 is associated with purified HCMV particles. (A) HCMV particles (indicated as virions) were purified by sucrose gradient from supernatants of infected HELFs (192 hpi, MOI of 1) and analyzed by immunoblotting for the viral proteins IEA, UL44, and pp65, and the cellular proteins IFI16 or p53. Total cell extract from MOCK- or HCMV-infected cells were included as controls.

(B) IFI16 interacts with pp65 in purified virions. HELFs were infected as described for panel A. Protein extracts were obtained from purified virions and immunoprecipitated with anti-pp65 *(upper panel)* or anti-IFI16 *(lower panel)* and the appropriate control antibodies (CTRL), and then immunoblotted with anti-IFI16 or anti-pp65 antibodies, respectively. Non-immunoprecipitated whole cell extracts (INPUT) were immunoblotted with anti-IFI16 or anti-pp65 antibodies and employed to normalize the proteins subjected to immunoprecipitation. (C) Immunoelectron microscopy analysis of purified virions stained, in the presence of 10% human serum, for IFI16 and HCMV gB and pp65, or left unstained (secAb). 15 nm gold conjugated secondary antibody was used to detect proteins. Scale bar, 100 nm.